

X 62 63940

CONFIDENTIAL

Copy 95  
RM L56F12

NACA RM L56F12

# NACA CASE FILE COPY

## RESEARCH MEMORANDUM

Attic 295683

NOT RELEASABLE TO PROJECT STORERS

INVESTIGATION AT TRANSONIC SPEEDS OF THE LOADING OVER A 45° SWEEPBACK WING HAVING AN ASPECT RATIO OF 3, A TAPER RATIO OF 0.2, AND NACA 65A004 AIRFOIL SECTIONS

By Jack F. Runckel and Edwin E. Lee, Jr.

Langley Aeronautical Laboratory  
Langley Field, Va.

CLASSIFICATION CHANGED TO  
DECLASSIFIED AUTHORITY

NTP July 1959 - June 1960

EXCLUDED FROM AUTOMATIC  
DECLASSIFICATION; E.O. 12958, 1.4  
DOES NOT APPLY

CLASSIFIED DOCUMENT

This material contains information affecting the National Defense of the United States within the meaning of the espionage laws, Title 18, U.S.C., Secs. 793 and 794, the transmission or revelation of which in any manner to an unauthorized person is prohibited by law.

### NATIONAL ADVISORY COMMITTEE FOR AERONAUTICS

WASHINGTON

October 8, 1956

11 OCT 1958 01 46

IN

CONFIDENTIAL T62-25959

ERRATA

NACA Research Memorandum L56F12

MAY 20 1957

By Jack F. Runckel and Edwin E. Lee, Jr.  
October 1956

A computational error in some of the data of this research memorandum necessitates corrections as follows:

√Page 1, second paragraph, lines 5 and 6:

Change 30 percent to 43 percent and 40 percent to 53 percent.

Page 12, third complete paragraph, lines 3 and 4:

Change 30 percent to 43 percent and 40 percent to 53 percent.

Page 14, paragraph numbered (4):

Change 30 percent to 43 percent and 40 percent to 53 percent.

Page 90:

Replace figure 12 with corrected figure 12 attached.

Page 93:

Replace figure 15 with corrected figure 15 attached.

On index cards inside the back cover (or on individual cards if detached):

In last line on front of card, change 30 percent to 43 percent.

In second line on back of card, change 40 percent to 53 percent.

CONFIDENTIAL

## NATIONAL ADVISORY COMMITTEE FOR AERONAUTICS

## RESEARCH MEMORANDUM

INVESTIGATION AT TRANSONIC SPEEDS OF THE LOADING OVER A  
45° SWEEPBACK WING HAVING AN ASPECT RATIO OF 3, A TAPER  
RATIO OF 0.2, AND NACA 65A004 AIRFOIL SECTIONS

By Jack F. Runckel and Edwin E. Lee, Jr.

## SUMMARY

An investigation at transonic speeds of the loading over a 45° sweptback wing having an aspect ratio of 3, a taper ratio of 0.2, and NACA 65A004 airfoil sections has been conducted in the Langley 16-foot transonic tunnel. Pressure measurements on the wing-body combination were obtained at angles of attack from 0° to 26° at Mach numbers from 0.80 to 0.98 and from 0° to about 12° at Mach numbers from 1.00 to 1.05. Reynolds number, based on the wing mean aerodynamic chord, varied from  $7 \times 10^6$  to  $8.5 \times 10^6$  over the test Mach number range.

Results of the investigation indicate that a highly swept shock originates at the wing-leading-edge—body juncture at moderate angles of attack and has a large influence on the loading over the inboard wing sections. The chordwise position of the wing center of pressure shifted from about ~~70~~<sup>43</sup> percent of the mean aerodynamic chord at a Mach number of 0.80 to about ~~53~~<sup>53</sup> percent of the mean aerodynamic chord at a Mach number of 1.05. The lateral position of the center of pressure shifted outboard a maximum of about 4 percent of the semispan over the same Mach number range.

## INTRODUCTION

Thin swept wings of low aspect ratio and low taper ratio appear to be desirable plan forms for the transonic and low supersonic speed range because they combine acceptable stability and performance characteristics with the structural advantages of the highly tapered plan form (ref. 1). However, very little data on the loading over swept wings that are thinner than 6 percent are available at transonic speeds.

CONFIDENTIAL

In order to increase the fund of information on thin wings at transonic speeds, a research program has been conducted at the Langley 16-foot transonic tunnel to determine the characteristics of unswept, swept, and delta wings. The characteristics of the unswept wing have been reported in reference 2. In the present paper, results are presented for a wing having  $45^\circ$  sweep of the quarter-chord line, a taper ratio of 0.2, an aspect ratio of 3, and NACA 65A004 airfoil sections parallel to the plane of symmetry. This wing was tested for the purpose of obtaining the steady-state aerodynamic loading characteristics, the longitudinal stability of the wing-body and wing-body-tail combinations, the effectiveness of lateral controls, and the loading on these controls. The longitudinal stability characteristics of this configuration have been reported in reference 3. Some data on the control loading were presented in reference 4. The present paper presents the steady-state aerodynamic loading characteristics of the wing in the presence of the body.

The model was tested at Mach numbers from 0.80 to 1.05 and at angles of attack from  $0^\circ$  to about  $26^\circ$  at subsonic speeds and from  $0^\circ$  to about  $12^\circ$  at supersonic speeds. Reynolds number, based on the wing mean aerodynamic chord, varied from  $7.0 \times 10^6$  to  $8.5 \times 10^6$  over the test Mach number range.

#### SYMBOLS

b wing span

c local chord measured parallel to body center line

c' wing mean aerodynamic chord

$\bar{c}$  average wing chord,  $S/b$

$c_{m_c/4}$  wing section pitching-moment coefficient about  $0.25c$ ,

$$\int_0^1 (P_L - P_U) \left(0.25 - \frac{x}{c}\right) d\left(\frac{x}{c}\right)$$

$c_n$  wing section normal-force coefficient,  $\int_0^1 (P_L - P_U) d\left(\frac{x}{c}\right)$

$c_m$  wing section pitching moment coefficient about  $0.25c'$ ,  
 $c_{m_c/4} - c_n \left(0.25 - \frac{x'}{c}\right)$



- $C_m$  wing pitching-moment coefficient about  $0.25c'$ ,  

$$\int_{0.16}^{1.0} c_m \frac{c^2}{cc'} d\left(\frac{y}{b/2}\right)$$
- $C_B$  wing bending-moment coefficient about body center line,  

$$\int_{0.16}^{1.0} \left(c_n \frac{c}{c} \frac{y}{b/2}\right) d\left(\frac{y}{b/2}\right)$$
- $C_N$  wing normal-force coefficient (perpendicular to body center line),  $\int_{0.16}^{1.0} c_n \frac{c}{c} d\left(\frac{y}{b/2}\right)$
- $L$  body length
- $M$  Mach number
- $m_c/4$  section pitching moment about  $0.25c$
- $n$  section normal force
- $p$  free-stream static pressure
- $P$  pressure coefficient,  $\frac{p_{\text{local}} - p}{q}$
- $q$  free-stream dynamic pressure
- $r$  body radius
- $S$  wing area (includes area blanketed by body)
- $\Delta S_\eta$  local section weighting area
- $x$  distance from leading edge of wing or nose of body (positive rearward)
- $x'$  distance from wing leading edge to a line perpendicular to plane of symmetry and passing through  $0.25c'$
- $\frac{x_{cp}}{c}$  section chordwise center-of-pressure position

$\frac{x_{cp}}{c}$	wing chordwise center-of-pressure position $\left(0.25 - \frac{C_m}{C_N}\right)$
y	spanwise distance measured from body center line
$\frac{y_{cp}}{b/2}$	wing spanwise center-of-pressure position
$\alpha$	angle of attack of fuselage center line
$\Delta\alpha$	angle of twist between body center line and wing tip, $\alpha_{tip} - \alpha_{body}$
$\frac{\partial\Delta\alpha}{\partial\alpha}$	influence coefficient of section pitching moment on wing-tip angle of attack
$\frac{\partial\Delta\alpha}{\partial\alpha}$	influence coefficient of section normal force on wing-tip angle of attack
$\phi$	meridian angle of body orifice
Subscripts:	
L	wing lower surface
U	wing upper surface
$\eta$	local spanwise wing station, A through F

## MODEL AND APPARATUS

### Model

The geometric details of the model are given in figure 1. The wing was constructed of aluminum alloy and was mounted in a midwing position on the body; it had no geometric incidence, twist, or dihedral. The body consisted of a cylindrical body of revolution, an ogival nose, and a slightly boattailed afterbody. The body ordinates are presented in figure 1. The ratio of body base diameter to the maximum diameter is 0.66 and the ratio of body maximum cross-sectional area to wing area is 0.0605. A photograph of the model mounted in the Langley 16-foot transonic tunnel is shown as figure 2.

### Tunnel and Model Support

The Langley 16-foot transonic tunnel, in which the tests were conducted, is an atmospheric tunnel and has an octagonal slotted test section permitting a continuous variation in speed to Mach numbers slightly above 1.0. The Reynolds number (based on the wing mean aerodynamic chord) for this investigation varied from  $7 \times 10^6$  to  $8 \times 10^6$  at a Mach number of 0.80 and from about  $7.3 \times 10^6$  to  $8.5 \times 10^6$  at a Mach number of 1.05.

The model support system was arranged so that the model was located near the center of the tunnel at all angles of attack; this system is described in reference 5.

### Instrumentation

Pressures over the wing were measured at six spanwise stations with orifices located at 16, 25, 40, 60, 75, and 95 percent of the semispan. At the innermost wing station the orifices were installed on the fuselage about 1/16 inch from the wing surface and extended slightly forward and rearward of the leading and trailing edges. Body pressure measurements were obtained along the  $0^\circ$  and  $180^\circ$  meridians from 0 percent to 78 percent of the body length and along the  $22.5^\circ$ ,  $337.5^\circ$  and  $180^\circ$  meridians from 82 percent to 98 percent of the body length. Pressures were also measured on the body in the region of the wing at meridian positions of  $22.5^\circ$ ,  $45^\circ$ ,  $135^\circ$ , and  $157.5^\circ$ . The orifice locations on the wing and body are given in figure 1. The model angle of attack was obtained from the static angle of attack corrected for deflections due to load. These deflections, which occurred in the balance and sting, were determined from static normal-force and pitching-moment calibrations of a six-component internal strain-gage balance.

### Flow-Visualization Technique

To supplement the pressure-distribution measurements on the wing, a visual study of the boundary-layer flow was made with a liquid film technique utilizing China clay. The upper surface of the wing was first painted with a flat black undercoat and then sprayed with a thin layer of white China clay. When a liquid having approximately the same index of refraction as the China clay was emitted from orifices on the wing and allowed to flow over the prepared surface, the wetted regions became transparent and caused the black undercoat to appear. After the flow of liquid was terminated, evaporation occurred on the wetted regions of the wing and caused these sections of the surface to regain their original white color. Since the flow-visualization studies were made after

the pressure-distribution measurements had been obtained, wing pressure orifices were utilized as sources of the fluid. Liquid was emitted from orifices at the following locations:

Spanwise station	$\frac{y}{b/2}$	Orifice locations, percent chord
A	0.16	2.5
B	.25	5, 10, 15, 20, 25, 45, 65
C	.40	5, 15, 20, 25, 30, 35, 40, 45, 50, 65
D	.60	5, 25, 45, 65
E	.75	5, 25, 45, 65
F	.95	5, 45,

The flow patterns on the wing were photographed with a shadowgraph camera apparatus.

#### Data Reduction

Pressures were recorded by photographing 100-tube mercury manometer boards. The film records were coded and transferred to cards by the use of a film-reading device coupled to a punch-card machine. The data were then processed on electronic computing machines to obtain individual pressure coefficients as well as wing-section normal-force and pitching-moment coefficients (using a rectangular step integration). The data cards were also fed to an automatic plotting device for the preparation of chordwise pressure-distribution plots.

#### Wing Twist

The wing-section data are presented herein for a range of body angles of attack. No aeroelastic corrections have been applied to correct the local wing-section angles of attack. However, the deflection characteristics of the wing have been determined from static loadings. In order to determine the influence on the tip deflection of a normal force acting at a given spanwise station, several normal loads were applied on the quarter-chord line at that station, and the angular deflection of the tip was recorded for each load applied. From a plot of tip deflection against the applied load, the slope or influence coefficient  $\frac{\partial \Delta \alpha}{\partial n}$  was obtained for the particular spanwise station. The influence coefficients for pitching moments were determined in a similar manner by applying the load at other chordwise positions at each spanwise station, and tip deflection was found to be a linear function of the moment about the local quarter-chord point. The influence coefficients  $\frac{\partial \Delta \alpha}{\partial n}$  and  $\frac{\partial \Delta \alpha}{\partial m}$  measured at various positions

along the exposed semispan are presented in figure 3. The spanwise variation of the local chord  $c$  is shown on figure 3. Selection of the incremental areas  $\Delta S_\eta$ , also presented in figure 3, was based on the location of the wing pressure-orifice stations. The area strip  $\Delta S_A$ , corresponding to station A, is that portion of the exposed wing area bounded by the wing-body juncture and a line parallel to the orifice stations, lying halfway between stations A and B. For stations B through E, the width of each corresponding area strip extends from midpoint to midpoint between adjacent pressure-orifice stations. The area for station F was taken as the area bounded by a line midway between stations E and F and the physical boundary of the wing tip. The angle of twist of the wing tip with respect to the body centerline can be determined from the following relation:

$$\Delta\alpha = q \left[ \sum_{\eta=A}^{\eta=F} \left( \frac{\partial \Delta\alpha}{\partial n} \right) c_n \Delta S_\eta + \sum_{\eta=A}^{\eta=F} \left( \frac{\partial \Delta\alpha}{\partial m} \right) c_{m_c} / 4 \ c \Delta S_\eta \right]$$

Calculation of the wing twist at a Mach number of 0.98 and a fuselage angle of attack of  $24.4^\circ$  resulted in a tip deflection of  $\Delta\alpha = -6.3^\circ$  or an actual section angle of attack at the wing tip of  $18.1^\circ$ . This value represents the maximum correction in section angle of attack for this investigation. For other spanwise stations, it is assumed that the twist varies linearly from the wing tip to the wing-body juncture.

### RESULTS AND DISCUSSION

Data were obtained over an angle-of-attack range from  $0^\circ$  to about  $26^\circ$  at subsonic speeds and from  $0^\circ$  to about  $12^\circ$  at supersonic speeds. Pressure distributions and/or tabulations are presented for Mach numbers of 0.80, 0.85, 0.90, 0.92, 0.94, 0.96, 0.98, 1.00, 1.03, and 1.05.

The results of the investigation are presented in the following figures and tables:

Illustrations of flow over the wing . . . . .	Fig. 4
Chordwise pressure distributions and contour plots . . .	Figs. 5 and 6
Pressure measurements on the body . . . . .	Fig. 7
Spanwise loading variation and normal-force variation . .	Figs. 8 to 10
Chordwise center-of-pressure locations . . . . .	Figs. 11 and 12
Bending-moment characteristics . . . . .	Fig. 13
Spanwise center-of-pressure characteristics . . . . .	Fig. 14
Wing stability characteristics . . . . .	Fig. 15
Pressure coefficients at six spanwise stations . . . . .	Table I
Section coefficients at wing stations . . . . .	Table II



## Flow Characteristics

The flow characteristics at transonic speeds of swept wings of 6-percent thickness ratio have been described in references 6, 7, and 8.

It would be expected that the flow pattern over the present wing would be modified somewhat from those observed for the 6-percent-thick wings in references 6, 7, and 8 because of greater leading-edge sweep, thinner sections, lower aspect ratio, and the difference in body shape and size of the present configuration. A brief description of the shocks associated with thinner wings in the transonic range has been presented in reference 4.

With thinner wing sections, lower velocities will be induced over the airfoil, and oblique shocks at the leading and trailing edges should be weaker. The reduced leading-edge radius of the 4-percent-thick airfoil sections will produce smaller negative pressure coefficients near the leading-edge region than those for the 6-percent-thick airfoil owing to the tendency of the sharper leading edge to separate the flow. The increase in leading-edge sweep would be expected to delay flow changes to somewhat higher Mach numbers.

Typical illustrations of the boundary-layer flow on the surface of the wing, obtained with the liquid film technique using China clay previously described, are shown in figure 4. At the lowest angles of attack such as shown for  $2^\circ$  at a Mach number of 0.80, the flow is essentially chordwise in direction. As the angle of attack is increased to about  $4^\circ$  at all Mach numbers, the flow of some liquid outboard along the leading edge indicates the formation of a disturbance in this region. In the angle-of-attack region from about  $5^\circ$  to  $12^\circ$ , the fluid lines on the wing indicate a division of the boundary-layer flow over the wing into streamwise and spanwise directions. At the highest angles of attack a large portion of the flow over the wing has separated and the flow becomes predominantly spanwise with inboard flow along the leading edge.

In figure 4, the photograph for a Mach number of 0.94 and an angle of attack of  $6^\circ$  shows some streamwise flow of fluid just outboard of station D, which was caused by a chordwise discontinuity of the wing leading-edge piece that tripped the boundary layer; this streamwise flow, therefore, should be discounted as representative of the flow in that region. The mismatch in the leading-edge piece was not present at the time the pressure distributions were obtained.

In the photographs for a Mach number of 0.94 at low angles of attack, the shadow of the main decelerating-flow shock is visible across the body and wings (arrow). The visible portion of the shock front occurs on the photograph where the shock becomes tangent to the shadow-graph light source. At higher angles of attack the flow-field shock moves rearward off the wing. At a supersonic Mach number of 1.03, the

decelerating-flow shock is behind the wing at all angles of attack and therefore is not visible in those photographs. Some turning of the flow near the wing trailing edge at low angles of attack at this Mach number indicates the presence of a weak oblique shock in this region.

### Chordwise Pressure Distributions

Chordwise pressure distributions are presented in figure 5 for the test Mach number range and increments of about  $4^\circ$  in angle of attack. (A more extensive coverage of the angle-of-attack range is illustrated for a Mach number of 0.94.) Throughout figure 5, the pressure distributions for station A include values of the pressure coefficient measured on the body just ahead of and behind the wing. When considering this spanwise station, the fact that all orifices are located on the body surface must be kept in mind.

At the subsonic Mach number of 0.80, the chordwise pressure distributions are generally similar in shape to those for thicker, higher aspect-ratio wings at this speed (see ref. 9); however, the peak negative pressures are lower for the present thinner wing as previously mentioned. Tip stall, characteristic of the swept wing, begins at about  $8.4^\circ$  angle of attack (fig. 5(a)) and spreads gradually inboard as the angle of attack is increased. The main difference between the present 4-percent-thick wing and the 6-percent-thick wings of references 6 and 9 is the strong disturbance that originates at the wing-leading-edge-body juncture and sweeps back off the wing outboard of the 0.60b/2 station at  $\alpha = 8.4^\circ$  (fig. 5(a)). This juncture shock is quite strong near the inboard stations, as shown by the subcritical pressures behind it, but the chordwise pressure gradient due to the shock diminishes outboard possibly because of increased boundary-layer thickness. Between  $16^\circ$  and  $20^\circ$  angle of attack, the high negative pressures in the leading-edge region of the inboard sections are greatly reduced causing a flattening of the normal-force curve of figure 10. At the highest angle of attack, the flow on the entire upper surface is separated.

As the Mach number is increased, little change in the pressure distributions occur until a Mach number of 0.90 is reached. At this speed, the main decelerating-flow shock becomes evident on the body at the higher angles of attack (fig. 7). This normal shock extends spanwise over the wing at  $8.4^\circ$  angle of attack, as is evident from the compressions near the trailing edge of the inboard sections.

The transonic Mach number of 0.94 has been found to be the region where the most severe changes in swept-wing stability usually occur (ref. 10). Studies of the flow over swept wings at this speed have shown that this phenomenon was due to the combination of the leading-edge,

trailing-edge, and decelerating-flow shocks near the tip, causing the flow over a large outboard region of the wing to separate (refs. 6 and 8). Additional angles of attack are, therefore, presented for this Mach number. At low angles of attack, figure 5(e), the swept-wing leading-edge shock and the decelerating-flow shock affect the loading diagrams. The wing trailing-edge shock is masked by the coincident decelerating-flow shock at this Mach number. Above  $8.3^\circ$  the primary leading-edge shock appears very weak and the sharply sweptback shock originating at the wing-leading-edge-body juncture develops and leaves the wing outboard of the  $0.60b/2$  station, with attendant separation starting at the tip section. At angles of attack where initial wing stall occurs ( $\alpha \approx 10^\circ$ , fig. 10), separation progresses inboard but is confined to the region forward of the juncture shock. By the time  $15.8^\circ$  is reached, the juncture shock has increased sweep but its influence is not felt beyond the  $0.40b/2$  station and regions outboard of this station are completely separated.

At a Mach number of 0.98 (fig. 5(g)), the decelerating-flow shock has passed beyond the wing and is no longer apparent on the pressure distributions. At  $\alpha = 8.4^\circ$  the juncture shock again appears and has somewhat greater sweep but the shock does not have quite as much influence on the pressure distributions as at the lower Mach numbers. No appreciable differences are noticed in the sonic- and low-supersonic-speed pressure distributions (figs. 5(h), (i), and (j)) when compared with those at  $M = 0.98$ . It is interesting to note the general similarity of the wing pressure distributions through the Mach number range with the predominant juncture shock existing from  $M = 0.80$  to the supersonic speeds. This shock front seems to develop its maximum strength when angles of attack of about  $8^\circ$  and above are reached.

In order to summarize the pressure distributions through the transonic-speed range, plan views of the wing with isobars are shown in figure 6. Three representative Mach numbers are illustrated for angles of attack below the wing-body stall angle.

At an angle of attack of about  $4.5^\circ$ , the main disturbance on the wing is confined to the leading edge. At angles of attack of about  $8.4^\circ$  and  $12.5^\circ$ , the strong oblique shock, mentioned in the discussion of the pressure distributions, extends from the leading edge of the wing-body juncture and remains inclined to the wing-body juncture at an angle which changes very little with Mach number.

Some uncertainty may exist as to whether the disturbance designated the juncture shock in this report is a leading-edge shock which has become more steeply inclined with increased angle of attack or whether this is a separate phenomena which develops only when sufficiently high angles of attack are reached. An inspection of the liquid-film photographs of figure 4 shows that a disturbance originates at the wing-leading-edge-fuselage juncture at low angles of attack and sweeps back

as the angle of attack is increased. This phenomenon is evidenced by the movement of the line of demarcation between the chordwise and spanwise boundary-layer flow. Although the shadow of this shock is not visible on the photographs in this region, it can be established from the pictures that at a Mach number of 0.94 the disturbance sweeps back rapidly as the angle of attack changes from  $4^\circ$  to  $6^\circ$ . It should be pointed out that the liquid-film pictures generally indicate the direction of the flow on the surface of the wing inside the boundary layer and that this direction may be different from that of the flow outside the boundary layer. On regions of the wing where the boundary layer has separated, however, some fluid may be affected by the main stream flow.

The movement of the juncture shock may be explained by considering the variation of the pressure field over the wing. An analysis of the pressure data presented in figure 5 of this report and the data for the swept wing reported in references 6 and 8 indicates that, in general, leading-edge suction increases slightly from root to tip over most of the exposed semispan for a given Mach number at low angles of attack. As a result, the flow tends to turn outboard toward the tip in passing over the forward portion of the wing.

With increasing angle of attack, the tip region stalls and separation progresses inboard and causes a loss of leading-edge suction in the vicinity of the tip. At the same time, the suction pressure near the leading edge increases over the inboard portion of the wing and causes a reversal in the spanwise pressure gradient and an inboard turning of the flow. The steeply inclined shock probably results from this inboard movement and produces the necessary outboard turning required to keep the flow essentially parallel to the wing-body juncture.

#### Wing Spanwise Load Distributions

Wing spanwise load distributions including the loading on the body surrounding the wing root sections are presented in figure 8 for several angles of attack at Mach numbers of 0.90 and 1.00. The body pressures that are included in the blanketed portion of the wing plan form have been plotted on a local-chord basis and integrated for section normal-force coefficient at spanwise wing stations equivalent to meridians  $0^\circ$  and  $180^\circ$ ,  $22.5^\circ$  and  $157.5^\circ$ , and  $45^\circ$  and  $135^\circ$ . The wing loading distribution varies considerably from the generally elliptic type expected from subsonic theoretical considerations of the wing alone such as reference 11. At the higher angles of attack, this wing exhibits considerable loss in load over the tip sections. At an angle of attack of about  $8.5^\circ$ , a fairly uniform load is maintained over the inboard portions of the wing and at high angles of attack (fig. 8,  $M = 0.90$ ) the loading distribution is almost triangular. Between the wing-body juncture and the body center line there is a gradual decrease in section load parameter

until an angle of attack of about  $12^\circ$  is reached. Above  $12^\circ$ , the  $22.5^\circ$  meridian station shows some slight loading increase.

The variation of spanwise loading parameter  $\frac{c_n c}{c}$  with wing normal-force coefficient is presented in figure 9. As the Mach number is increased, the loading increases somewhat on the outboard stations - a characteristic of thin swept wings at transonic speeds (ref. 12). A more inboard location of the peak load and generally trapezoidal shape is in contrast with somewhat thicker swept wings (ref. 13). Between normal-force coefficients of about 0.4 and 0.6, the spanwise distributions of loading indicate the typical swept-wing flow separation over the outboard regions as was indicated in the chordwise pressure distributions of figure 5. The effect of this tip separation is indicated by the curves of figure 10 for the variation of angle of attack with normal force, where the initial inflection in normal-force-curve slope generally occurs near a normal-force coefficient of about 0.5.

#### Chordwise Center-of-Pressure Characteristics

The distribution of the section center of pressure along the semi-span is presented in figure 11 for constant values of wing normal-force coefficient. At low normal-force coefficients, the outboard wing sections have the most forward center-of-pressure positions. As separation begins to develop over the outboard region of the wing at the higher values of normal-force coefficient, the centers of pressure move rearward, and this rearward shift progresses inboard on the wing.

The variation with Mach number of the chordwise center-of-pressure location on the mean aerodynamic chord is shown in figure 12. The center-of-pressure location varies from about ~~43~~ 48 percent of the mean aerodynamic chord at a Mach number of 0.80 to about ~~43~~ 53 percent of the mean aerodynamic chord at the highest test Mach number of 1.05 for all normal-force coefficients.

#### Wing Bending-Moment Characteristics

The data of figure 13 show there is only a small change in the values of the bending-moment coefficient of the wing about the body center-line for the test Mach number range. A slight increase occurs at a normal-force coefficient of 0.6 in the Mach number region of 0.96, but the change in this coefficient in the transonic range is much smaller than that for the thicker swept wings. This difference is due to the similarity of the spanwise loading at all Mach numbers for the wing of this investigation.



### Lateral Location of Center of Pressure

Since the bending-moment coefficient remains fairly constant through the Mach number range for a given normal-force coefficient, only small shifts in the lateral center-of-pressure position would be expected. In figure 14 the wing spanwise center-of-pressure characteristics are presented. A maximum lateral shift of about 4 percent of the semispan occurred for the test Mach number range at the highest normal-force coefficient ( $C_N = 0.6$ ). The outboard shift in center of pressure in the transonic range has been found to be much less for highly tapered wings than for wings of medium taper (ref. 1). The most outboard positions of the lateral center of pressure are noted for the supersonic Mach numbers as a result of the gradual outboard shift of the region of higher load with Mach number as seen on spanwise loading distributions of figure 9. At higher normal-force coefficients, the center of load should remain near the inner third of the exposed semispan since the spanwise loading shape is almost triangular at high angles of attack. (See fig. 8.) A comparison of the experimental and theoretical (ref. 11) lateral center-of-pressure positions indicates that the theoretical positions are about 8 percent of the semispan further outboard owing to the assumption of nearly elliptical spanwise loading.

### Pitching-Moment Characteristics of Wing

The variation of wing pitching-moment coefficient about 0.25c' with wing normal-force coefficient is presented in figure 15. Results of the investigation of the wing-body characteristics of the present model reported in reference 3 showed that this configuration has pitch-up tendencies between Mach numbers of 0.90 and 0.96. The wing characteristics of figure 15 show corresponding pitch-ups at Mach numbers of 0.90 and 0.94 indicating that the pitch-up of the wing-body combination of reference 3 is due primarily to separation at the wing tips. The flow phenomena occurring at transonic speeds (separation over the outboard wing sections reinforced by shock interaction) that cause the unstable moment breaks of swept wings have been discussed in reference 6. It is believed that the pitch-up tendencies of the present thin wing are milder than those of the 6-percent-thick wing of reference 6 because on the present 4-percent-thick wing the shocks are weaker and probably cause less separation. Also, because of the greater taper ratio, less wing area is affected when separation starts at the tips.

### CONCLUDING REMARKS

A wind-tunnel investigation was made at transonic speeds of the loading on a  $45^\circ$  sweptback wing having an aspect ratio of 3, a taper

ratio of 0.2, and NACA 65A004 airfoil sections. The results of this investigation have led to the following observations:

1. Comparisons of the pressure distributions over the present wing with those of thicker swept wings at transonic speeds showed generally similar loading shapes and characteristic inboard progression of tip separation with increasing angle of attack. The effect of the wing trailing-edge shock and the main decelerating-flow shock on the loading was less pronounced for this wing with thin sections.
2. The disturbance exerting the greatest influence on the flow over the upper surface of the wing was a shock emanating from the wing-leading-edge-body juncture. This shock moved back from the leading edge with increasing angle of attack and passed off the wing trailing edge at about the midsemispan position at angles of attack above  $8^\circ$  at all Mach numbers.
3. The spanwise loading on the wing was characterized by a slight outboard shift in center of load with an increase in Mach number and a small inboard shift in lateral center of pressure with increasing normal force.
4. The chordwise center of pressure shifted from about ~~36~~<sup>43</sup> percent of the mean aerodynamic chord at a Mach number of 0.80 to about ~~40~~<sup>53</sup> percent of the mean aerodynamic chord at a Mach number of 1.05.
5. The coincidence of the wing pitching-moment breaks with those of the wing-body combination indicate that the configuration pitch-up is primarily due to separation at the wing tips.

Langley Aeronautical Laboratory,  
National Advisory Committee for Aeronautics,  
Langley Field, Va., May 21, 1956.

## REFERENCES

1. Davis, Don D., Jr., and Hieser, Gerald: Loads on Thin Wings at Transonic Speeds. NACA RM L55E11c, 1955.
2. Hieser, Gerald, Henderson, James H., and Swihart, John M.: Transonic Aerodynamic and Loads Characteristics of a 4-Percent-Thick Unswept-Wing—Fuselage Combination. NACA RM L54B24, 1954.
3. Critzos, Chris C.: A Transonic Investigation of the Static Longitudinal-Stability Characteristics of a  $45^\circ$  Sweptback Wing-Fuselage Combination With and Without Horizontal Tail. NACA RM L56A18, 1956.
4. Runckel, Jack F., and Gray, W. H.: An Investigation of Loads on Ailerons at Transonic Speeds. NACA RM L55E13, 1955.
5. Hallissy, Joseph M., and Bowman, Donald R.: Transonic Characteristics of a  $45^\circ$  Sweptback Wing-Fuselage Combination. Effect of Longitudinal Wing Position and Division of Wing and Fuselage Forces and Moments. NACA RM L52K04, 1953.
6. West, F. E., Jr., and Henderson, James H.: Relationship of Flow Over a  $45^\circ$  Sweptback Wing With and Without Leading-Edge Chord-Extensions to Longitudinal Stability Characteristics at Mach Numbers From 0.60 to 1.03. NACA RM L53H18b, 1953.
7. Whitcomb, Richard T., and Kelly, Thomas C.: A Study of the Flow Over a  $45^\circ$  Sweptback Wing-Fuselage Combination at Transonic Mach Numbers. NACA RM L52D01, 1952.
8. Solomon, William, and Schmeer, James W.: Effect of Longitudinal Wing Position on the Pressure Characteristics at Transonic Speeds of a  $45^\circ$  Sweptback Wing-Fuselage Model. NACA RM L52K05a, 1953.
9. Loving, Donald L., and Estabrooks, Bruce B.: Transonic-Wing Investigation in the Langley 8-Foot High-Speed Tunnel at High Subsonic Mach Numbers and at a Mach Number of 1.2. Analysis of Pressure Distribution of Wing-Fuselage Configuration Having a Wing of  $45^\circ$  Sweepback, Aspect Ratio 4, Taper Ratio 0.6, and NACA 65A006 Airfoil Section. NACA RM L51F07, 1951.
10. Runckel, Jack F., and Schmeer, James W.: The Aerodynamic Characteristics at Transonic Speeds of a Model With a  $45^\circ$  Sweptback Wing, Including the Effect of Leading-Edge Slats and a Low Horizontal Tail. NACA RM L53J08, 1954.

11. DeYoung, John, and Harper, Charles W.: Theoretical Symmetric Span Loading at Subsonic Speeds for Wings Having Arbitrary Plan Form. NACA Rep. 921, 1948.
12. Williams, Claude V., and Kuhn, Richard E.: A Study of Aerodynamic Loads on Sweptback Wings at Transonic Speeds. NACA RM L53E08b, 1953.
13. Loving, Donald L., and Williams, Claude V.: Aerodynamic Loading Characteristics of a Wing-Fuselage Combination Having a Wing of  $45^\circ$  Sweepback Measured in the Langley 8-Foot Transonic Tunnel. NACA RM L52B27, 1952.





TABLE I - Continued  
PRESSURE COEFFICIENTS AT SIX SPANWISE STATIONS

(a) M = 0.80 - Continued

Table with columns for x/c and stations (.16, .25, .40, .60, .75, .95) for Upper and Lower surfaces at alpha = 6.4 degrees.

Table with columns for x/c and stations (.16, .25, .40, .60, .75, .95) for Upper and Lower surfaces at alpha = 8.4 degrees.

Table with columns for x/c and stations (.16, .25, .40, .60, .75, .95) for Upper and Lower surfaces at alpha = 10.5 degrees.

Table with columns for x/c and stations (.16, .25, .40, .60, .75, .95) for Upper and Lower surfaces at alpha = 12.5 degrees.



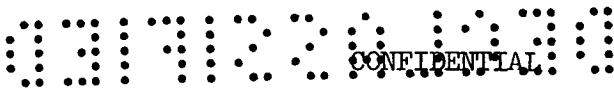


TABLE L - Continued  
PRESSURE COEFFICIENTS AT SIX SPANWISE STATIONS

(a) M = 0.80 - Concluded

x/c	Upper surface						Lower surface					
	Station, fraction of semispan						Station, fraction of semispan					
	.16	.25	.40	.60	.75	.95	.16	.25	.40	.60	.75	.95
$\alpha = 19.7$												
-.0500												
.0000	-.241	-.928	-.896	-.766	-.745	-.555	-.082					
.0125	-.997	-.928	-.869	-.758	-.682	-.549	.467	.597	.438	.349	.296	.173
.0250	-.951	-.928	-.860	-.760	-.672	-.545	.748	.663	.535	.442	.393	.279
.0500	-.934	-.923	-.862	-.753	-.664	-.542	.870	.637	.556	.474	.422	.316
.0750	-.920	-.921	-.846	-.751	-.663	-.542	.785	.633	.553	.464	.418	.311
.1000	-.912	-.918	-.858	-.745	-.652	-.539	.739	.597	.523	.452	.404	.291
.1500	-.907	-.913	-.853	-.742	-.658	-.537	.631	.546	.478	.414	.373	.251
.2000	-.895	-.902	-.848	-.738	-.649	-.532	.561	.501	.440	.385	.343	.199
.2500	-.833	-.893	-.839	-.738	-.645	-.532	.509	.457	.397	.335	.300	.148
.3000	-.781	-.880	-.835	-.730	-.644	-.533	.472	.417	.358	.302	.269	.097
.3500	-.723	-.868	-.829	-.724	-.637	-.530	.459	.377	.323	.266	.234	.047
.4000	-.679	-.843	-.822	-.694	-.633	-.530	.399	.349	.302	.247	.206	.001
.4500	-.675	-.813	-.812	-.710	-.628	-.533	.370	.315	.267	.208	.173	-.038
.5000	-.659	-.795	-.804	-.704	-.619	-.533	.319	.281	.232	.178	.131	-.081
.5500	-.647	-.764	-.789	-.696	-.614	-.533	.287	.255	.206	.146	.099	-.104
.6000	-.633	-.744	-.779	-.687	-.610	-.530	.257	.221	.169	.105	.062	-.140
.6500	-.598	-.723	-.769	-.677	-.610	-.529	.235	.185	.160	.075	.027	-.183
.7000	-.596	-.698	-.751	-.667	-.601	-.527	.188	.157	.107	.033	-.001	-.185
.7500	-.570	-.677	-.736	-.661	-.593	-.523	.172	.135	.068	.007	-.039	-.216
.8000	-.612	-.648	-.722	-.646	-.584	-.518	.138	.107	.048	-.031	-.082	-.235
.8500	-.546	-.618	-.707	-.645	-.580	-.516	.106	.070	-.003	-.084	-.120	-.262
.9000	-.513	-.577	-.688	-.635	-.581	-.507	.068	.019	-.065	-.139	-.176	-.292
.9500	-.459	-.518	-.672	-.630	-.578	-.500	.020	-.061	-.158	-.227	-.231	-.363
1.0000							-.224					
1.0500							-.420					

$\alpha = 21.8$

x/c	Upper surface						Lower surface					
	Station, fraction of semispan						Station, fraction of semispan					
	.16	.25	.40	.60	.75	.95	.16	.25	.40	.60	.75	.95
$\alpha = 21.8$												
-.0500												
.0000	-.341	-.816	-.822	-.747	-.805	-.591	-.097					
.0125	-.890	-.821	-.796	-.740	-.707	-.586	.448	.462	.429	.329	.263	.128
.0250	-.854	-.819	-.789	-.742	-.700	-.579	.762	.684	.541	.440	.381	.257
.0500	-.839	-.818	-.794	-.739	-.691	-.579	.923	.691	.578	.489	.424	.310
.0750	-.833	-.818	-.784	-.738	-.689	-.579	.824	.674	.564	.488	.430	.312
.1000	-.825	-.816	-.784	-.733	-.684	-.578	.781	.644	.555	.480	.420	.295
.1500	-.819	-.823	-.792	-.733	-.684	-.572	.671	.596	.514	.445	.394	.262
.2000	-.805	-.821	-.791	-.731	-.682	-.570	.602	.548	.477	.418	.366	.211
.2500	-.797	-.817	-.789	-.730	-.679	-.570	.559	.505	.441	.370	.324	.164
.3000	-.788	-.789	-.789	-.728	-.674	-.569	.514	.465	.403	.337	.294	.131
.3500	-.769	-.810	-.785	-.723	-.671	-.570	.499	.424	.368	.304	.260	.063
.4000	-.740	-.800	-.783	-.701	-.670	-.567	.441	.393	.342	.282	.230	.015
.4500	-.720	-.780	-.780	-.717	-.684	-.570	.410	.361	.309	.246	.195	-.024
.5000	-.701	-.777	-.777	-.714	-.681	-.569	.356	.325	.274	.214	.156	-.070
.5500	-.693	-.761	-.772	-.708	-.655	-.568	.324	.293	.244	.182	.123	-.094
.6000	-.683	-.756	-.769	-.703	-.652	-.568	.291	.256	.204	.138	.083	-.136
.6500	-.671	-.751	-.762	-.697	-.651	-.565	.268	.220	.190	.105	.048	-.179
.7000	-.676	-.742	-.755	-.688	-.643	-.564	.220	.188	.139	.060	.017	-.186
.7500	-.665	-.736	-.746	-.682	-.639	-.560	.199	.165	.099	.031	-.024	-.220
.8000	-.713	-.724	-.735	-.666	-.634	-.556	.158	.131	.067	-.010	-.067	-.236
.8500	-.654	-.704	-.724	-.646	-.625	-.551	.122	.089	.016	-.065	-.132	-.271
.9000	-.628	-.679	-.710	-.660	-.624	-.546	.077	.029	-.053	-.117	-.172	-.324
.9500	-.581	-.638	-.698	-.655	-.620	-.535	.019	-.063	-.151	-.213	-.230	-.386
1.0000							-.324					
1.0500							-.336					

$\alpha = 23.9$

x/c	Upper surface						Lower surface					
	Station, fraction of semispan						Station, fraction of semispan					
	.16	.25	.40	.60	.75	.95	.16	.25	.40	.60	.75	.95
$\alpha = 23.9$												
-.0500												
.0000	-.464	-.763	-.777	-.743	-.811	-.599	-.145					
.0125	-.827	-.766	-.763	-.738	-.708	-.594	.403	.593	.405	.298	.226	.088
.0250	-.799	-.766	-.760	-.740	-.701	-.589	.765	.697	.541	.423	.361	.236
.0500	-.785	-.768	-.766	-.738	-.692	-.589	.948	.720	.602	.492	.419	.299
.0750	-.777	-.770	-.751	-.738	-.691	-.588	.849	.706	.585	.500	.428	.310
.1000	-.770	-.770	-.766	-.733	-.682	-.588	.808	.678	.581	.495	.425	.298
.1500	-.760	-.777	-.768	-.735	-.687	-.585	.701	.631	.546	.464	.406	.289
.2000	-.754	-.781	-.768	-.732	-.682	-.582	.638	.587	.512	.441	.381	.225
.2500	-.753	-.784	-.768	-.736	-.680	-.582	.595	.542	.474	.395	.342	.180
.3000	-.753	-.787	-.768	-.734	-.680	-.581	.551	.507	.431	.363	.312	.131
.3500	-.749	-.786	-.768	-.731	-.677	-.581	.537	.462	.399	.329	.278	.080
.4000	-.738	-.786	-.769	-.709	-.675	-.580	.478	.430	.374	.305	.251	.032
.4500	-.736	-.774	-.769	-.725	-.673	-.582	.445	.397	.337	.267	.216	-.010
.5000	-.736	-.781	-.770	-.723	-.669	-.581	.391	.357	.302	.232	.177	-.052
.5500	-.730	-.773	-.768	-.719	-.665	-.581	.357	.325	.273	.198	.140	-.079
.6000	-.727	-.774	-.767	-.714	-.661	-.581	.320	.283	.231	.155	.098	-.125
.6500	-.727	-.772	-.762	-.710	-.661	-.578	.300	.251	.219	.115	.062	-.167
.7000	-.719	-.768	-.756	-.702	-.655	-.576	.247	.211	.154	.073	.030	-.177
.7500	-.713	-.769	-.748	-.698	-.648	-.574	.223	.186	.108	.039	-.015	-.215
.8000	-.751	-.765	-.746	-.686	-.646	-.570	.182	.151	.081	-.001	-.060	-.224
.8500	-.716	-.755	-.741	-.689	-.636	-.567	.142	.099	.025	-.059	-.102	-.273
.9000	-.704	-.741	-.734	-.685	-.635	-.560	.089	.037	-.053	-.119	-.166	-.317
.9500	-.677	-.720	-.730	-.679	-.628	-.550	.016	-.070	-.156	-.219	-.228	-.370
1.0000							-.414					
1.0500							-.416					

















TABLE I - Continued  
PRESSURE COEFFICIENTS AT SIX SPANWISE STATIONS

(c) M = 0.90 - Continued

Table for alpha = 11.5. Columns include x/c (0.16 to 0.95) for Upper and Lower surfaces. Rows list pressure coefficients for various spanwise stations from -0.0500 to 1.0500.

Table for alpha = 13.6. Columns include x/c (0.16 to 0.95) for Upper and Lower surfaces. Rows list pressure coefficients for various spanwise stations from -0.0500 to 1.0500.

Table for alpha = 15.8. Columns include x/c (0.16 to 0.95) for Upper and Lower surfaces. Rows list pressure coefficients for various spanwise stations from -0.0500 to 1.0500.

Table for alpha = 17.9. Columns include x/c (0.16 to 0.95) for Upper and Lower surfaces. Rows list pressure coefficients for various spanwise stations from -0.0500 to 1.0500.

TABLE L - Continued  
PRESSURE COEFFICIENTS AT SIX SPANWISE STATIONS

(c) M = 0.90 - Concluded

x/c	Upper surface						Lower surface					
	Station, fraction of semispan						Station, fraction of semispan					
	.16	.25	.40	.60	.75	.95	.16	.25	.40	.60	.75	.95
a = 20.0												
-.0500												
.0000												
.0125												
.0250												
.0500												
.0750												
.1000												
.1500												
.2000												
.2500												
.3000												
.3500												
.4000												
.4500												
.5000												
.5500												
.6000												
.6500												
.7000												
.7500												
.8000												
.8500												
.9000												
.9500												
1.0000												
1.0500												

a = 22.0												
-.0500												
.0000												
.0125												
.0250												
.0500												
.0750												
.1000												
.1500												
.2000												
.2500												
.3000												
.3500												
.4000												
.4500												
.5000												
.5500												
.6000												
.6500												
.7000												
.7500												
.8000												
.8500												
.9000												
.9500												
1.0000												
1.0500												

a = 24.1												
-.0500												
.0000												
.0125												
.0250												
.0500												
.0750												
.1000												
.1500												
.2000												
.2500												
.3000												
.3500												
.4000												
.4500												
.5000												
.5500												
.6000												
.6500												
.7000												
.7500												
.8000												
.8500												
.9000												
.9500												
1.0000												
1.0500												

a = 26.2												
-.0500												
.0000												
.0125												
.0250												
.0500												
.0750												
.1000												
.1500												
.2000												
.2500												
.3000												
.3500												
.4000												
.4500												
.5000												
.5500												
.6000												
.6500												
.7000												
.7500												
.8000												
.8500												
.9000												
.9500												
1.0000												
1.0500												









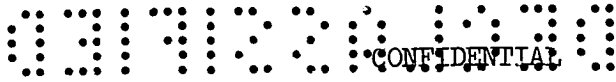


TABLE L - Continued  
PRESSURE COEFFICIENTS AT SIX SPANWISE STATIONS

(d) M = 0.92 - Concluded

x/c	Upper surface						Lower surface					
	Station, fraction of semispan						Station, fraction of semispan					
	.16	.25	.40	.60	.75	.95	.16	.25	.40	.60	.75	.95
α = 20.0												
-0.0500	-0.130	-1.294	-1.042	-0.842	-0.775	-0.642						
.0000							.536	.664	.499	.401	.328	.180
.0125	-1.039	-1.237	-1.025	-0.835	-0.763	-0.636	.807	.725	.587	.488	.424	.298
.0250	-1.111	-1.237	-1.014	-0.831	-0.752	-0.631	.926	.713	.604	.519	.452	.343
.0500	-1.147	-1.222	-1.016	-0.828	-0.745	-0.629	.841	.687	.583	.510	.453	.343
.0750	-1.116	-1.206	-0.992	-0.825	-0.739	-0.628	.791	.652	.570	.499	.439	.328
.1000	-1.049	-1.198	-1.005	-0.825	-0.736	-0.628	.679	.600	.530	.463	.412	.297
.1500	-0.922	-1.178	-0.981	-0.812	-0.729	-0.628	.614	.555	.488	.438	.385	.252
.2000	-0.839	-1.149	-0.972	-0.806	-0.727	-0.620	.570	.512	.451	.391	.346	.204
.2500	-0.726	-1.116	-0.975	-0.793	-0.722	-0.624	.527	.475	.413	.361	.316	.156
.3000	-0.676	-1.063	-0.939	-0.783	-0.715	-0.622	.508	.433	.382	.327	.284	.103
.3500	-0.661	-1.013	-0.953	-0.777	-0.709	-0.623	.455	.404	.359	.309	.260	.050
.4000	-0.614	-0.949	-0.930	-0.748	-0.703	-0.620	.424	.374	.327	.272	.230	.007
.4500	-0.626	-0.882	-0.914	-0.763	-0.700	-0.622	.374	.339	.295	.243	.192	.037
.5000	-0.640	-0.846	-0.908	-0.758	-0.698	-0.621	.342	.316	.270	.216	.164	-0.067
.5500	-0.627	-0.791	-0.876	-0.753	-0.692	-0.619	.311	.277	.235	.184	.125	-0.107
.6000	-0.627	-0.761	-0.855	-0.747	-0.687	-0.619	.299	.246	.195	.155	.099	.151
.6500	-0.620	-0.730	-0.836	-0.742	-0.681	-0.619	.244	.220	.180	.116	.077	-0.158
.7000	-0.614	-0.715	-0.820	-0.738	-0.677	-0.616	.230	.199	.149	.097	.044	-0.195
.7500	-0.620	-0.677	-0.799	-0.727	-0.675	-0.615	.199	.177	.130	.065	.007	-0.241
.8000	-0.655	-0.650	-0.778	-0.719	-0.667	-0.614	.172	.152	.107	.028	.024	-0.272
.8500	-0.586	-0.623	-0.759	-0.711	-0.653	-0.611	.152	.132	.085	-0.008	-0.071	-0.306
.9000	-0.551	-0.583	-0.741	-0.702	-0.646	-0.608	.108	.048	-0.008	-0.071	-0.206	-0.342
.9500	-0.479	-0.477	-0.718	-0.698	-0.655	-0.601	.096	.039	-0.022	-0.079	-0.115	-0.342
1.0000							-0.139					
1.0500							-0.295					
α = 22.1												
-0.0500	-0.217	-0.910	-0.879	-0.811	-0.841	-0.678						
.0000							.518	.671	.492	.381	.296	.145
.0125	-0.941	-0.897	-0.865	-0.808	-0.808	-0.672	.823	.744	.594	.462	.340	.283
.0250	-0.904	-0.897	-0.860	-0.803	-0.793	-0.666	.981	.746	.623	.529	.454	.341
.0500	-0.893	-0.891	-0.845	-0.805	-0.776	-0.662	.882	.723	.614	.528	.462	.349
.0750	-0.891	-0.891	-0.854	-0.802	-0.766	-0.663	.834	.693	.602	.518	.456	.340
.1000	-0.892	-0.891	-0.870	-0.805	-0.766	-0.661	.723	.647	.563	.490	.431	.313
.1500	-0.881	-0.891	-0.860	-0.797	-0.760	-0.658	.657	.601	.526	.464	.405	.272
.2000	-0.869	-0.891	-0.859	-0.800	-0.757	-0.655	.615	.559	.488	.419	.366	.227
.2500	-0.820	-0.887	-0.861	-0.787	-0.753	-0.650	.572	.519	.450	.390	.338	.183
.3000	-0.782	-0.882	-0.853	-0.785	-0.747	-0.648	.552	.479	.415	.357	.308	.129
.3500	-0.745	-0.873	-0.851	-0.782	-0.747	-0.651	.500	.449	.395	.337	.283	.081
.4000	-0.709	-0.862	-0.848	-0.757	-0.743	-0.647	.467	.416	.359	.303	.255	.033
.4500	-0.711	-0.839	-0.844	-0.772	-0.740	-0.650	.412	.380	.327	.273	.219	-0.10
.5000	-0.709	-0.837	-0.839	-0.770	-0.740	-0.646	.384	.353	.301	.242	.186	-0.041
.5500	-0.703	-0.815	-0.832	-0.767	-0.734	-0.646	.351	.314	.266	.206	.151	-0.081
.6000	-0.704	-0.802	-0.818	-0.751	-0.713	-0.646	.335	.282	.222	.176	.123	-0.128
.6500	-0.696	-0.798	-0.816	-0.755	-0.725	-0.646	.277	.223	.206	.138	.097	-0.140
.7000	-0.694	-0.788	-0.815	-0.755	-0.719	-0.643	.232	.207	.147	.081	.026	-0.177
.7500	-0.691	-0.769	-0.810	-0.743	-0.714	-0.640	.198	.170	.111	.042	.009	-0.256
.8000	-0.684	-0.739	-0.789	-0.736	-0.699	-0.637	.157	.125	.054	.005	.005	-0.296
.8500	-0.684	-0.739	-0.789	-0.736	-0.699	-0.637	.111	.046	-0.017	-0.070	-0.103	-0.325
.9000	-0.664	-0.718	-0.780	-0.732	-0.707	-0.631						
.9500	-0.625	-0.662	-0.767	-0.727	-0.704	-0.623						
1.0000							-0.177					
1.0500							-0.447					
α = 24.2												
-0.0500	-0.299	-0.797	-0.798	-0.774	-0.845	-0.692						
.0000							.488	.676	.490	.367	.280	.114
.0125	-0.860	-0.795	-0.788	-0.773	-0.790	-0.686	.831	.770	.615	.485	.410	.268
.0250	-0.822	-0.795	-0.783	-0.772	-0.776	-0.680	1.012	.787	.657	.546	.467	.342
.0500	-0.822	-0.794	-0.789	-0.772	-0.768	-0.677	.908	.768	.651	.551	.482	.336
.0750	-0.823	-0.794	-0.778	-0.762	-0.762	-0.677	.861	.746	.647	.548	.478	.350
.1000	-0.818	-0.794	-0.794	-0.774	-0.757	-0.674	.763	.698	.612	.521	.463	.332
.1500	-0.795	-0.802	-0.791	-0.771	-0.756	-0.671	.700	.657	.578	.501	.441	.296
.2000	-0.774	-0.807	-0.793	-0.771	-0.756	-0.668	.661	.612	.543	.459	.406	.284
.2500	-0.769	-0.816	-0.789	-0.766	-0.754	-0.664	.617	.573	.504	.433	.379	.209
.3000	-0.764	-0.811	-0.793	-0.768	-0.752	-0.661	.598	.551	.473	.399	.346	.180
.3500	-0.742	-0.809	-0.792	-0.766	-0.749	-0.664	.549	.504	.451	.377	.321	.111
.4000	-0.736	-0.804	-0.791	-0.748	-0.748	-0.659	.514	.468	.415	.343	.293	.089
.4500	-0.736	-0.787	-0.789	-0.764	-0.747	-0.661	.462	.434	.382	.314	.257	.022
.5000	-0.726	-0.794	-0.789	-0.763	-0.746	-0.660	.427	.404	.356	.282	.226	-0.10
.5500	-0.726	-0.783	-0.788	-0.762	-0.746	-0.661	.398	.365	.318	.246	.188	-0.053
.6000	-0.727	-0.783	-0.785	-0.758	-0.743	-0.659	.381	.328	.277	.216	.158	-0.099
.6500	-0.727	-0.783	-0.784	-0.758	-0.743	-0.659	.321	.300	.252	.175	.135	-0.115
.7000	-0.732	-0.781	-0.784	-0.755	-0.731	-0.657	.307	.276	.219	.151	.096	-0.151
.7500	-0.730	-0.777	-0.784	-0.749	-0.732	-0.652	.268	.247	.192	.115	.057	-0.183
.8000	-0.727	-0.777	-0.779	-0.747	-0.726	-0.652	.236	.208	.150	.071	.020	-0.240
.8500	-0.736	-0.766	-0.775	-0.746	-0.711	-0.649	.191	.161	.090	.030	-0.031	-0.279
.9000	-0.724	-0.763	-0.771	-0.744	-0.718	-0.639	.143	.076	.017	-0.051	-0.080	-0.325
.9500	-0.700	-0.734	-0.765	-0.744	-0.717	-0.631						
1.0000							-0.186					
1.0500							-0.525					
α = 26.3												
-0.0500	-0.387	-0.767	-0.784	-0.796	-0.871	-0.719						
.0000							.435	.673	.475	.340	.247	.071
.0125	-0.827	-0.767	-0.779	-0.795	-0.813	-0.713	.821	.787	.618	.470	.392	.241
.0250	-0.806	-0.761	-0.776	-0.796	-0.806	-0.711	1.019	.817	.677	.553	.463	.325
.0500	-0.801	-0.767	-0.783	-0.797	-0.792	-0.709	.928	.809	.680	.565	.487	.347
.0750	-0.796	-0.771	-0.774	-0.796	-0.792	-0.707	.891	.785	.676	.565	.489	.349
.1000	-0.796	-0.776	-0.789	-0.799	-0.790	-0.707	.793	.705	.649	.547	.480	.333
.1500	-0.774	-0.787	-0.789	-0.795	-0.786	-0.704	.739	.702	.616	.524	.480	.304
.2000	-0.752	-0.796	-0.794	-0.800	-0.784	-0.702	.703	.662	.563	.487	.428	.266
.2500	-0.746	-0.800	-0.801	-0.795	-0.784	-0.699	.660	.622	.547	.463	.403	.225
.3000	-0.742	-0.800	-0.800	-0.797	-0.782	-0.695	.641	.583	.513	.431	.372	.177
.3500	-0.733	-0.803	-0.800	-0.797	-0.777	-0.695	.593	.552	.489	.408	.349	.129
.4000	-0.733	-0.803	-0.802	-0.777	-0.773	-0.695	.556	.514	.456	.371	.321	.086
.4500	-0.747	-0.801	-0.802	-0.777	-0.773	-0.695	.505	.481	.422	.341	.282	.037
.5000	-0.744	-0.803	-0.802	-0.795	-0.773	-0.690	.475	.448	.392	.313	.251	.000
.5500	-0.756	-0.800	-0.802	-0.795	-0.771	-0.690	.442	.408	.354	.272	.213	-0.034
.6000	-0.760	-0.806	-0.800	-0.790	-0.771	-0.690	.426	.375	.310	.239	.181	-0.087
.6500	-0.764	-0.808	-0.800	-0.791	-0.765	-0.690	.364	.342	.288	.197	.157	-0.101
.7000	-0.771	-0.811	-0.									

TABLE I - Continued
PRESSURE COEFFICIENTS AT SIX SPANWISE STATIONS

(c) M = 0.94

Table with three main sections for alpha = 0.4, alpha = 1.4, and alpha = 2.4. Each section contains data for x/c from -0.5000 to 1.0500 and stations .16, .25, .40, .60, .75, .95. The data is organized into two columns: Upper surface and Lower surface.



TABLE I - Continued  
PRESSURE COEFFICIENTS AT SIX SPANWISE STATIONS

(e) M = 0.94 - Continued

Table with columns for x/c, Station, fraction of semispan (0.16, 0.25, 0.40, 0.60, 0.75, 0.95) for Upper surface and Lower surface. Includes data for alpha = 6.4 degrees.

Table with columns for x/c, Station, fraction of semispan (0.16, 0.25, 0.40, 0.60, 0.75, 0.95) for Upper surface and Lower surface. Includes data for alpha = 8.3 degrees.

Table with columns for x/c, Station, fraction of semispan (0.16, 0.25, 0.40, 0.60, 0.75, 0.95) for Upper surface and Lower surface. Includes data for alpha = 10.4 degrees.

Table with columns for x/c, Station, fraction of semispan (0.16, 0.25, 0.40, 0.60, 0.75, 0.95) for Upper surface and Lower surface. Includes data for alpha = 12.5 degrees.

TABLE I. - Continued  
PRESSURE COEFFICIENTS AT SIX SPANWISE STATIONS

(e) M = 0.94 - Continued

Table with columns for z/c, Upper surface (Station, fraction of semispan: .16, .25, .40, .60, .75, .95), Lower surface (Station, fraction of semispan: .16, .25, .40, .60, .75, .95), and alpha = 11.6. Rows include values for -0.0500 to 1.0500.

Table with columns for z/c, Upper surface (Station, fraction of semispan: .16, .25, .40, .60, .75, .95), Lower surface (Station, fraction of semispan: .16, .25, .40, .60, .75, .95), and alpha = 13.7. Rows include values for -0.0500 to 1.0500.

Table with columns for z/c, Upper surface (Station, fraction of semispan: .16, .25, .40, .60, .75, .95), Lower surface (Station, fraction of semispan: .16, .25, .40, .60, .75, .95), and alpha = 15.8. Rows include values for -0.0500 to 1.0500.

Table with columns for z/c, Upper surface (Station, fraction of semispan: .16, .25, .40, .60, .75, .95), Lower surface (Station, fraction of semispan: .16, .25, .40, .60, .75, .95), and alpha = 18.0. Rows include values for -0.0500 to 1.0500.

TABLE L - Continued  
 PRESSURE COEFFICIENTS AT SIX SPANWISE STATIONS

(e)  $M = 0.94$  - Concluded

x/c	Upper surface						Lower surface					
	Station, fraction of semispan						Station, fraction of semispan					
	.16	.25	.40	.60	.75	.95	.16	.25	.40	.60	.75	.95
$\alpha = 20.1$												
-.0500												
.0000	-1.104	-1.321	-1.184	-.902	-.825	-.704						
.0125	-.982	-1.443	-1.163	-.902	-.847	-.698	.554	.680	.510	.411	.332	.184
.0250	-1.056	-1.439	-1.151	-.902	-.842	-.692	.822	.737	.596	.496	.429	.305
.0500	-1.105	-1.422	-1.162	-.907	-.831	-.692	.940	.726	.611	.524	.462	.350
.0750	-1.077	-1.416	-1.138	-.908	-.824	-.688	.889	.699	.591	.518	.462	.356
.1000	-1.019	-1.378	-1.168	-.913	-.820	-.688	.809	.667	.577	.505	.448	.342
.1500	-.884	-1.384	-1.159	-.907	-.817	-.685	.694	.618	.536	.471	.421	.310
.2000	-.764	-1.347	-1.145	-.909	-.813	-.683	.628	.568	.498	.443	.395	.268
.2500	-.669	-1.241	-1.136	-.895	-.805	-.680	.584	.525	.460	.398	.356	.222
.3000	-.639	-1.059	-1.108	-.889	-.800	-.677	.543	.488	.421	.370	.327	.275
.3500	-.630	-.924	-1.089	-.887	-.791	-.677	.526	.446	.387	.335	.296	.216
.4000	-.630	-.829	-1.055	-.848	-.785	-.674	.472	.420	.366	.314	.273	.270
.4500	-.639	-.775	-1.033	-.871	-.781	-.672	.443	.388	.335	.280	.246	.225
.5000	-.609	-.762	-1.008	-.865	-.776	-.672	.390	.354	.302	.252	.206	-.023
.5500	-.614	-.735	-.981	-.861	-.768	-.669	.360	.330	.278	.224	.182	-.050
.6000	-.623	-.723	-.955	-.853	-.766	-.667	.327	.291	.244	.192	.144	-.090
.6500	-.624	-.705	-.931	-.847	-.758	-.666	.315	.263	.219	.164	.117	-.136
.7000	-.615	-.705	-.914	-.842	-.745	-.663	.261	.237	.190	.126	.096	-.144
.7500	-.623	-.707	-.891	-.826	-.746	-.661	.251	.222	.160	.110	.065	-.176
.8000	-.649	-.687	-.861	-.814	-.727	-.659	.221	.198	.143	.079	.030	-.210
.8500	-.632	-.662	-.825	-.805	-.714	-.656	.197	.170	.108	.041	-.001	-.254
.9000	-.602	-.626	-.788	-.791	-.719	-.652	.160	.132	.059	.009	-.048	-.287
.9500	-.524	-.504	-.752	-.788	-.719	-.643	.121	.065	-.004	-.058	-.087	-.322
1.0000							-.128					
1.0500							-.244					
$\alpha = 22.2$												
-.0500												
.0000	-1.190	-1.107	-1.031	-.895	-.864	-.708						
.0125	-1.070	-1.079	-1.020	-.897	-.856	-.704	.540	.689	.510	.396	.313	.156
.0250	-1.060	-1.078	-1.010	-.894	-.842	-.701	.840	.765	.616	.500	.428	.294
.0500	-1.060	-1.076	-1.014	-.894	-.828	-.698	.998	.768	.647	.546	.474	.356
.0750	-1.060	-1.076	-.994	-.890	-.820	-.695	.901	.749	.624	.546	.483	.367
.1000	-.939	-1.074	-.983	-.890	-.814	-.693	.821	.653	.578	.497	.444	.348
.1500	-.995	-1.066	-.995	-.882	-.812	-.690	.744	.672	.586	.509	.453	.335
.2000	-.913	-1.056	-.990	-.877	-.805	-.689	.681	.628	.551	.487	.429	.296
.2500	.784	-1.051	-.989	-.866	-.798	-.684	.636	.584	.514	.446	.391	.261
.3000	-.742	-1.036	-.980	-.861	-.792	-.684	.594	.546	.475	.418	.364	.208
.3500	-.736	-1.018	-.977	-.857	-.784	-.685	.577	.505	.443	.381	.335	.159
.4000	-.683	-.985	-.963	-.822	-.778	-.683	.526	.478	.420	.365	.312	.104
.4500	-.701	-.937	-.934	-.840	-.772	-.683	.492	.444	.390	.329	.281	.061
.5000	-.703	-.921	-.943	-.835	-.768	-.682	.439	.411	.359	.302	.247	.014
.5500	-.689	-.875	-.929	-.829	-.761	-.680	.410	.382	.332	.271	.218	-.014
.6000	-.691	-.851	-.913	-.822	-.756	-.680	.375	.344	.298	.241	.181	-.053
.6500	-.691	-.836	-.900	-.817	-.747	-.679	.347	.311	.267	.213	.153	-.103
.7000	-.679	-.806	-.889	-.814	-.742	-.677	.306	.286	.242	.173	.132	-.113
.7500	-.683	-.771	-.877	-.802	-.740	-.675	.295	.266	.206	.152	.099	-.149
.8000	-.737	-.741	-.856	-.794	-.733	-.674	.262	.242	.185	.130	.081	-.181
.8500	-.684	-.676	-.821	-.771	-.727	-.673	.231	.207	.147	.094	.045	-.213
.9000	-.652	-.674	-.821	-.778	-.725	-.669	.187	.165	.094	.045	-.019	-.263
.9500	-.581	-.575	-.801	-.772	-.722	-.664	.153	.091	.032	-.030	-.065	-.306
1.0000							-.131					
1.0500							-.351					
$\alpha = 24.3$												
-.0500												
.0000	-.290	-.946	-.928	-.888	-.889	-.710						
.0125	-.978	-.936	-.922	-.885	-.855	-.710	.502	.683	.495	.369	.312	.152
.0250	-.939	-.936	-.913	-.883	-.832	-.701	.842	.778	.611	.489	.416	.268
.0500	-.939	-.931	-.923	-.883	-.808	-.697	1.025	.796	.664	.549	.497	.381
.0750	-.939	-.931	-.907	-.883	-.795	-.696	.921	.779	.660	.558	.513	.399
.1000	-.939	-.931	-.923	-.885	-.792	-.694	.876	.754	.655	.554	.509	.394
.1500	-.930	-.910	-.922	-.881	-.791	-.694	.775	.699	.619	.532	.495	.376
.2000	-.816	-.935	-.921	-.887	-.785	-.688	.674	.666	.584	.511	.475	.342
.2500	-.970	-.936	-.923	-.875	-.782	-.683	.675	.624	.550	.468	.441	.304
.3000	-.821	-.932	-.919	-.876	-.780	-.680	.634	.582	.514	.443	.416	.283
.3500	-.795	-.930	-.920	-.870	-.778	-.680	.612	.541	.483	.408	.388	.216
.4000	-.755	-.921	-.916	-.844	-.774	-.680	.562	.514	.458	.390	.365	.168
.4500	-.773	-.897	-.915	-.863	-.772	-.680	.528	.484	.426	.357	.338	.122
.5000	-.778	-.902	-.915	-.858	-.769	-.678	.475	.445	.392	.329	.300	.077
.5500	-.770	-.881	-.909	-.853	-.765	-.679	.445	.416	.366	.298	.271	.047
.6000	-.774	-.876	-.904	-.848	-.762	-.678	.412	.376	.329	.262	.236	.004
.6500	-.776	-.868	-.899	-.844	-.757	-.678	.399	.345	.299	.230	.207	-.039
.7000	-.764	-.861	-.894	-.842	-.752	-.674	.338	.316	.267	.191	.184	-.056
.7500	-.772	-.840	-.890	-.833	-.752	-.671	.322	.293	.230	.168	.151	-.090
.8000	-.814	-.833	-.881	-.828	-.745	-.670	.285	.264	.207	.132	.114	-.114
.8500	-.771	-.816	-.871	-.826	-.729	-.668	.252	.226	.165	.091	.076	-.148
.9000	-.764	-.797	-.859	-.821	-.740	-.658	.211	.182	.107	.054	.028	-.199
.9500	-.721	-.718	-.846	-.818	-.738	-.654	.168	.098	.035	-.028	-.019	-.262
1.0000							-.149					
1.0500							-.387					
$\alpha = 26.4$												
-.0500												
.0000	-.377	-.928	-.925	-.909	-.975	-.817						
.0125	-.971	-.920	-.917	-.909	-.927	-.812						
.0250	-.941	-.920	-.914	-.908	-.912	-.807	.634	.797	.624	.477	.396	.246
.0500	-.938	-.913	-.922	-.909	-.898	-.804	1.034	.800	.665	.557	.489	.335
.0750	-.942	-.916	-.913	-.908	-.895	-.804	.939	.820	.687	.577	.493	.342
.1000	-.942	-.922	-.932	-.915	-.894	-.802	.907	.799	.684	.573	.497	.343
.1500	-.921	-.925	-.923	-.906	-.888	-.799	.807	.750	.655	.557	.489	.352
.2000	-.896	-.933	-.925	-.913	-.888	-.796	.752	.715	.622	.536	.469	.321
.2500	-.874	-.932	-.937	-.899	-.888	-.789	.720	.674	.591	.497	.438	.286
.3000	-.843	-.929	-.928	-.901	-.882	-.786	.677	.637	.553	.469	.413	.248
.3500	-.822	-.924	-.919	-.876	-.862	-.790	.652	.604	.522	.441	.386	.201
.4000	-.793	-.922	-.926	-.874	-.877	-.784	.609	.566	.501	.419	.360	.193
.4500	-.811	-.900	-.926	-.895	-.876	-.785	.574	.530	.465	.386	.332	.108
.5000	-.813	-.905	-.926	-.893	-.878	-.783	.520	.494	.432	.356	.299	.040
.5500	-.816	-.893	-.922	-.889	-.872	-.781	.484	.459	.404	.328	.279	.029
.6000	-.818	-.889	-.920	-.886	-.871	-.783	.458	.424	.365	.287	.229	-.016
.6500	-.824	-.888	-.918	-.887	-.862	-.783	.442	.389	.336	.253	.200	-.065
.7000	-.825	-.890	-.922	-.891	-.855	-.782	.379	.350	.301	.213	.174	-.102
.7500	-.834	-.879	-.924	-.877	-.861	-.782	.362	.333	.282	.196	.158	-.122
.8000	-.872	-.877	-.915	-.874	-.853	-.778	.325	.302	.237	.151	.097	-.157
.8500	-.839	-.868	-.907	-.872	-.833	-.773	.287	.265	.190	.109	.059	-.208
.9000	-.828	-.854	-.897	-.871	-.845	-.764	.237	.209	.127	.065	.006	-.202
.9500	-.801	-.792	-.885	-.870	-.845	-.756	.189	.123	.052	-.021	-.049	-.307
1.0000							-.145					
1.0500							-.484					

TABLE L - Continued  
PRESSURE COEFFICIENTS AT SIX SPANWISE STATIONS

(f) M = 0.96

x/c	Upper surface						Lower surface					
	Station, fraction of semispan						Station, fraction of semispan					
	.16	.25	.40	.60	.75	.95	.16	.25	.40	.60	.75	.95
$\alpha = 0.4$												
.0500	.267	.493	.407	.379	.501	.574	.071					
.1000	.267	.493	.407	.379	.501	.574	.149	.032	-.022	-.031	-.085	-.085
.1500	.267	.493	.407	.379	.501	.574	.160	.029	-.030	-.029	-.077	-.094
.2000	.267	.493	.407	.379	.501	.574	.106	.034	-.029	-.077	.102	-.153
.2500	.267	.493	.407	.379	.501	.574	.085	.026	-.037	-.088	-.115	-.163
.3000	.267	.493	.407	.379	.501	.574	.054	.006	-.039	-.101	-.131	-.183
.3500	.267	.493	.407	.379	.501	.574	.016	.012	-.055	-.126	-.155	-.193
.4000	.267	.493	.407	.379	.501	.574	.006	-.024	-.079	-.140	-.165	-.190
.4500	.267	.493	.407	.379	.501	.574	-.005	-.040	-.088	-.160	-.180	-.235
.5000	.267	.493	.407	.379	.501	.574	-.024	-.056	-.111	-.178	-.202	-.290
.5500	.267	.493	.407	.379	.501	.574	-.026	-.088	-.130	-.201	-.219	-.296
.6000	.267	.493	.407	.379	.501	.574	-.062	-.092	-.147	-.189	-.222	-.280
.6500	.267	.493	.407	.379	.501	.574	-.082	-.095	-.172	-.204	-.247	-.227
.7000	.267	.493	.407	.379	.501	.574	-.076	-.139	-.184	-.220	-.271	-.160
.7500	.267	.493	.407	.379	.501	.574	-.187	-.190	-.226	-.241	-.285	.007
.8000	.267	.493	.407	.379	.501	.574	-.145	-.164	-.200	-.241	-.257	-.034
.8500	.267	.493	.407	.379	.501	.574	-.145	-.170	-.189	-.242	-.226	-.041
.9000	.267	.493	.407	.379	.501	.574	-.154	-.193	-.226	-.245	-.178	-.005
.9500	.267	.493	.407	.379	.501	.574	-.187	-.190	-.226	-.241	-.188	-.085
1.0000	.267	.493	.407	.379	.501	.574	-.177	-.173	-.186	-.097	-.027	.028
1.0500	.267	.493	.407	.379	.501	.574	-.163	-.154	-.121	-.017	.014	.051
							-.147	-.118	-.034	.059	.052	.073
							-.087	-.028	.029	.059	.094	.093
							.014					
							.021					

$\alpha = 1.4$												
.0500	.269	.470	.336	.286	.409	.540	.069					
.1000	.269	.470	.336	.286	.409	.540	.193	.129	.106	.110	.091	.075
.1500	.269	.470	.336	.286	.409	.540	.204	.092	.067	.036	.028	.029
.2000	.269	.470	.336	.286	.409	.540	.156	.075	.046	.009	.001	.040
.2500	.269	.470	.336	.286	.409	.540	.131	.058	.028	-.022	-.027	.083
.3000	.269	.470	.336	.286	.409	.540	.099	.041	.008	-.035	-.050	.099
.3500	.269	.470	.336	.286	.409	.540	.054	.028	-.007	-.069	-.081	.115
.4000	.269	.470	.336	.286	.409	.540	.039	.010	-.023	-.071	-.100	.188
.4500	.269	.470	.336	.286	.409	.540	.030	-.010	-.051	-.099	-.126	.228
.5000	.269	.470	.336	.286	.409	.540	.013	-.029	-.077	-.125	-.153	.269
.5500	.269	.470	.336	.286	.409	.540	.001	-.057	-.099	-.149	-.171	.275
.6000	.269	.470	.336	.286	.409	.540	-.030	-.087	-.117	-.151	-.180	.245
.6500	.269	.470	.336	.286	.409	.540	-.050	-.077	-.125	-.177	-.202	.204
.7000	.269	.470	.336	.286	.409	.540	-.052	-.121	-.142	-.194	-.220	.122
.7500	.269	.470	.336	.286	.409	.540	-.088	-.130	-.153	-.204	-.221	.053
.8000	.269	.470	.336	.286	.409	.540	-.132	-.136	-.152	-.214	-.207	.042
.8500	.269	.470	.336	.286	.409	.540	-.115	-.149	-.181	-.208	-.198	.040
.9000	.269	.470	.336	.286	.409	.540	-.135	-.170	-.202	-.206	-.124	.009
.9500	.269	.470	.336	.286	.409	.540	-.161	-.172	-.203	-.175	-.075	.010
1.0000	.269	.470	.336	.286	.409	.540	-.152	-.158	-.168	-.108	-.078	.028
1.0500	.269	.470	.336	.286	.409	.540	-.141	-.142	-.099	-.021	.003	.050
							-.129	-.104	-.026	.024	.044	.077
							-.077	-.028	.024	.051	.093	.096
							.007					
							.011					

$\alpha = 2.4$												
.0500	.265	.381	.159	.057	.435	.046	.059					
.1000	.265	.381	.159	.057	.435	.046	.228	.211	.209	.213	.203	.205
.1500	.265	.381	.159	.057	.435	.046	.194	.157	.150	.132	.124	.070
.2000	.265	.381	.159	.057	.435	.046	.140	.121	.104	.081	.070	.074
.2500	.265	.381	.159	.057	.435	.046	.165	.096	.074	.048	.029	.038
.3000	.265	.381	.159	.057	.435	.046	.131	.083	.057	.022	.001	.030
.3500	.265	.381	.159	.057	.435	.046	.084	.057	.030	-.007	-.031	.025
.4000	.265	.381	.159	.057	.435	.046	.064	.036	-.001	-.029	-.052	.057
.4500	.265	.381	.159	.057	.435	.046	.052	.010	-.024	-.067	-.085	.124
.5000	.265	.381	.159	.057	.435	.046	.030	-.007	-.050	-.091	-.107	.171
.5500	.265	.381	.159	.057	.435	.046	.021	-.038	-.072	-.108	-.125	.234
.6000	.265	.381	.159	.057	.435	.046	-.015	-.049	-.083	-.123	-.137	.4276
.6500	.265	.381	.159	.057	.435	.046	-.031	-.062	-.101	-.149	-.158	.293
.7000	.265	.381	.159	.057	.435	.046	-.040	-.101	-.123	-.159	-.170	.292
.7500	.265	.381	.159	.057	.435	.046	-.081	-.108	-.136	-.171	-.165	.231
.8000	.265	.381	.159	.057	.435	.046	-.096	-.120	-.155	-.176	-.154	.145
.8500	.265	.381	.159	.057	.435	.046	-.099	-.144	-.175	-.172	-.130	.084
.9000	.265	.381	.159	.057	.435	.046	-.132	-.162	-.170	-.142	-.107	.040
.9500	.265	.381	.159	.057	.435	.046	-.148	-.152	-.162	-.121	.091	.002
1.0000	.265	.381	.159	.057	.435	.046	-.137	-.137	-.118	-.087	-.068	.020
1.0500	.265	.381	.159	.057	.435	.046	-.120	-.112	-.075	-.029	-.035	.044
							-.108	-.085	-.025	.010	.012	.063
							-.065	-.036	.016	.032	.073	.081
							-.009					
							-.014					

$\alpha = 4.4$												
.0500	.280	.102	-.220	-.383	.382	-.524	.070					
.1000	.280	.102	-.220	-.383	.382	-.524	.316	.354	.346	.336	.326	.316
.1500	.280	.102	-.220	-.383	.382	-.524	.288	.245	.217	.196	.191	.192
.2000	.280	.102	-.220	-.383	.382	-.524	.257	.211	.177	.153	.147	.151
.2500	.280	.102	-.220	-.383	.382	-.524	.216	.178	.158	.125	.112	.113
.3000	.280	.102	-.220	-.383	.382	-.524	.161	.138	.115	.088	.077	.081
.3500	.280	.102	-.220	-.383	.382	-.524	.139	.110	.079	.058	.044	.022
.4000	.280	.102	-.220	-.383	.382	-.524	.123	.083	.050	.017	.004	.046
.4500	.280	.102	-.220	-.383	.382	-.524	.102	.058	.021	-.009	-.018	.095
.5000	.280	.102	-.220	-.383	.382	-.524	.083	.028	-.028	-.020	-.038	.164
.5500	.280	.102	-.220	-.383	.382	-.524	.037	.013	-.013	-.042	-.054	.222
.6000	.280	.102	-.220	-.383	.382	-.524	.033	-.005	-.036	-.068	-.073	.252
.6500	.280	.102	-.220	-.383	.382	-.524	.007	-.032	-.056	-.082	-.091	.287
.7000	.280	.102	-.220	-.383	.382	-.524	-.002	-.044	-.069	-.094	-.101	.281
.7500	.280	.102	-.220	-.383	.382	-.524	-.032	-.068	-.087	-.104	-.108	.277
.8000	.280	.102	-.220	-.383	.382	-.524	-.048	-.096	-.118	-.110	-.097	.291
.8500	.280	.102	-.220	-.383	.382	-.524	-.081	-.101	-.107	-.107	-.102	.238
.9000	.280	.102	-.220	-.383	.382	-.524	-.096	-.096	-.098	-.094	-.085	.150
.9500	.280	.102	-.220	-.383	.382	-.524	-.080	-.080	-.076	-.060	-.072	.041
1.0000	.280	.102	-.220	-.383	.382	-.524	-.072	-.070	-.057	-.036	-.052	.019
1.0500	.280	.102	-.220	-.383	.382	-.524	-.060	-.060	-.043	-.030	-.046	.052
							-.056	-.041	-.004	.011	.034	.078
							-.036					
							-.052					

TABLE I - Continued  
PRESSURE COEFFICIENTS AT SIX SPANWISE STATIONS

(f) M = 0.96 - Continued

x/c	Upper surface					Lower surface						
	Station, fraction of semispan					Station, fraction of semispan						
	.16	.25	.40	.60	.75	.95	.16	.25	.40	.60	.75	.95
$\alpha = 6.4$												
-0.0500												
0.0000												
0.0125												
0.0250												
0.0500												
0.0750												
0.1000												
0.1500												
0.2000												
0.2500												
0.3000												
0.3500												
0.4000												
0.4500												
0.5000												
0.5500												
0.6000												
0.6500												
0.7000												
0.7500												
0.8000												
0.8500												
0.9000												
0.9500												
1.0000												
1.0500												
$\alpha = 8.4$												
-0.0500												
0.0000												
0.0125												
0.0250												
0.0500												
0.0750												
0.1000												
0.1500												
0.2000												
0.2500												
0.3000												
0.3500												
0.4000												
0.4500												
0.5000												
0.5500												
0.6000												
0.6500												
0.7000												
0.7500												
0.8000												
0.8500												
0.9000												
0.9500												
1.0000												
1.0500												
$\alpha = 10.4$												
-0.0500												
0.0000												
0.0125												
0.0250												
0.0500												
0.0750												
0.1000												
0.1500												
0.2000												
0.2500												
0.3000												
0.3500												
0.4000												
0.4500												
0.5000												
0.5500												
0.6000												
0.6500												
0.7000												
0.7500												
0.8000												
0.8500												
0.9000												
0.9500												
1.0000												
1.0500												
$\alpha = 12.5$												
-0.0500												
0.0000												
0.0125												
0.0250												
0.0500												
0.0750												
0.1000												
0.1500												
0.2000												
0.2500												
0.3000												
0.3500												
0.4000												
0.4500												
0.5000												
0.5500												
0.6000												
0.6500												
0.7000												
0.7500												
0.8000												
0.8500												
0.9000												
0.9500												
1.0000												
1.0500												







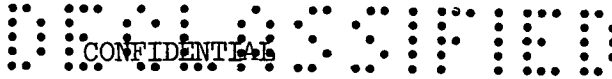


TABLE I - Continued  
PRESSURE COEFFICIENTS AT SIX SPANWISE STATIONS

(g) M = 0.98

Table for alpha = 0.5 showing pressure coefficients for upper and lower surfaces at six spanwise stations (0.16, 0.25, 0.40, 0.60, 0.75, 0.95) for various x/c values from -0.0500 to 1.0500.

alpha = 1.5

Table for alpha = 1.5 showing pressure coefficients for upper and lower surfaces at six spanwise stations (0.16, 0.25, 0.40, 0.60, 0.75, 0.95) for various x/c values from -0.0500 to 1.0500.

alpha = 2.4

Table for alpha = 2.4 showing pressure coefficients for upper and lower surfaces at six spanwise stations (0.16, 0.25, 0.40, 0.60, 0.75, 0.95) for various x/c values from -0.0500 to 1.0500.

alpha = 4.5

Table for alpha = 4.5 showing pressure coefficients for upper and lower surfaces at six spanwise stations (0.16, 0.25, 0.40, 0.60, 0.75, 0.95) for various x/c values from -0.0500 to 1.0500.



TABLE L - Continued  
PRESSURE COEFFICIENTS AT SIX SPANWISE STATIONS

(g) M = 0.98 - Continued

Table with columns: x/c, Station, fraction of semispan (.16, .25, .40, .60, .75, .95) for Upper surface and Lower surface. Includes rows for alpha = 11.6 degrees.

alpha = 11.6

Table with columns: x/c, Station, fraction of semispan (.16, .25, .40, .60, .75, .95) for Upper surface and Lower surface. Includes rows for alpha = 13.7 degrees.

alpha = 13.7

Table with columns: x/c, Station, fraction of semispan (.16, .25, .40, .60, .75, .95) for Upper surface and Lower surface. Includes rows for alpha = 15.9 degrees.

alpha = 15.9

Table with columns: x/c, Station, fraction of semispan (.16, .25, .40, .60, .75, .95) for Upper surface and Lower surface. Includes rows for alpha = 18.1 degrees.

alpha = 18.1

TABLE L - Continued  
PRESSURE COEFFICIENTS AT SIX SPANWISE STATIONS

(g) M = 0.98 - Concluded

Table with columns for x/c and stations (0.16, 0.25, 0.40, 0.60, 0.75, 0.95) for upper and lower surfaces. Includes a parameter a = 20.2 and a grid of pressure coefficient values.

Table with columns for x/c and stations (0.16, 0.25, 0.40, 0.60, 0.75, 0.95) for upper and lower surfaces. Includes a parameter a = 22.3 and a grid of pressure coefficient values.

Table with columns for x/c and stations (0.16, 0.25, 0.40, 0.60, 0.75, 0.95) for upper and lower surfaces. Includes a parameter a = 24.4 and a grid of pressure coefficient values.

Table with columns for x/c and stations (0.16, 0.25, 0.40, 0.60, 0.75, 0.95) for upper and lower surfaces. Includes a parameter a = 26.5 and a grid of pressure coefficient values.









TABLE L - Continued  
PRESSURE COEFFICIENTS AT SIX SPANWISE STATIONS

(i) M = 1.03 - Concluded

x/c	Upper surface						Lower surface					
	Station, fraction of semispan						Station, fraction of semispan					
	.16	.25	.40	.60	.75	.95	.16	.25	.40	.60	.75	.95
$\alpha = 6.4$												
-.0500												
.0000	.192	-.034	-.371	-.539	.265	-.703	-.110					
.0125	-.038	-.895	-.824	-1.031	-1.133	-1.157	.312	.441	.431	.422	.409	.401
.0250	-.141	-.837	-.724	-1.003	-1.088	-1.142	.375	.372	.376	.363	.353	.342
.0500	-.175	-.324	-.608	-.895	-1.075	-1.110	.363	.314	.320	.301	.301	.290
.0750	-.194	-.293	-.522	-.873	-.995	-1.072	.340	.283	.274	.260	.256	.254
.1000	-.208	-.279	-.482	-.748	-.936	-1.041	.301	.263	.247	.230	.222	.216
.1500	-.187	-.258	-.411	-.641	-.869	-1.006	.249	.219	.203	.194	.185	.174
.2000	-.187	-.245	-.346	-.503	-.781	-.941	.221	.191	.165	.163	.153	.132
.2500	-.186	-.249	-.341	-.448	-.616	-.955	.202	.163	.139	.121	.112	.072
.3000	-.211	-.241	-.328	-.411	-.578	-.932	.184	.140	.110	.096	.084	.022
.3500	-.213	-.241	-.326	-.403	-.559	-.876	.162	.108	.089	.043	.067	-.047
.4000	-.204	-.256	-.325	-.392	-.534	-.850	.106	.093	.081	.063	.047	-.105
.4500	-.220	-.267	-.335	-.396	-.504	-.804	.119	.075	.060	.035	.025	-.147
.5000	-.247	-.286	-.341	-.399	-.469	-.717	.058	.057	.036	.017	.003	-.190
.5500	-.266	-.283	-.335	-.392	-.442	-.598	.035	.044	.018	.002	-.025	-.211
.6000	-.256	-.297	-.337	-.392	-.446	-.567	.059	.024	.007	-.006	-.042	-.217
.6500	-.256	-.282	-.327	-.366	-.429	-.578	.043	-.014	-.026	-.012	-.036	-.233
.7000	-.236	-.297	-.364	-.396	-.410	-.589	-.005	-.013	-.030	-.012	-.032	-.240
.7500	-.279	-.305	-.329	-.354	-.404	-.595	.010	.4001	-.010	.031	.042	.252
.8000	-.272	-.301	-.314	-.338	-.382	-.556	.010	.001	.005	-.027	-.044	-.251
.8500	-.282	-.296	-.312	-.336	-.354	-.511	.005	.006	.012	-.015	-.033	-.230
.9000	-.277	-.290	-.294	-.268	-.269	-.464	.010	.008	.008	.005	-.037	-.232
.9500	-.243	-.233	-.178	-.125	-.111	-.421	.012	.000	.002	.017	.032	-.169
1.0000							-.054					
1.0500							-.050					

$\alpha = 8.5$

x/c	Upper surface						Lower surface					
	Station, fraction of semispan						Station, fraction of semispan					
	.16	.25	.40	.60	.75	.95	.16	.25	.40	.60	.75	.95
$\alpha = 8.5$												
-.0500												
.0000	.170	-.265	-.593	-.729	.065	-.741	-.090					
.0125	-.076	-1.009	-.862	-.864	-.967	-.814	.381	.437	.408	.472	.454	.428
.0250	-.200	-.945	-.795	-.854	-.908	-.803	.485	.474	.464	.441	.419	.362
.0500	-.232	-.593	-.759	-.830	-.866	-.780	.491	.411	.406	.382	.371	.343
.0750	-.264	-.459	-.721	-.815	-.836	-.782	.461	.374	.352	.337	.331	.308
.1000	-.272	-.413	-.657	-.796	-.825	-.772	.413	.353	.332	.308	.300	.270
.1500	-.248	-.347	-.691	-.757	-.794	-.754	.346	.304	.283	.261	.253	.227
.2000	-.231	-.308	-.643	-.720	-.766	-.740	.309	.270	.242	.227	.216	.183
.2500	-.229	-.302	-.567	-.729	-.728	-.716	.285	.239	.213	.188	.179	.147
.3000	-.253	-.292	-.508	-.707	-.712	-.691	.262	.211	.182	.162	.152	.080
.3500	-.253	-.287	-.439	-.695	-.697	-.683	.237	.183	.159	.106	.126	.003
.4000	-.249	-.292	-.365	-.665	-.680	-.651	.173	.163	.146	.119	.106	-.054
.4500	-.261	-.300	-.343	-.662	-.659	-.627	.190	.161	.122	.094	.079	-.096
.5000	-.285	-.319	-.338	-.641	-.629	-.603	.123	.121	.098	.075	.052	-.142
.5500	-.300	-.315	-.335	-.613	-.611	-.576	.095	.106	.083	.059	.034	-.153
.6000	-.293	-.332	-.340	-.594	-.575	-.559	.122	.061	.064	.040	.007	-.142
.6500	-.300	-.317	-.338	-.541	-.54	-.551	.109	.048	.027	.025	.013	-.193
.7000	-.272	-.332	-.348	-.560	-.503	-.536	.054	.043	.026	.024	.011	-.198
.7500	-.307	-.338	-.348	-.509	-.455	-.528	.071	.053	.042	.005	.000	-.207
.8000	-.303	-.331	-.344	-.461	-.420	-.516	.066	.054	.040	.006	.010	-.207
.8500	-.314	-.330	-.332	-.422	-.345	-.501	.058	.051	.039	.017	.000	-.190
.9000	-.310	-.318	-.319	-.325	-.334	-.488	.055	.042	.031	.027	-.014	-.189
.9500	-.265	-.257	-.244	-.168	-.293	-.478	.044	.022	.013	.002	-.055	-.188
1.0000							-.063					
1.0500												

$\alpha = 10.5$

x/c	Upper surface						Lower surface					
	Station, fraction of semispan						Station, fraction of semispan					
	.16	.25	.40	.60	.75	.95	.16	.25	.40	.60	.75	.95
$\alpha = 10.5$												
-.0500												
.0000	.138	-.522	-.763	-.878	-.158	-.664	+.042					
.0125	-.116	-1.040	-.883	-.839	-.897	-.643	.458	.616	.552	.503	.468	.433
.0250	-.266	-.941	-.857	-.838	-.858	-.636	.598	.468	.459	.489	.455	.388
.0500	-.304	-.821	-.855	-.826	-.836	-.630	.624	.507	.476	.440	.416	.371
.0750	-.342	-.782	-.837	-.824	-.823	-.630	.585	.468	.432	.401	.383	.342
.1000	-.348	-.752	-.852	-.813	-.813	-.628	.524	.439	.406	.373	.351	.305
.1500	-.311	-.613	-.850	-.810	-.808	-.624	.442	.389	.361	.328	.306	.264
.2000	-.278	-.301	-.824	-.810	-.799	-.619	.396	.350	.316	.293	.268	.215
.2500	-.266	-.269	-.781	-.820	-.794	-.608	.367	.316	.284	.252	.233	.154
.3000	-.287	-.285	-.762	-.815	-.791	-.599	.340	.285	.249	.221	.201	.102
.3500	-.282	-.298	-.717	-.813	-.785	-.594	.309	.253	.221	.165	.173	.044
.4000	-.283	-.307	-.632	-.786	-.768	-.579	.244	.232	.206	.176	.149	-.013
.4500	-.294	-.321	-.529	-.789	-.749	-.564	.259	.209	.179	.150	.123	-.049
.5000	-.317	-.343	-.394	-.778	-.718	-.550	.186	.186	.156	.127	.098	-.091
.5500	-.330	-.341	-.307	-.760	-.691	-.535	.146	.166	.139	.104	.072	-.108
.6000	-.325	-.356	-.307	-.757	-.660	-.522	.184	.137	.114	.084	.049	-.125
.6500	-.330	-.341	-.319	-.716	-.640	-.508	.167	.105	.079	.063	.038	-.170
.7000	-.297	-.357	-.345	-.750	-.610	-.493	.111	.076	.071	.084	.058	-.173
.7500	-.331	-.363	-.348	-.714	-.577	-.482	.124	.102	.083	.039	.024	-.182
.8000	-.328	-.357	-.348	-.684	-.559	-.470	.113	.098	.078	.041	.024	-.184
.8500	-.338	-.352	-.346	-.613	-.518	-.457	.101	.092	.071	.047	.024	-.181
.9000	-.339	-.337	-.340	-.548	-.504	-.446	.091	.075	.058	.064	-.005	-.177
.9500	-.275	-.260	-.278	-.465	-.481	-.438	.072	.047	.029	.065	-.055	-.186
1.0000							-.082					
1.0500							-.079					





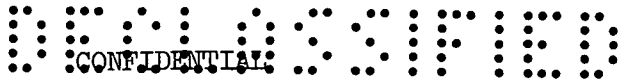
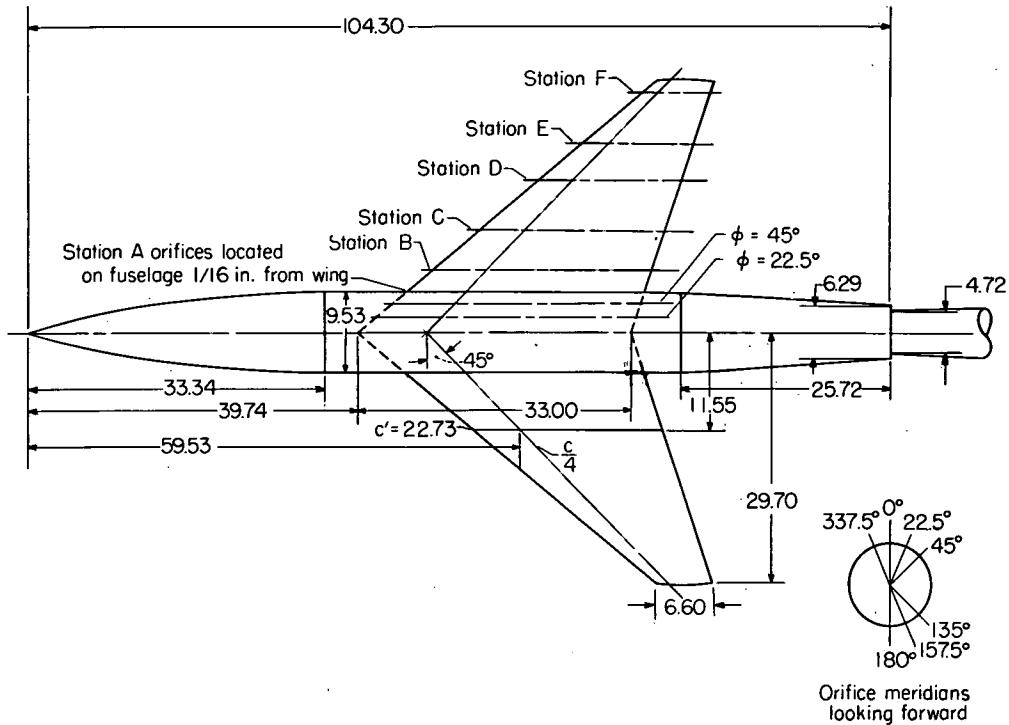


TABLE II  
SECTION COEFFICIENTS AT WING STATIONS

M	α, deg	y/b/2 = 0.16			y/b/2 = 0.25			y/b/2 = 0.40			y/b/2 = 0.60			y/b/2 = 0.75			y/b/2 = 0.95		
		c <sub>n</sub>	c <sub>mc</sub> /4	x <sub>cp</sub> /c	c <sub>n</sub>	c <sub>mc</sub> /4	x <sub>cp</sub> /c	c <sub>n</sub>	c <sub>mc</sub> /4	x <sub>cp</sub> /c	c <sub>n</sub>	c <sub>mc</sub> /4	x <sub>cp</sub> /c	c <sub>n</sub>	c <sub>mc</sub> /4	x <sub>cp</sub> /c	c <sub>n</sub>	c <sub>mc</sub> /4	x <sub>cp</sub> /c
0.80	4.5	0.206	-0.020	0.347	0.226	-0.013	0.308	0.252	-0.008	0.282	0.290	-0.002	0.257	0.293	0.013	0.206	0.257	-0.010	0.289
	8.4	.429	-.038	.339	.478	-.015	.281	.555	-.003	.245	.721	-.051	.321	.600	-.089	.398	.227	-.008	.285
	12.5	.639	-.057	.339	.723	-.027	.287	.917	-.055	.310	.870	-.153	.426	.634	-.088	.389	.301	-.017	.306
	15.7	.838	-.085	.351	1.001	-.058	.308	1.089	-.148	.386	.856	-.142	.416	.673	-.103	.403	.405	-.041	.351
	19.7	1.047	-.157	.400	1.065	-.171	.411	1.014	-.178	.426	.857	-.144	.418	.743	-.120	.412	.486	-.059	.371
23.9	1.146	-.212	.435	1.122	-.212	.439	1.036	-.195	.438	.915	-.163	.428	.814	-.140	.423	.544	-.073	.384	
0.85	4.5	.217	-.024	.361	.238	-.015	.313	.271	-.011	.291	.305	-.006	.270	.321	.014	.206	.283	-.015	.303
	8.5	.440	-.044	.350	.485	-.022	.295	.556	-.005	.259	.725	-.054	.324	.623	-.088	.391	.253	-.009	.286
	12.5	.640	-.066	.353	.726	-.040	.305	.925	-.072	.328	.823	-.146	.427	.630	-.089	.391	.330	-.019	.308
	15.7	.855	-.104	.372	1.015	-.079	.323	1.079	-.163	.401	.872	-.146	.417	.704	-.109	.405	.333	-.001	.253
	19.8	1.068	-.164	.404	1.099	-.179	.418	1.039	-.186	.429	.886	-.156	.426	.784	-.133	.420	.514	-.062	.371
24.0	1.152	-.216	.438	1.128	-.218	.443	1.049	-.202	.443	.944	-.175	.435	.849	-.152	.429	.566	-.075	.383	
0.90	4.5	.244	-.034	.389	.262	-.023	.338	.294	-.016	.304	.330	-.010	.280	.383	-.002	.255	.397	-.027	.318
	8.4	.488	-.071	.395	.526	-.046	.337	.605	-.031	.301	.766	-.071	.343	.623	-.105	.394	.327	-.024	.323
	12.5	.679	-.091	.384	.753	-.058	.327	.948	-.096	.351	.800	-.144	.430	.671	-.110	.414	.411	-.042	.352
	15.8	.871	-.125	.394	.934	-.097	.348	1.090	-.172	.408	.898	-.158	.426	.762	-.126	.415	.478	-.055	.365
	20.0	1.092	-.168	.404	1.170	-.183	.406	1.106	-.200	.431	.937	-.171	.432	.835	-.151	.431	.568	-.077	.386
24.1	1.202	-.230	.441	1.183	-.233	.447	1.102	-.219	.449	1.003	-.196	.445	.926	-.176	.440	.637	-.094	.398	
0.92	4.4	.249	-.040	.411	.269	-.030	.362	.303	-.022	.323	.341	-.014	.291	.397	.000	.250	.406	-.017	.292
	8.5	.502	-.085	.419	.541	-.060	.361	.620	-.046	.324	.766	-.078	.352	.769	-.108	.390	.353	-.029	.332
	12.4	.675	-.092	.386	.745	-.060	.331	.900	-.081	.340	.829	-.149	.430	.666	-.115	.423	.421	-.048	.364
	15.8	.879	-.134	.402	.991	-.105	.356	1.118	-.176	.407	.917	-.167	.432	.799	-.138	.423	.517	-.065	.376
	20.0	1.113	-.174	.406	1.232	-.184	.399	1.179	-.215	.432	.998	-.187	.437	.884	-.162	.433	.609	-.087	.393
24.2	1.237	-.238	.442	1.224	-.242	.448	1.155	-.233	.452	1.051	-.209	.449	.979	-.191	.445	.688	-.107	.406	
0.94	0.4	.007	.000	.250	.010	.000	.250	.003	-.002	.002	.003	.008	.003	.003	.000	.006	-.001	.006	
	2.4	.129	-.024	.436	.139	-.019	.387	.157	-.016	.352	.176	-.009	.301	.193	.002	.240	.163	-.026	.160
	4.4	.258	-.050	.444	.278	-.040	.394	.316	-.035	.361	.361	-.027	.325	.405	-.011	.277	.371	-.015	.210
	6.4	.386	-.074	.444	.417	-.062	.399	.469	-.060	.378	.558	-.055	.349	.632	-.052	.332	.484	-.041	.335
	8.3	.500	-.095	.436	.541	-.074	.387	.624	-.065	.351	.766	-.097	.377	.771	-.109	.391	.410	-.032	.328
10.4	.622	-.111	.428	.677	-.082	.371	.762	-.065	.335	.968	-.155	.410	.787	-.120	.402	.389	-.039	.370	
11.6	.677	-.113	.417	.737	-.078	.356	.829	-.053	.314	1.014	-.158	.406	.752	-.125	.416	.401	-.048	.370	
12.5	.701	-.108	.404	.799	-.071	.344	.861	-.054	.313	.987	-.152	.404	.735	-.129	.426	.446	-.061	.387	
13.7	.758	-.112	.398	.843	-.078	.343	1.026	-.115	.362	.925	-.171	.435	.751	-.136	.431	.495	-.065	.381	
15.8	.885	-.143	.412	.989	-.110	.361	1.172	-.175	.399	.971	-.184	.439	.843	-.155	.434	.572	-.079	.388	
20.1	1.117	-.185	.416	1.283	-.183	.393	1.302	-.236	.431	1.106	-.215	.444	.977	-.185	.439	.677	-.103	.402	
24.3	1.316	-.250	.440	1.330	-.258	.444	1.282	-.261	.455	1.160	-.234	.452	1.049	-.210	.450	.765	-.129	.419	
0.96	4.4	.239	-.044	.434	.265	-.038	.393	.304	-.036	.368	.353	-.034	.346	.397	-.016	.290	.383	-.037	.347
	8.4	.476	-.085	.429	.529	-.071	.384	.615	-.067	.359	.760	-.108	.392	.720	-.080	.361	.472	-.039	.333
	12.5	.705	-.123	.424	.777	-.099	.377	.910	-.097	.357	1.158	-.237	.455	.872	-.139	.409	.450	-.053	.368
	15.9	.882	-.140	.409	.981	-.104	.356	1.181	-.156	.382	1.113	-.210	.439	.906	-.176	.444	.613	-.093	.402
	20.2	1.111	-.187	.418	1.259	-.177	.391	1.386	-.246	.427	1.180	-.236	.450	1.035	-.203	.446	.728	-.116	.409
24.4	1.367	-.252	.434	1.441	-.266	.435	1.424	-.290	.454	1.280	-.261	.454	1.155	-.230	.449	.838	-.146	.424	
0.98	4.5	.228	-.041	.430	.255	-.035	.387	.296	-.034	.365	.343	-.037	.358	.399	-.027	.318	.404	-.018	.266
	8.4	.452	-.080	.427	.506	-.068	.384	.589	-.065	.360	.734	-.107	.396	.710	-.086	.371	.542	-.054	.350
	12.5	.678	-.118	.424	.756	-.098	.380	.895	-.107	.370	1.143	-.247	.467	.962	-.170	.427	.547	-.063	.365
	15.9	.900	-.165	.433	1.004	-.134	.383	1.173	-.169	.394	1.245	-.251	.452	1.077	-.197	.433	.657	-.108	.414
	20.2	1.104	-.188	.420	1.218	-.173	.392	1.408	-.259	.434	1.240	-.254	.455	1.064	-.216	.453	.770	-.126	.414
24.4	1.357	-.253	.436	1.448	-.268	.435	1.438	-.294	.454	1.293	-.268	.457	1.166	-.225	.452	.850	-.148	.424	
1.00	4.4	.217	-.036	.416	.242	-.032	.382	.279	-.030	.358	.322	-.034	.356	.368	-.025	.318	.369	-.015	.209
	8.5	.447	-.080	.429	.500	-.067	.384	.584	-.066	.363	.723	-.107	.398	.700	-.087	.374	.558	-.059	.356
	12.3	.646	-.113	.425	.723	-.095	.381	.854	-.102	.369	1.090	-.232	.463	.926	-.162	.425	.564	-.071	.376
1.03	2.5	.114	-.020	.425	.131	-.018	.387	.148	-.017	.365	.172	-.017	.349	.203	-.019	.344	.189	.010	.197
	6.4	.344	-.066	.442	.391	-.059	.401	.441	-.059	.384	.513	-.053	.353	.591	-.050	.335	.671	-.058	.336
	10.5	.558	-.099	.427	.623	-.084	.385	.729	-.083	.364	.907	-.166	.433	.828	-.134	.412	.541	-.063	.366
1.05	4.5	.216	-.039	.431	.247	-.035	.392	.273	-.034	.375	.321	-.031	.347	.369	-.024	.342	.373	-.003	.258
	8.5	.437	-.081	.431	.491	-.073	.399	.557	-.070	.376	.663	-.083	.375	.720	-.096	.383	.711	-.090	.377
	12.3	.656	-.119	.431	.741	-.104	.390	.878	-.113	.379	1.080	-.231	.464	.934	-.166	.428	.582	-.075	.379



Body ordinates			
x	r	x	r
0.000	0.000	24.000	4.396
0.500	0.144	26.000	4.536
1.000	0.286	28.000	4.643
1.500	0.426	30.000	4.716
2.000	0.564	32.000	4.755
3.000	0.832	33.333	4.763
4.000	1.091	78.582	4.763
5.000	1.341	79.000	4.757
6.000	1.582	79.250	4.752
7.000	1.812	79.500	4.746
8.000	2.035	80.000	4.728
9.000	2.249	80.500	4.708
10.000	2.454	81.000	4.685
10.500	2.551	81.916	4.639
11.000	2.649	83.500	4.557
11.625	2.766	85.250	4.458
12.000	2.834	87.000	4.345
14.000	3.182	88.000	4.278
16.000	3.493	89.000	4.209
18.000	3.770	90.965	4.067
19.000	3.896	97.362	3.624
20.000	4.014	104.300	3.143
22.000	4.223		

Wing data		
Aspect ratio	3.0	
Taper ratio	0.2	
Wing area	8.165 sq ft	
Airfoil section	65A004	
Wing orifice locations		
Spanwise station location, percent semispan		
A	16.00	
B	25.00	
C	40.00	
D	60.00	
E	75.00	
F	95.00	
Location of each orifice, percent chord		
0	25.00	65.00
1.25	30.00	70.00
2.50	35.00	75.00
5.00	40.00	80.00
7.50	45.00	85.00
10.00	50.00	90.00
15.00	55.00	95.00
20.00	60.00	

Body orifice locations			
Percent length	Angle from top looking forward	Percent length	Angle from top looking forward
2.00	0°, 180°	39.00	22.5°, 157.5°
4.00		41.70	
8.00		43.70	
12.00		47.60	
20.00		50.40	
28.00		53.30	
33.00		56.20	
38.00		59.10	
42.00		62.00	
46.00		64.80	
50.00		67.70	
54.00		70.60	
58.00		73.50	
62.00		40.50	45°, 135°
66.00		43.30	
70.00		46.20	
74.00		48.10	
78.00		52.00	
82.00	22.5°, 180°, 337.5°	54.80	
86.00		57.70	
90.00		60.60	
94.00		63.40	
98.00		66.30	
		69.20	
		72.20	

Figure 1.- Geometric details of model. All dimensions are in inches unless otherwise stated.



Figure 2.- Model installed in the test section of the Langley 16-foot transonic tunnel. L-87668

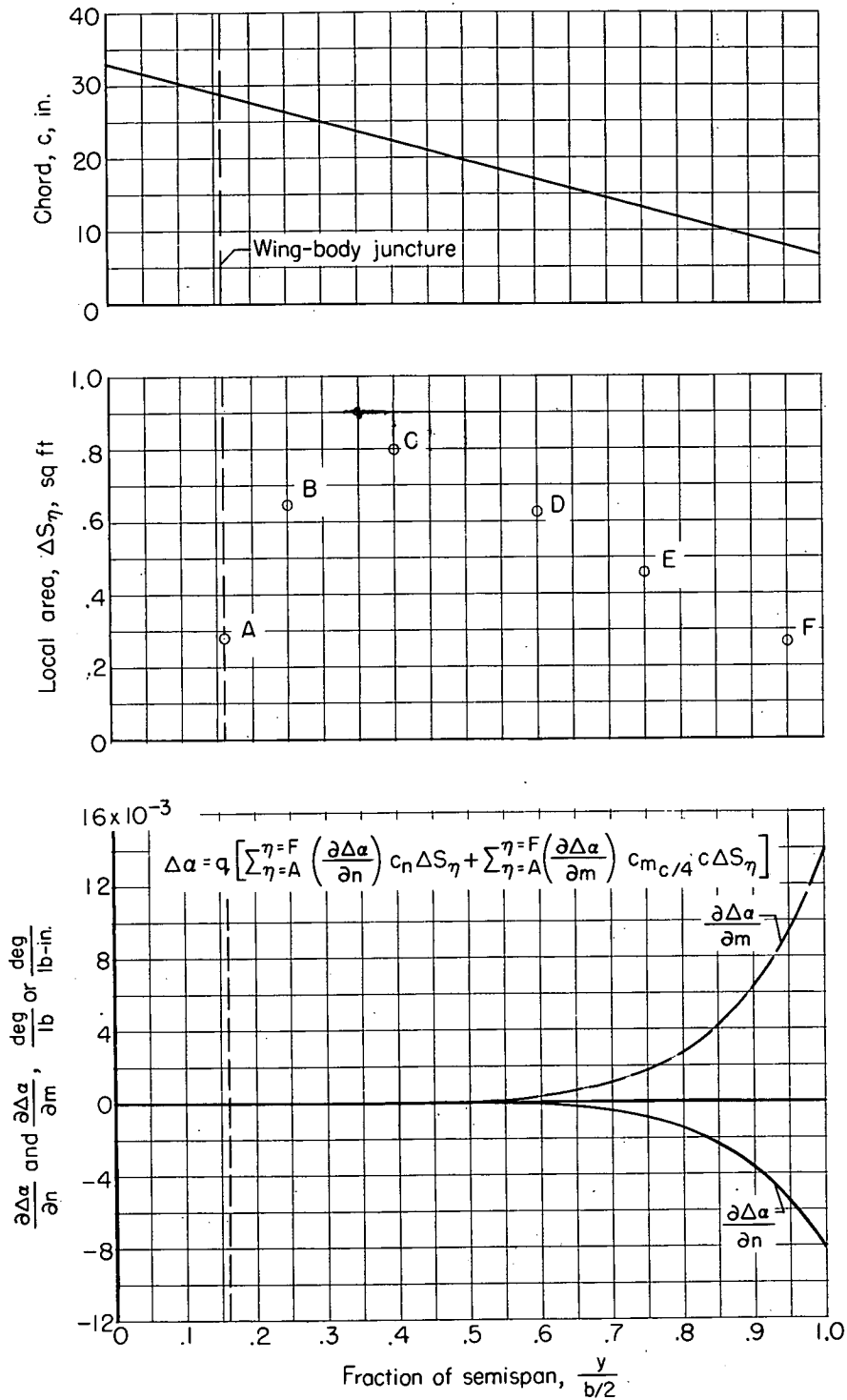
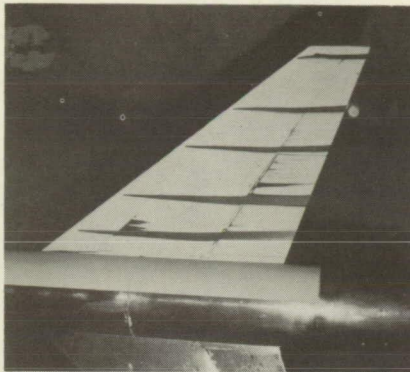
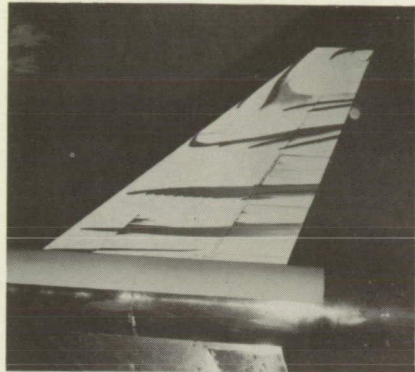


Figure 3.- Deflection characteristics of wing.

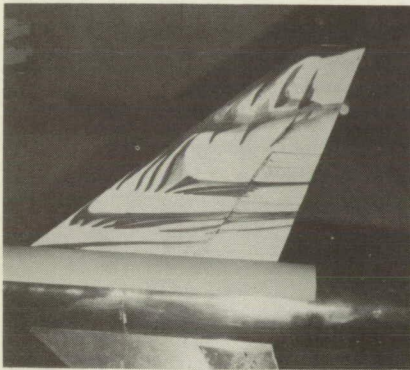




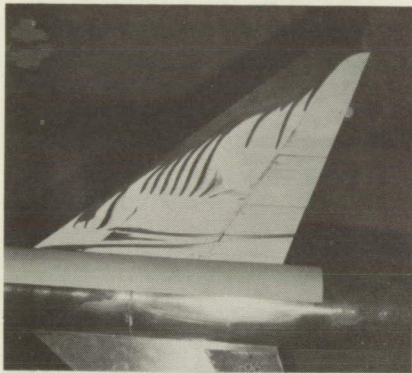
$\alpha \approx 2^\circ$



$\alpha \approx 4^\circ$



$\alpha \approx 6^\circ$



$\alpha \approx 8^\circ$



$\alpha \approx 12^\circ$

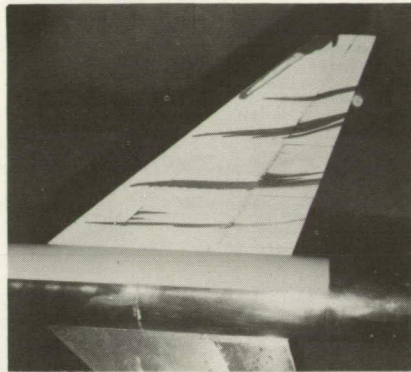
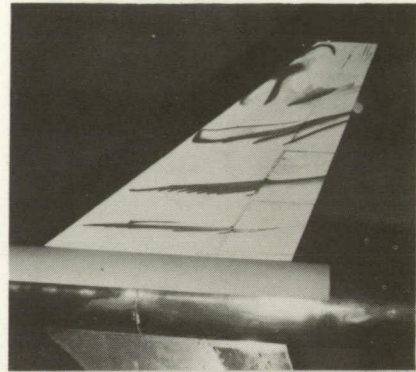
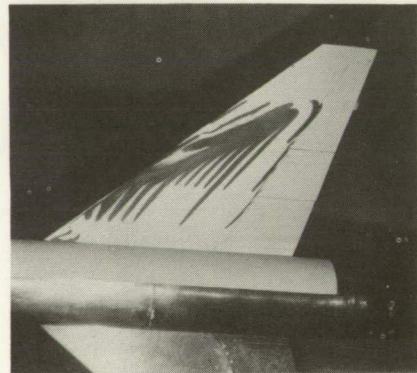


$\alpha \approx 19^\circ$

(a)  $M = 0.80$ .

L-93525

Figure 4.- Boundary-layer-flow patterns on the wing.

 $\alpha \approx 4^\circ$  $\alpha \approx 5^\circ$  $\alpha \approx 6^\circ$  $\alpha \approx 8^\circ$  $\alpha \approx 12^\circ$  $\alpha \approx 19^\circ$ (b)  $M = 0.94$ .

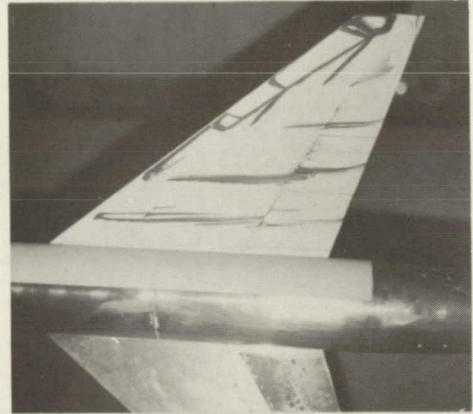
L-93526

Figure 4.- Continued.





$\alpha \approx 4^\circ$



$\alpha \approx 6^\circ$



$\alpha \approx 8^\circ$

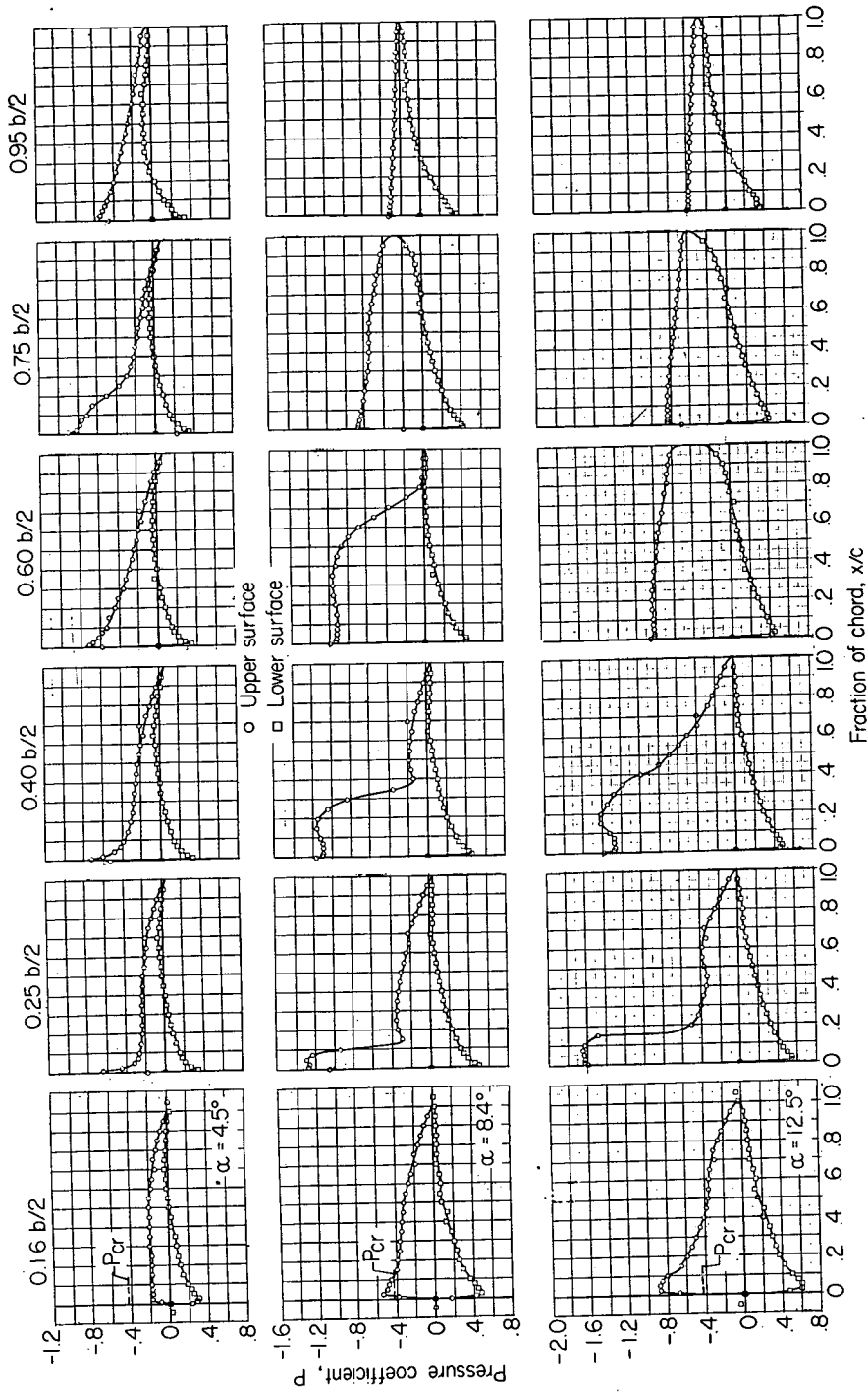


$\alpha \approx 10^\circ$

(c)  $M = 1.03$ .

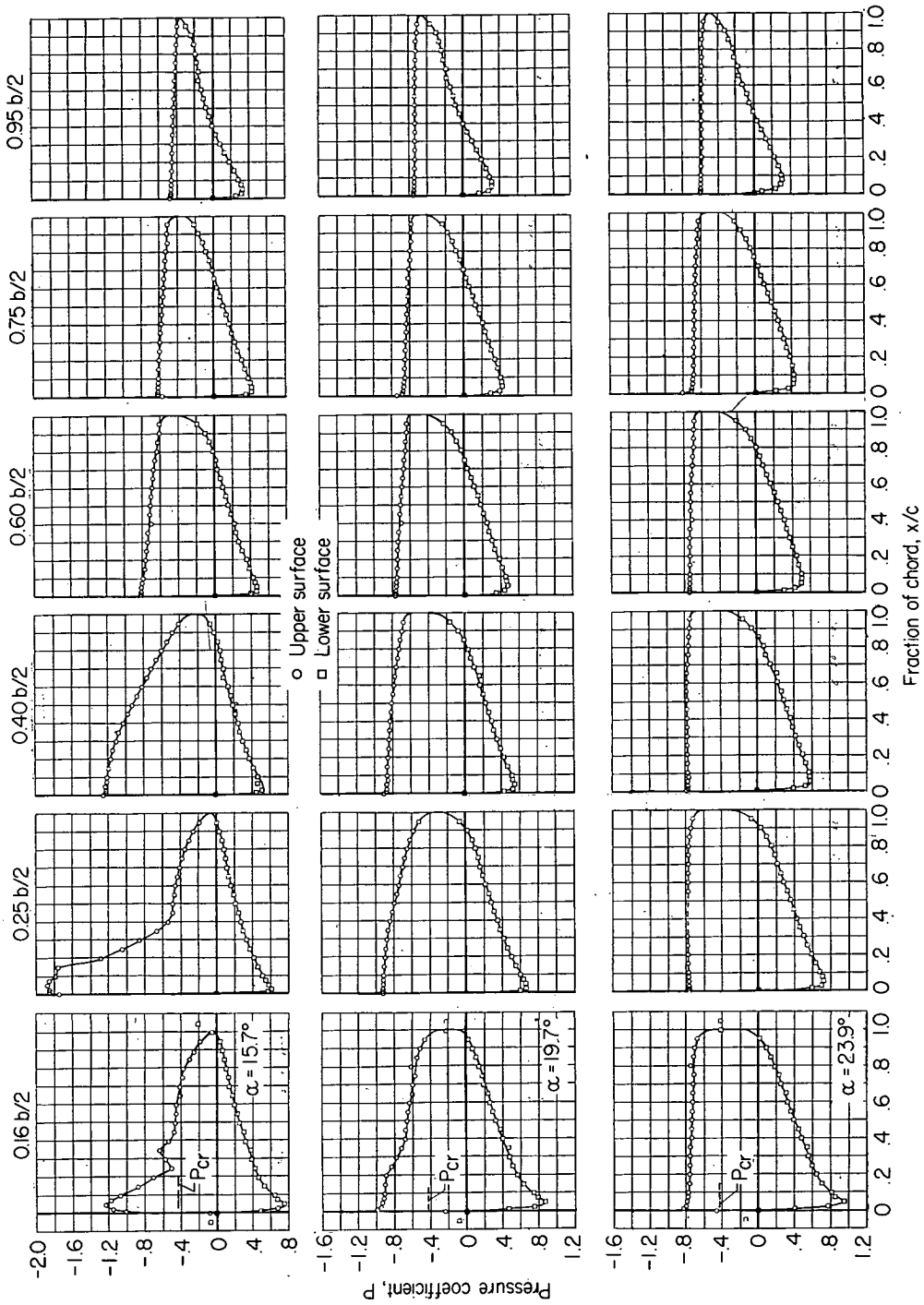
L-93527

Figure 4.- Concluded.



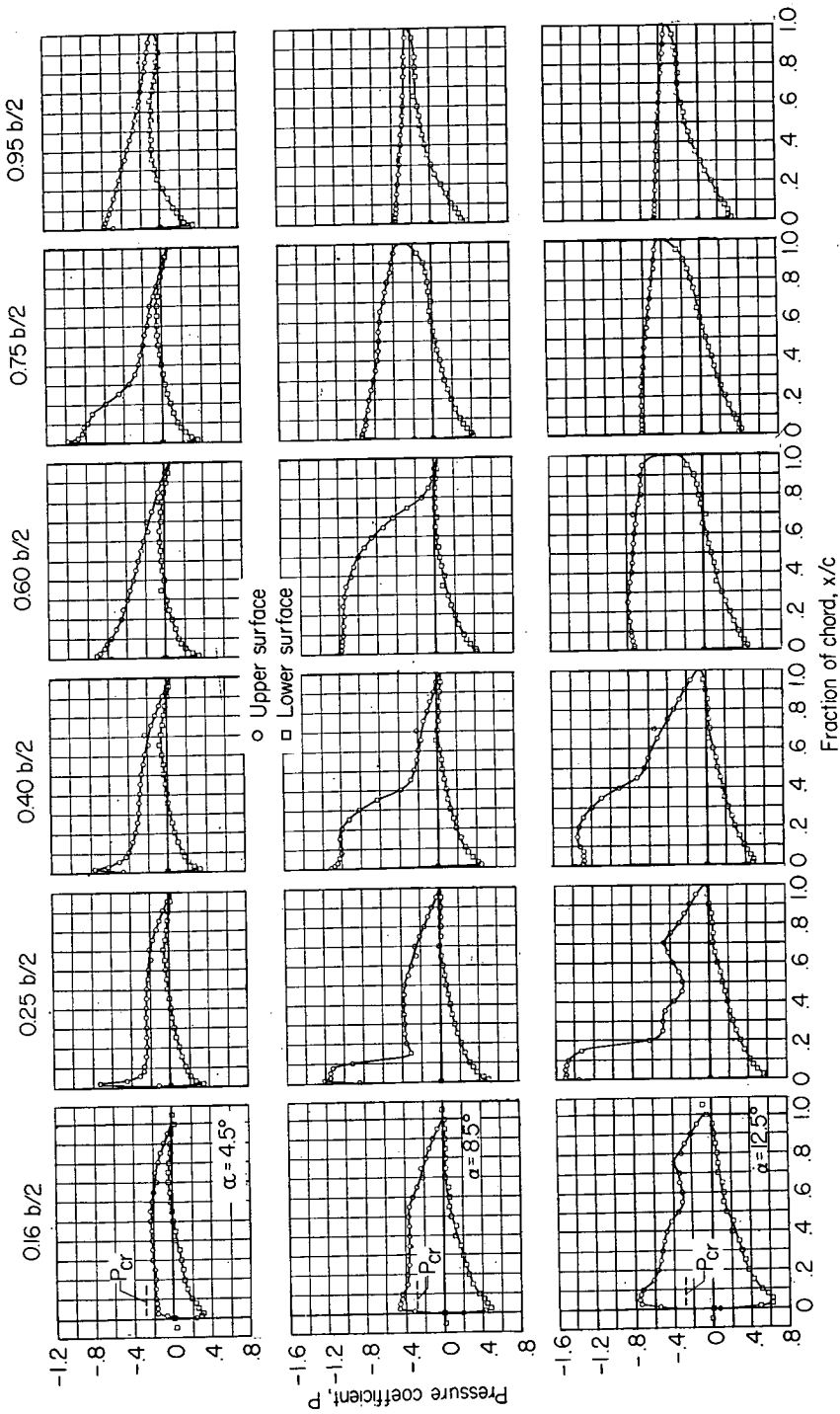
(a)  $M = 0.80$ .

Figure 5.- Chordwise pressure distributions on the wing.



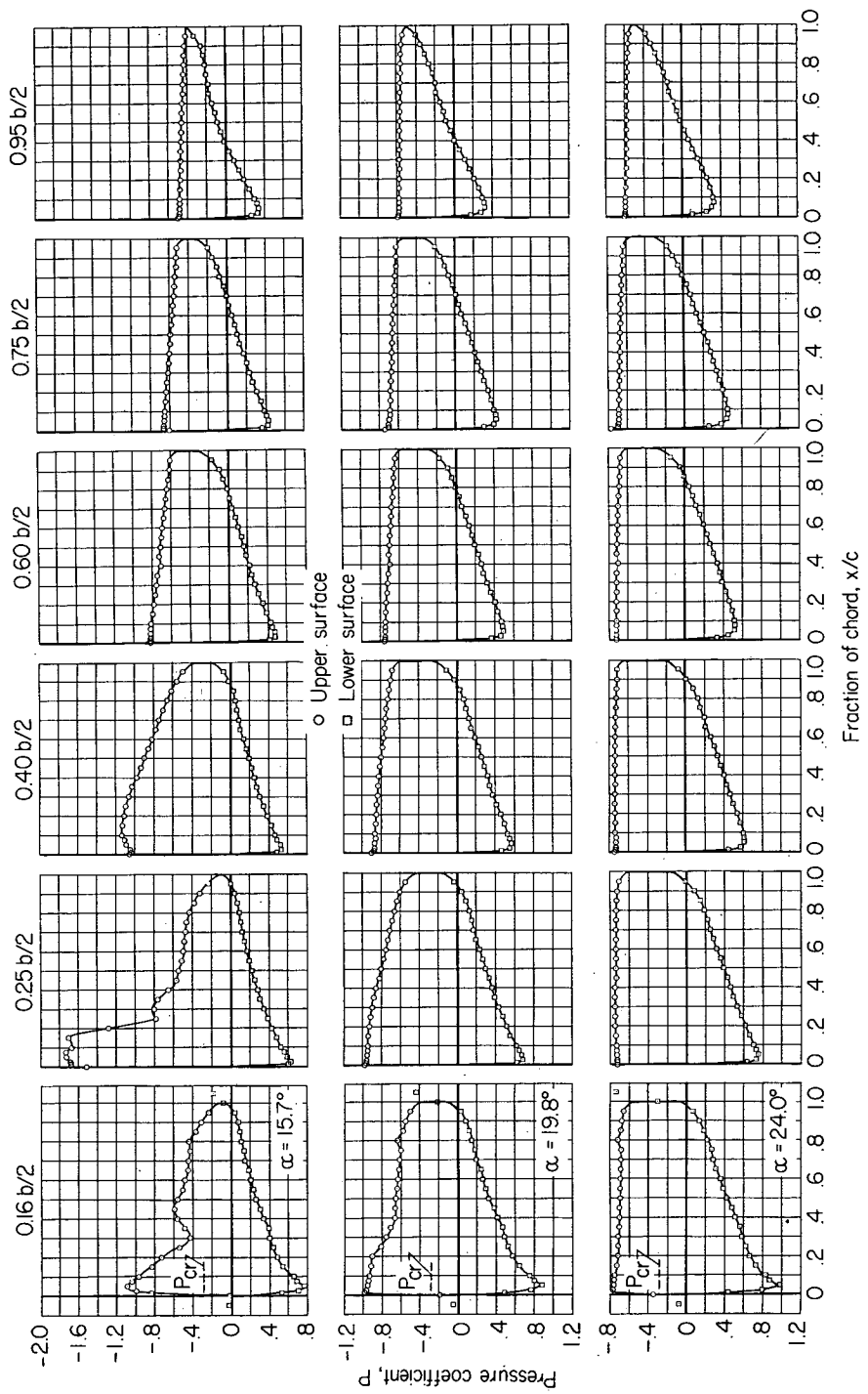
(a) Concluded.

Figure 5.- Continued.



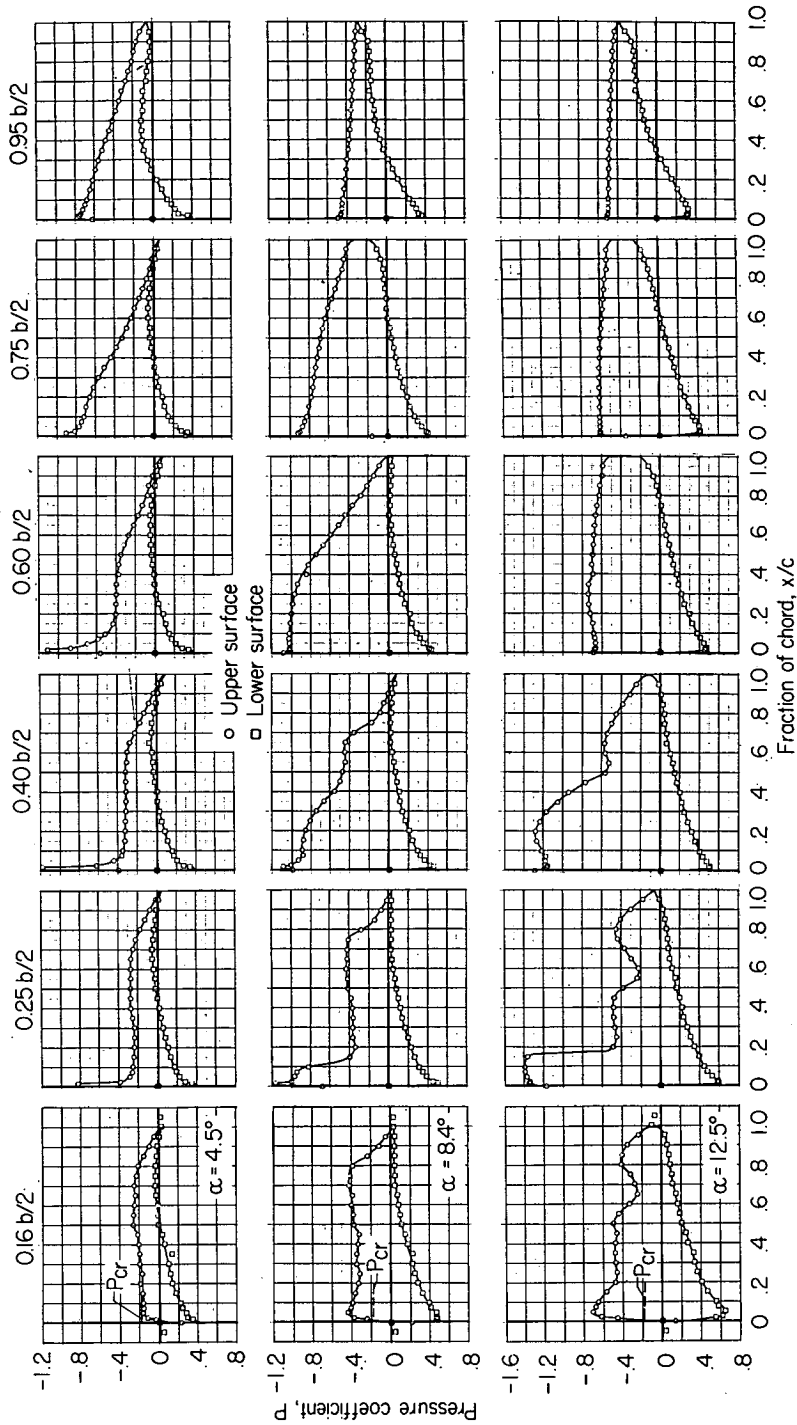
(b)  $M = 0.85$ .

Figure 5.- Continued.



(b) Concluded.

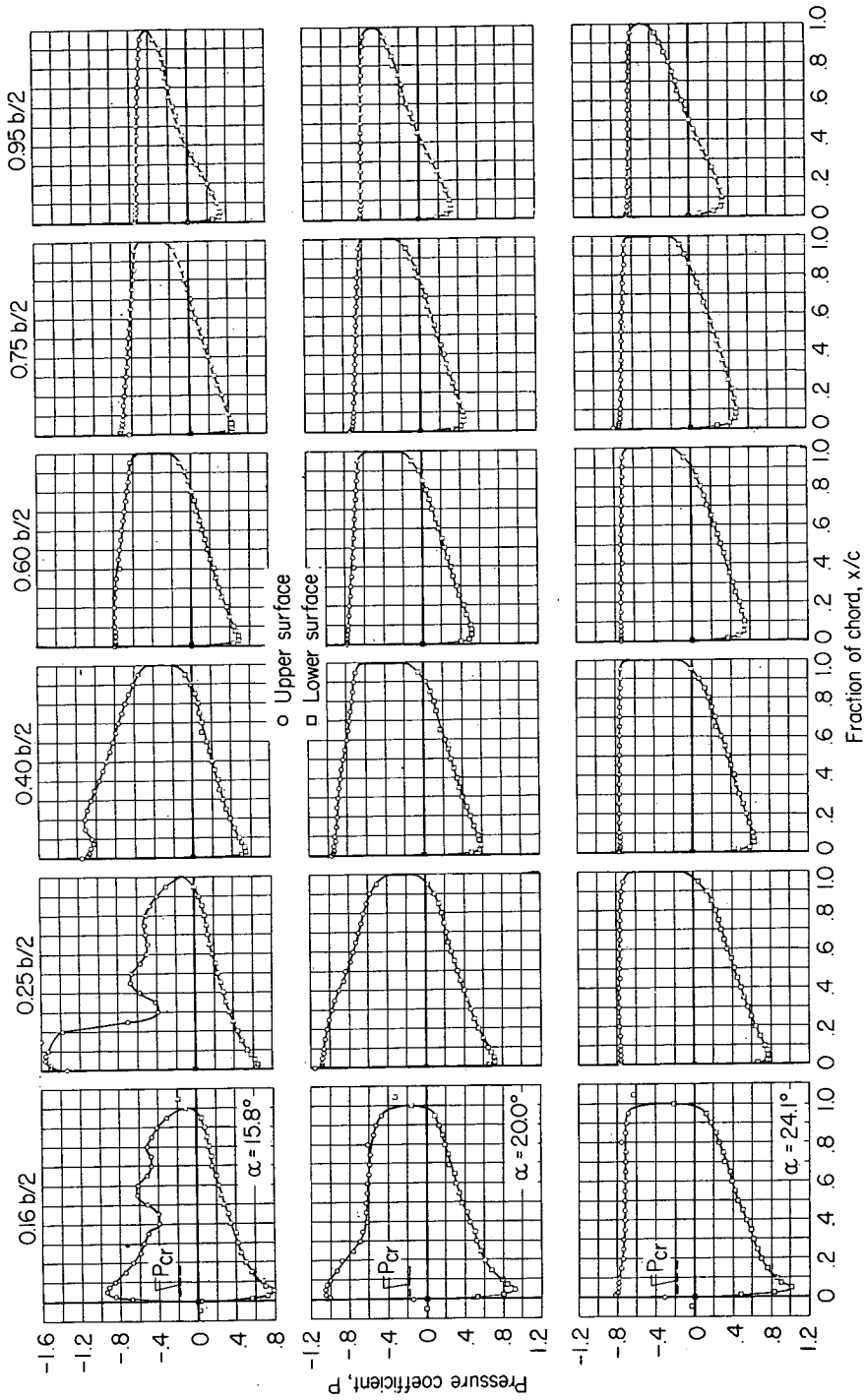
Figure 5.- Continued.



(c)  $M = 0.90$ .

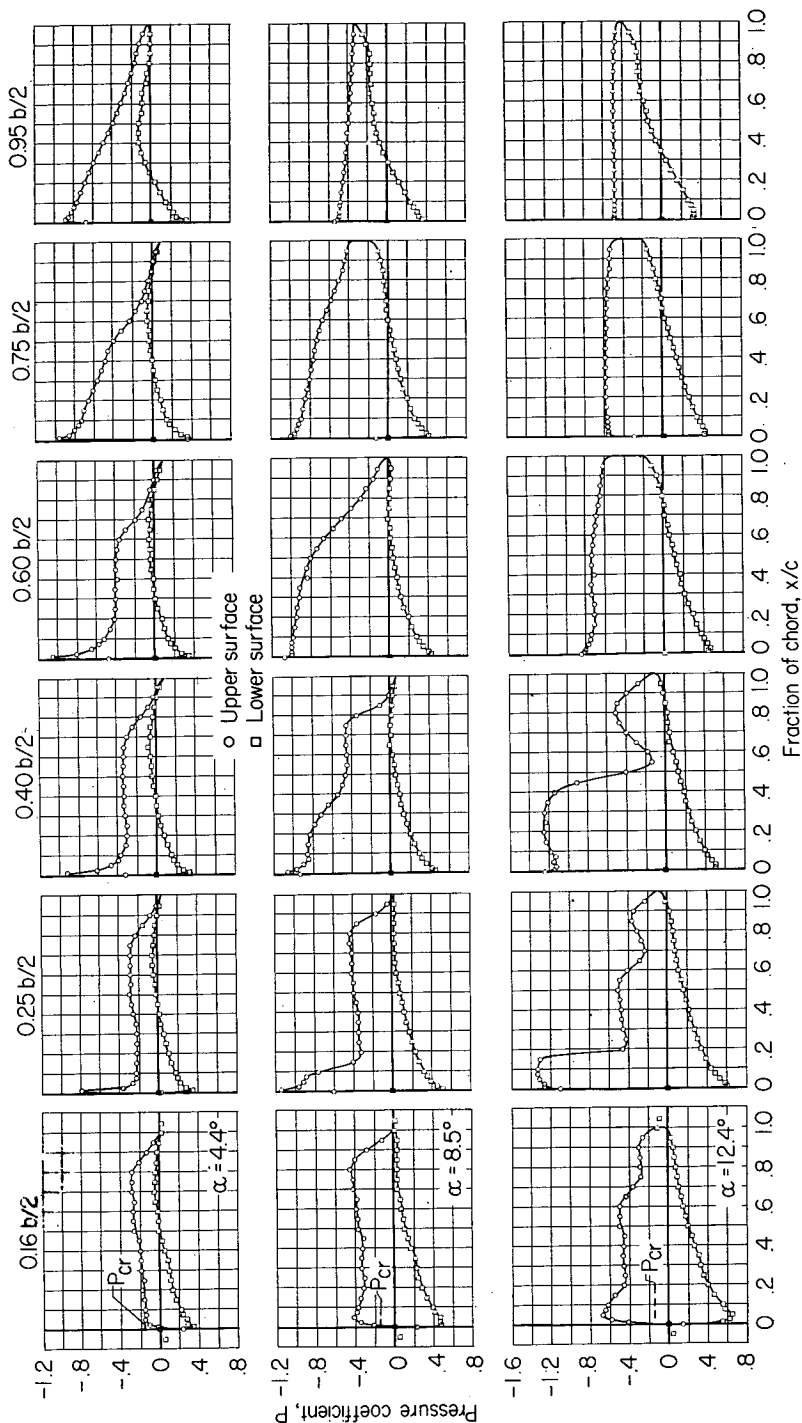
Figure 5.- Continued.





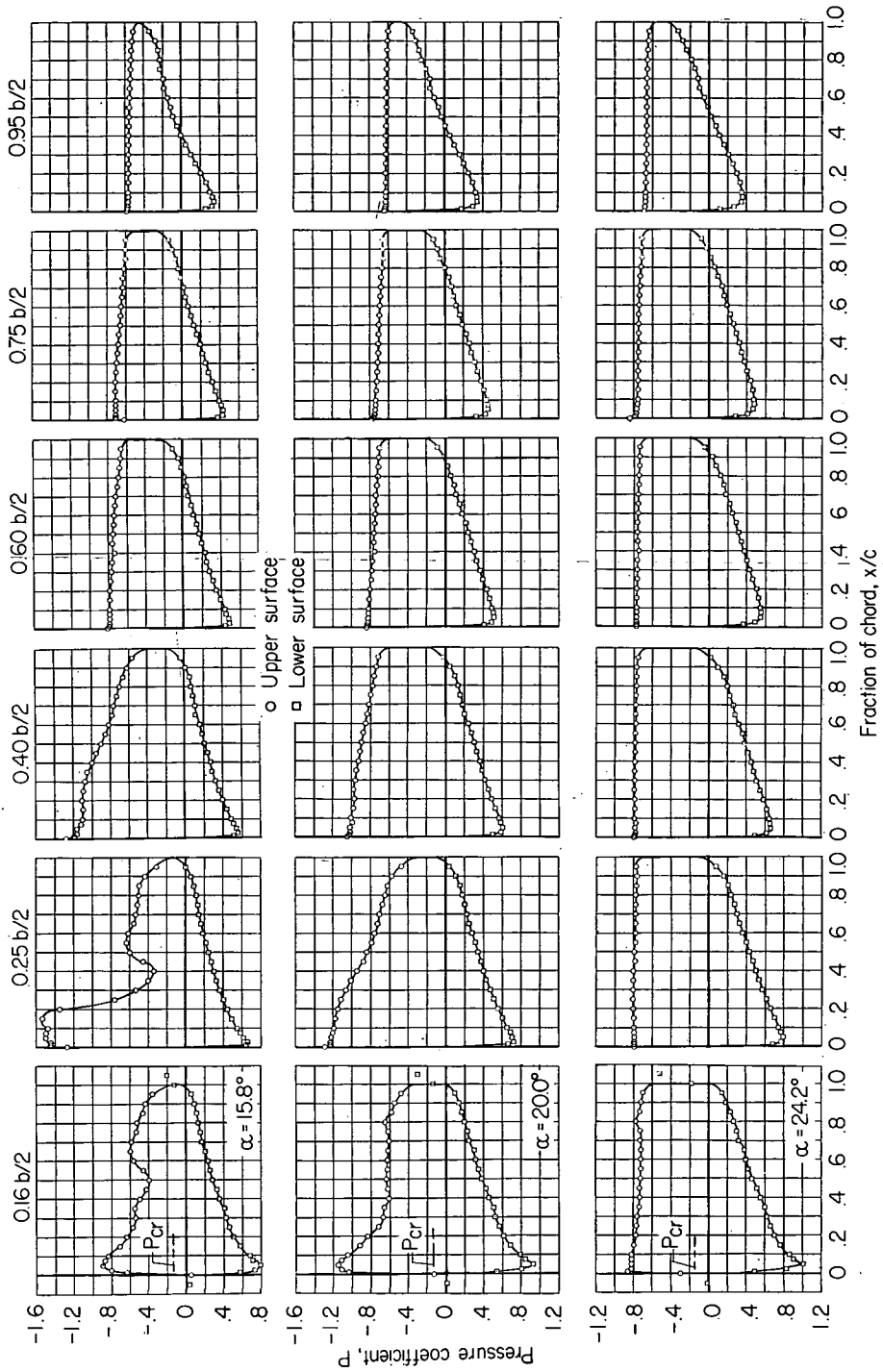
(c) Concluded.

Figure 5.- Continued.



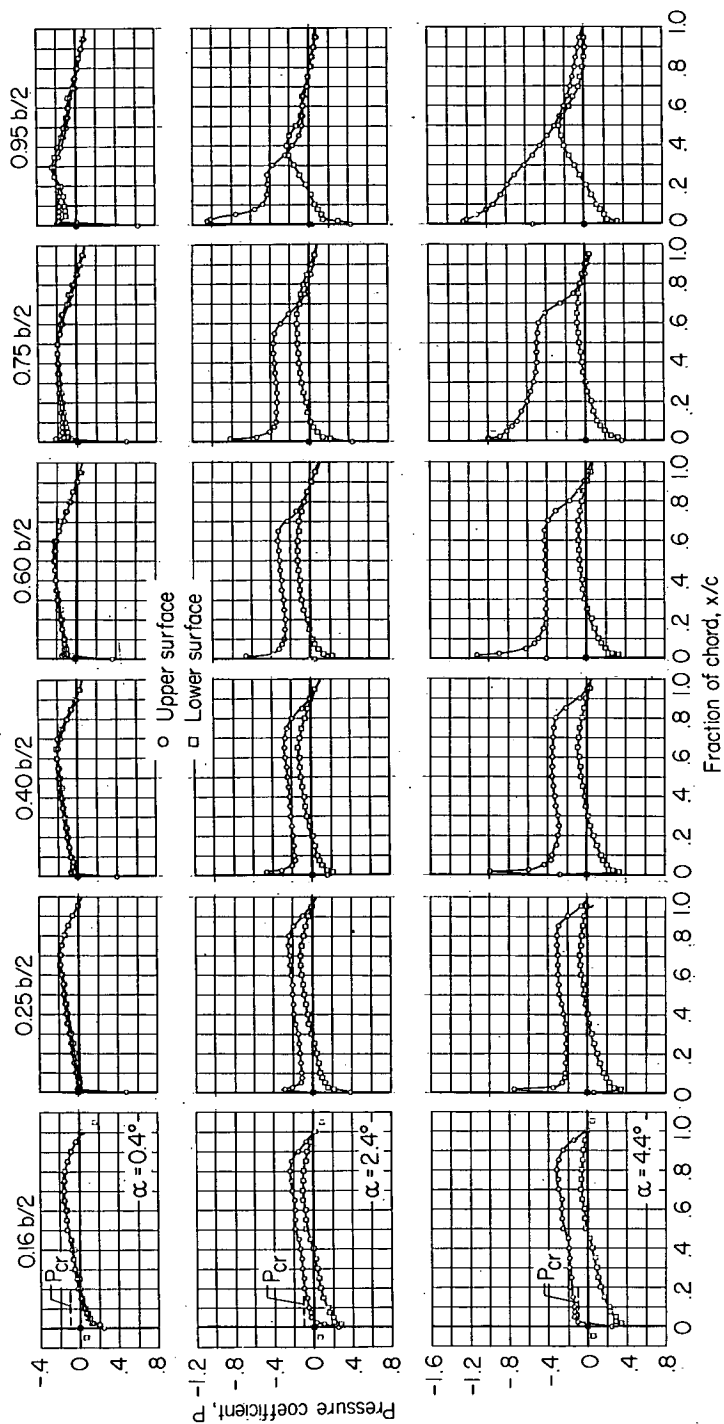
(d)  $M = 0.92$ .

Figure 5.- Continued.



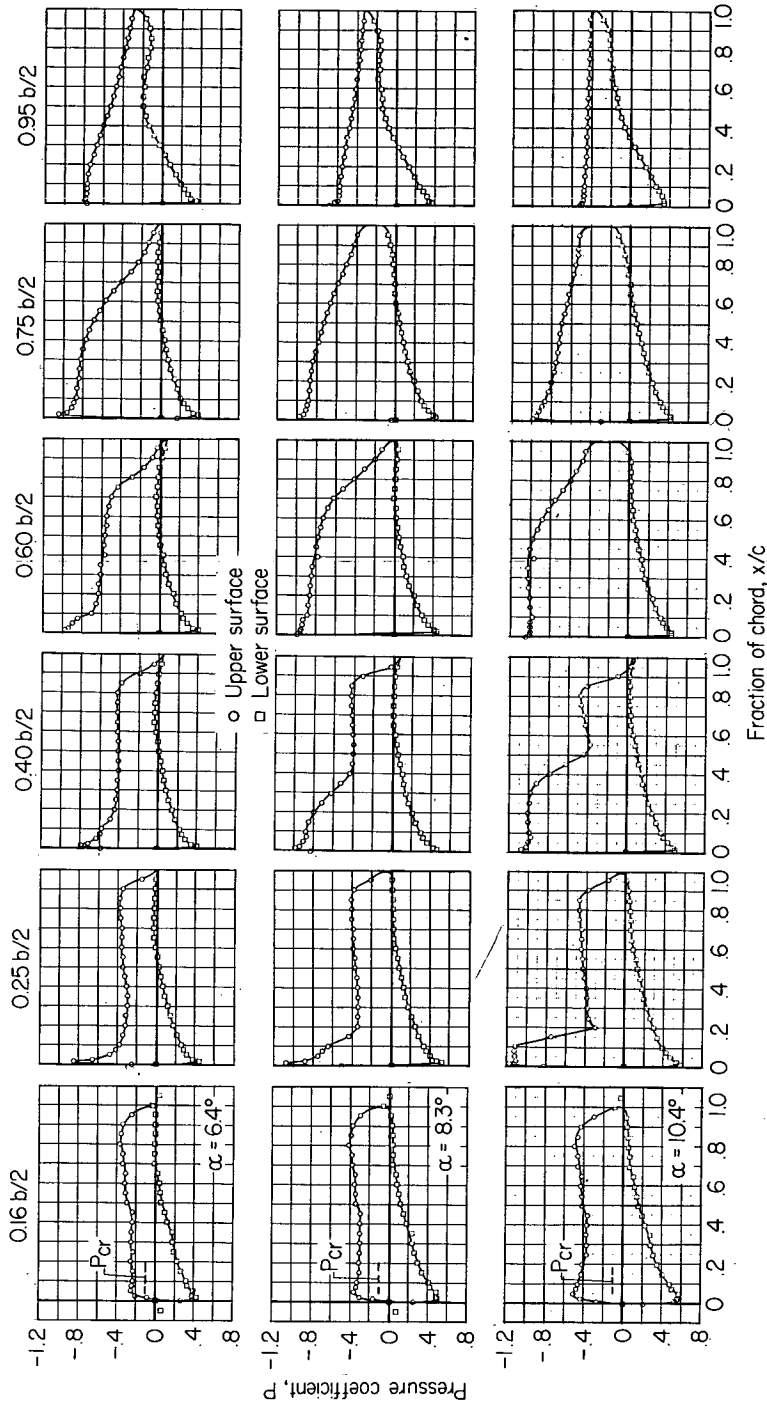
(d) Concluded.

Figure 5.- Continued.



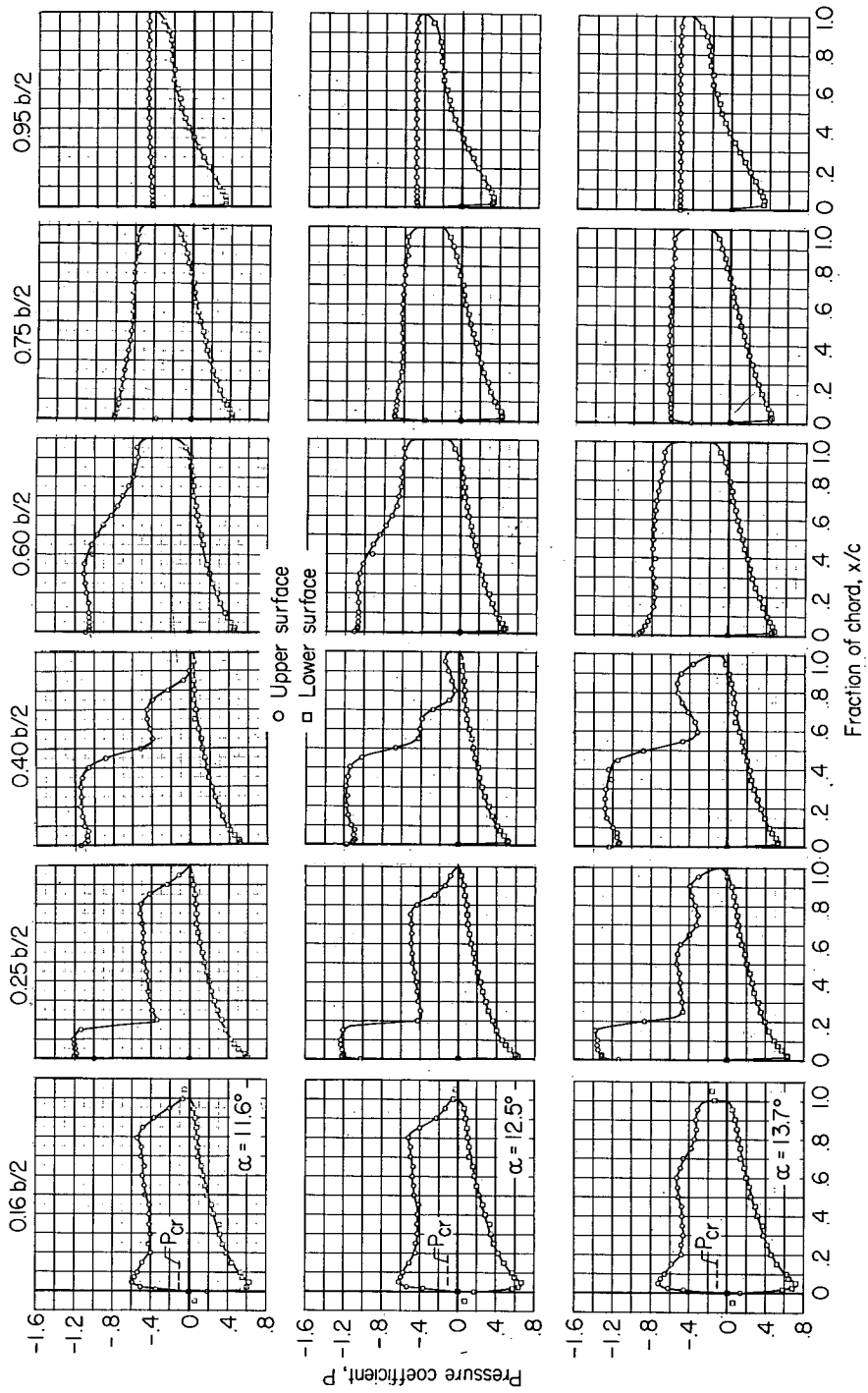
(e)  $M = 0.94$ .

Figure 5.- Continued.



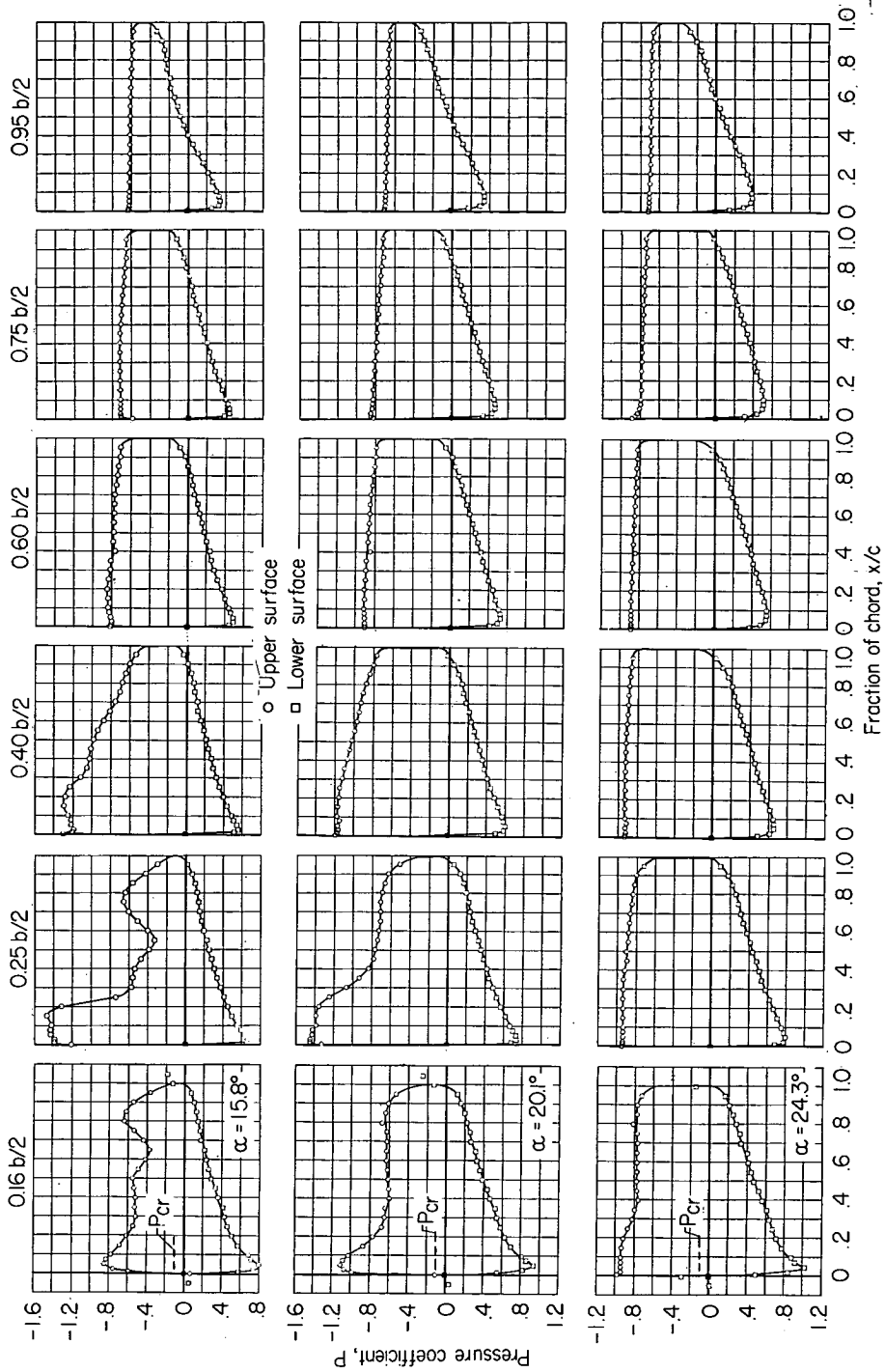
(e) Continued.

Figure 5.- Continued.



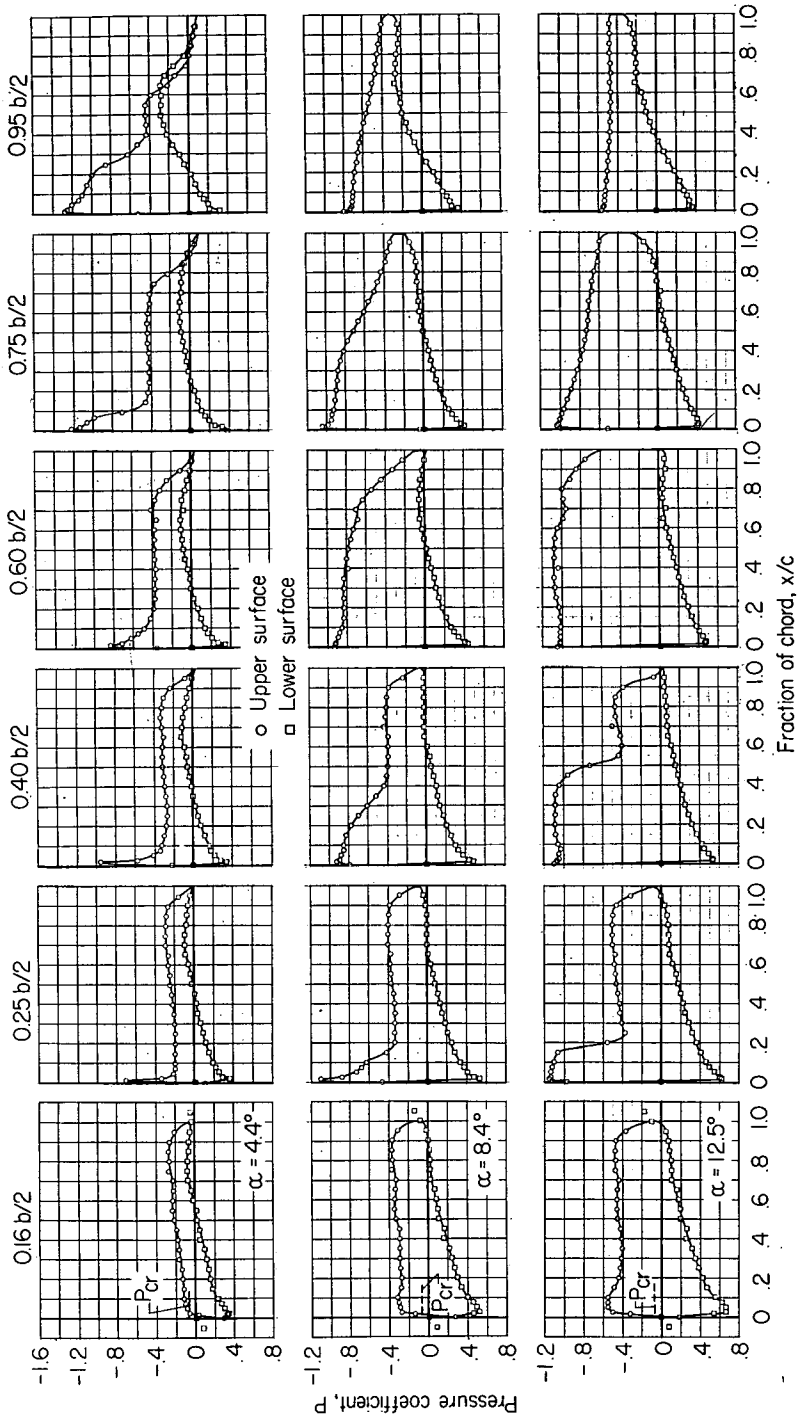
(e) Continued.

Figure 5.- Continued.



(e) Concluded.

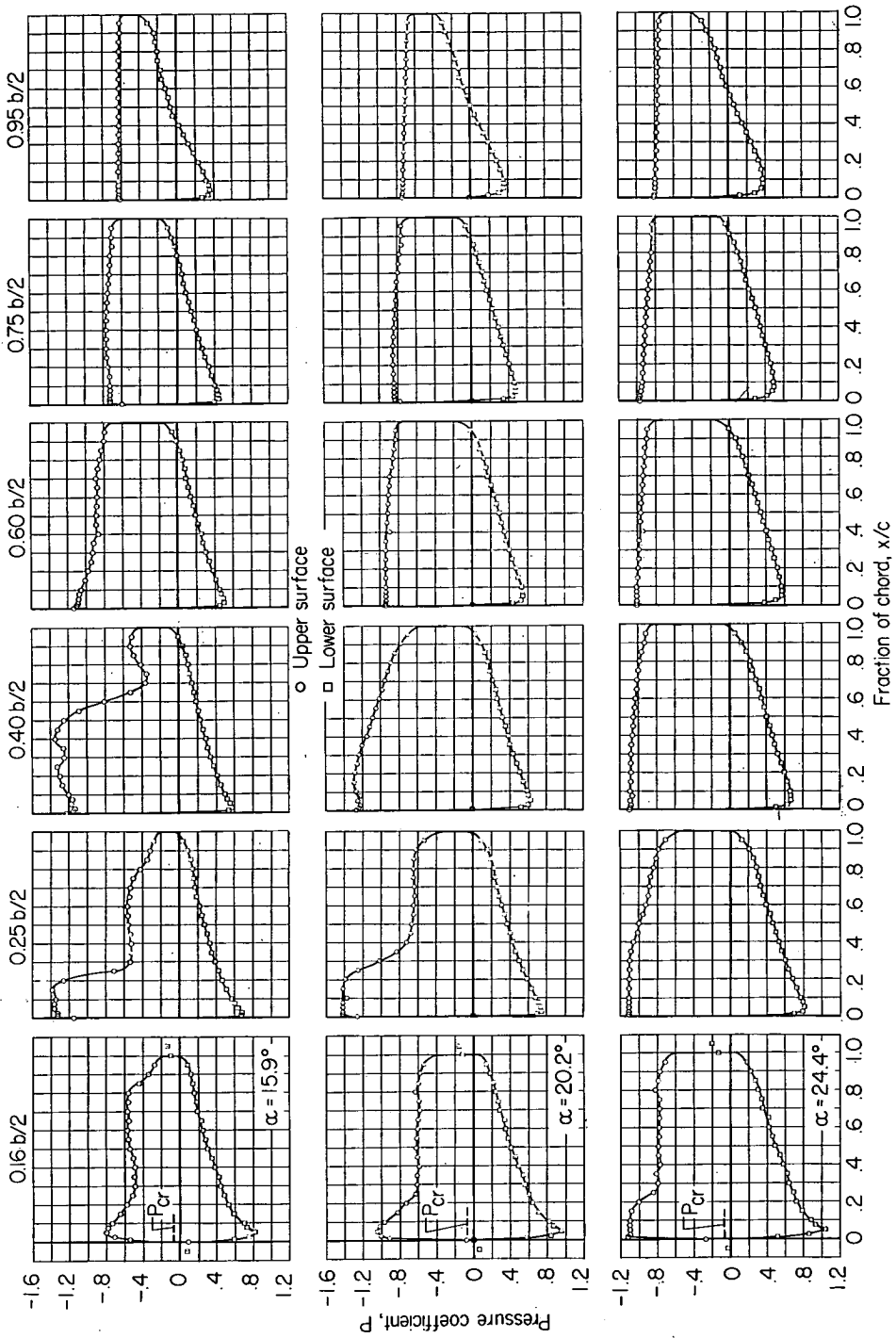
Figure 5.- Continued.



(f)  $M = 0.96$ .

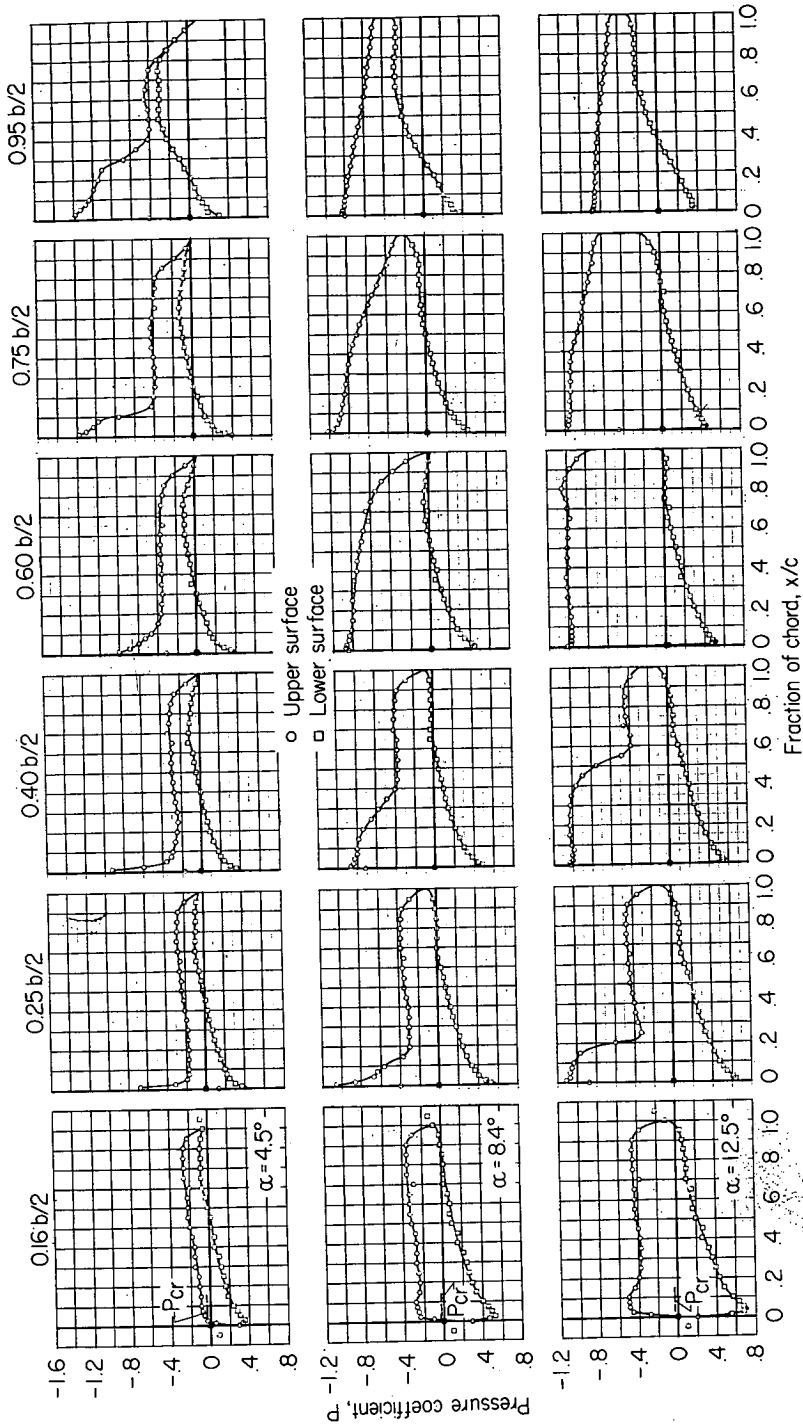
Figure 5.- Continued.





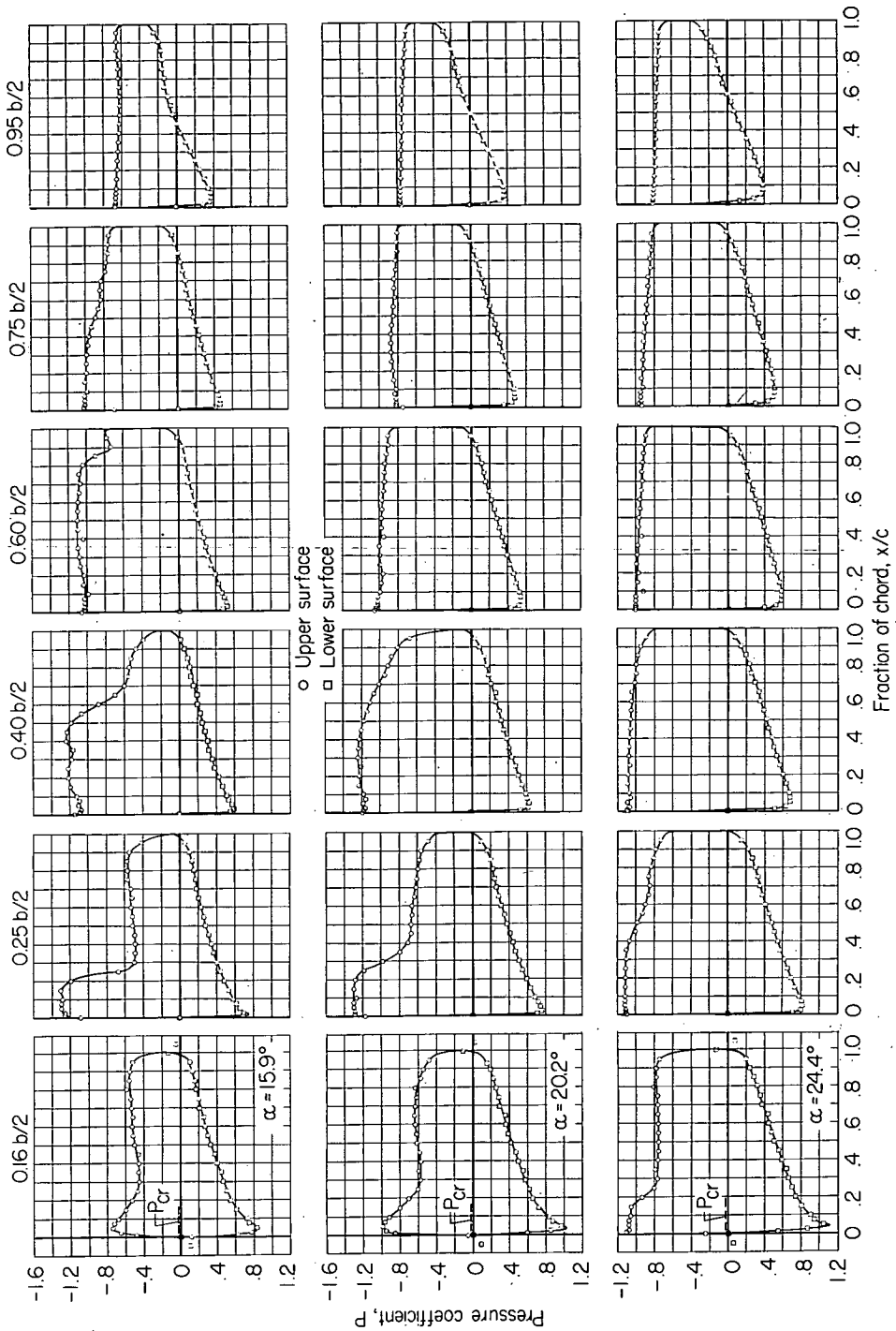
(f) Concluded.

Figure 5.- Continued.



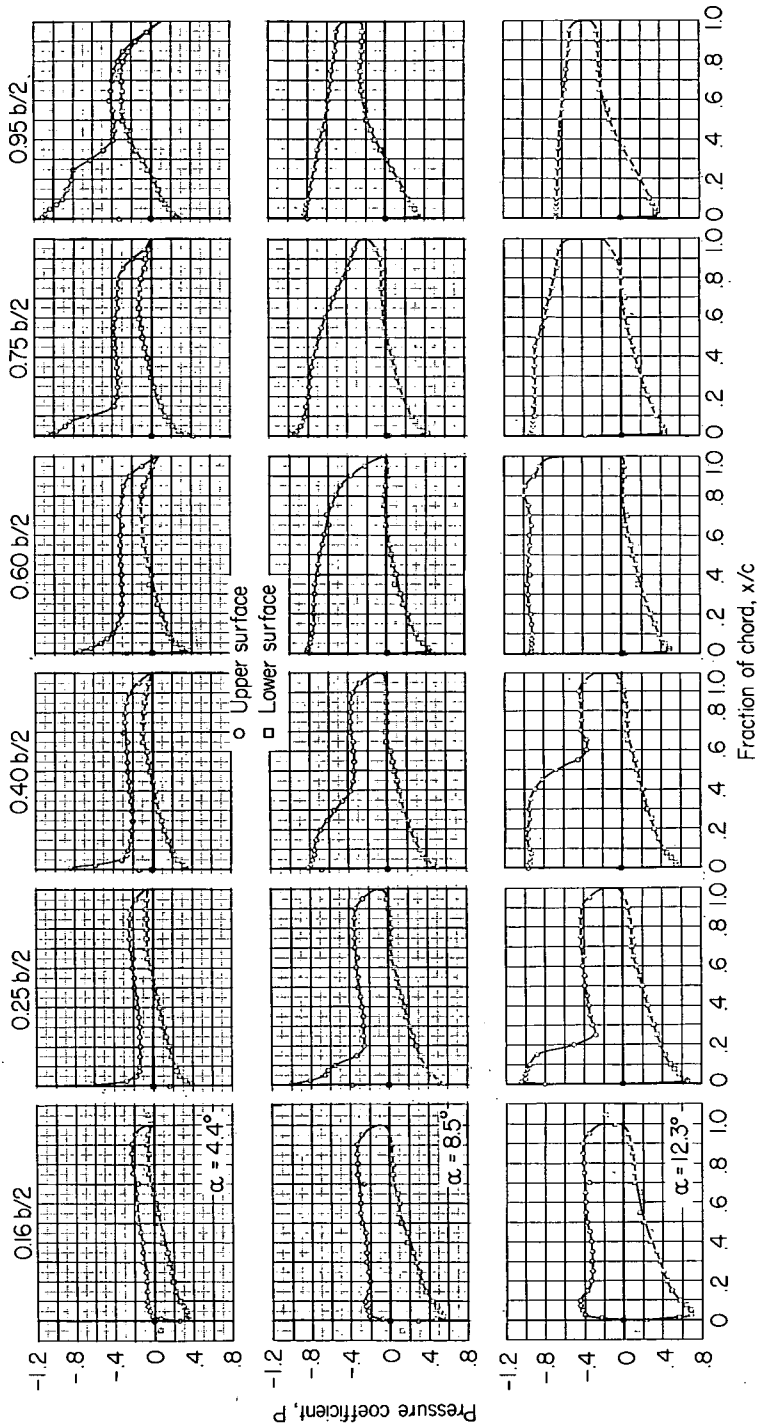
(g)  $M = 0.98$ .

Figure 5.- Continued.



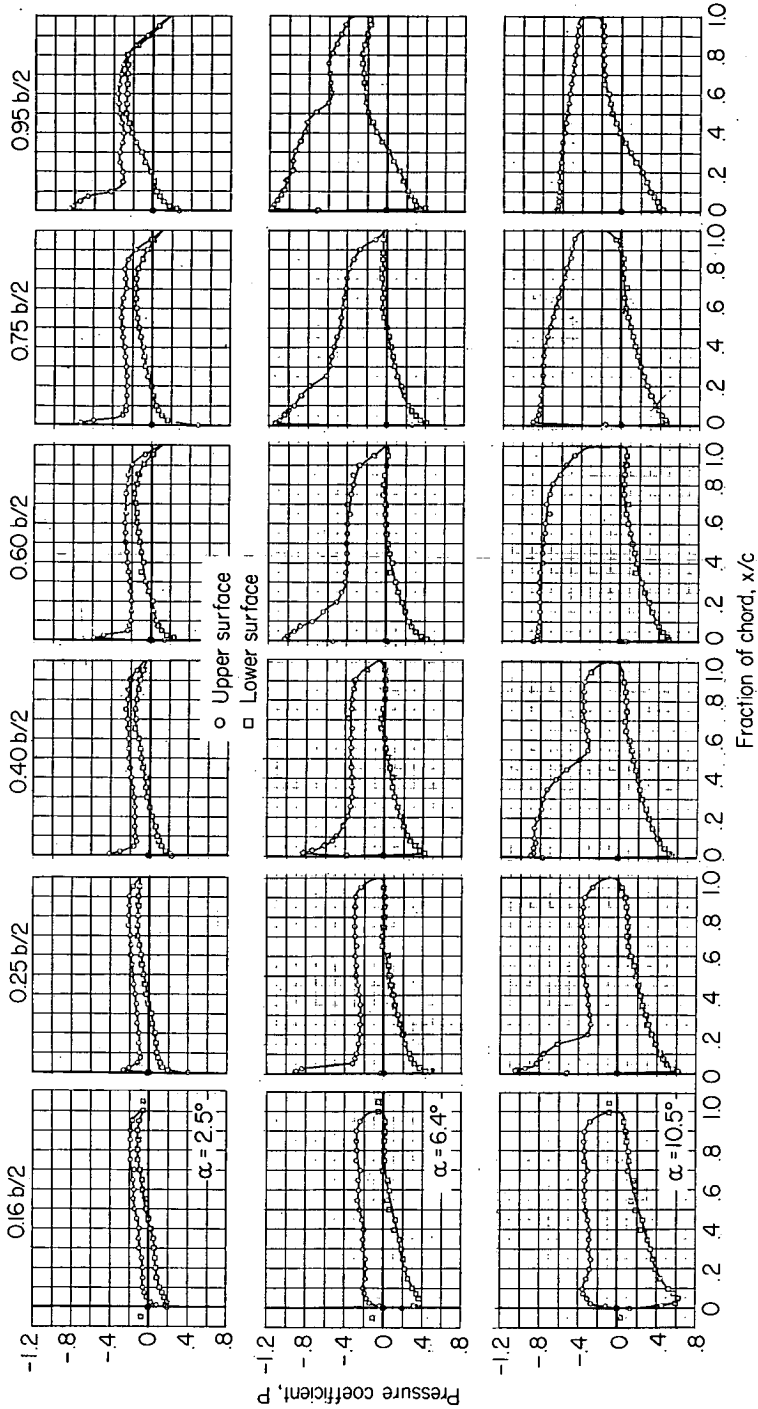
(g) Concluded.

Figure 5.- Continued.



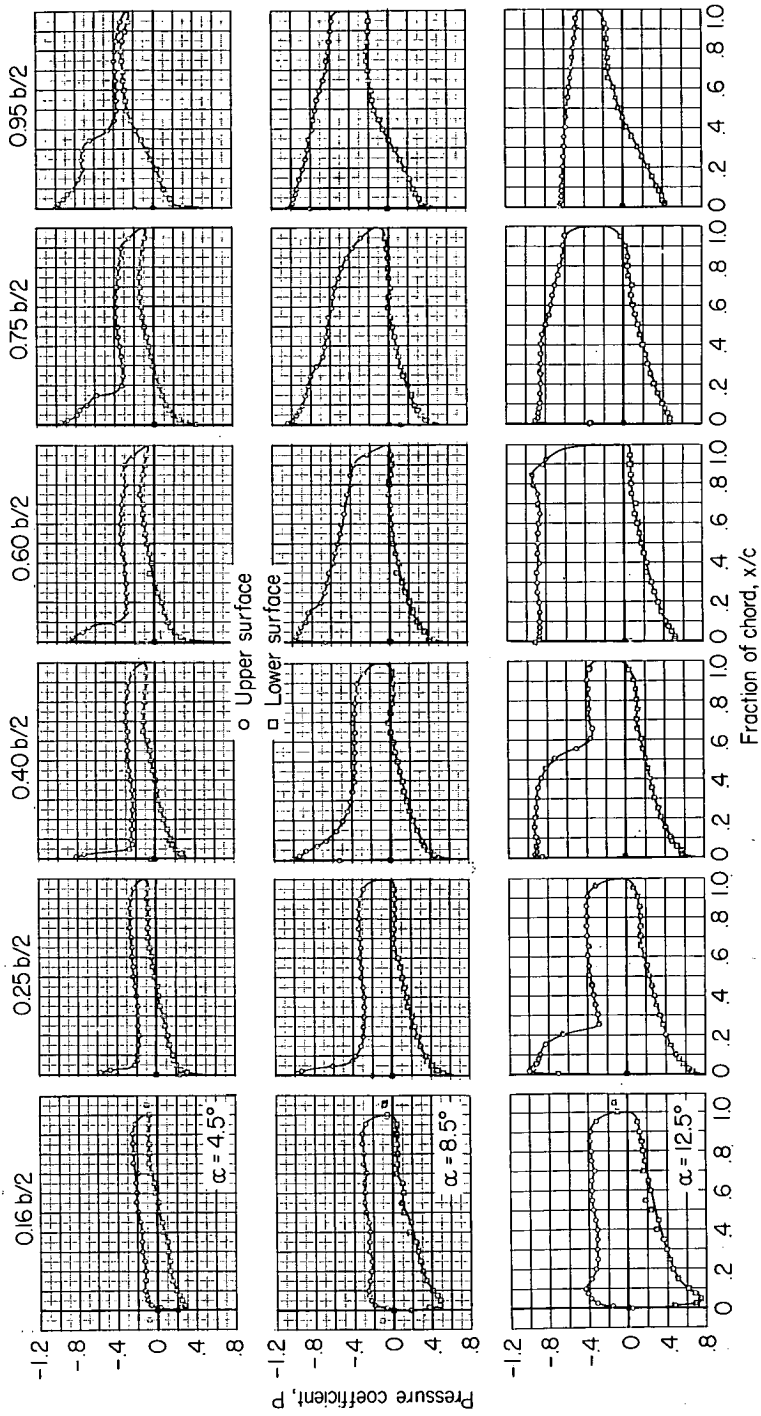
(h)  $M = 1.00$ .

Figure 5.- Continued.



(1)  $M = 1.03$ .

Figure 5.- Continued.



(j)  $M = 1.05$ .

Figure 5.- Concluded.

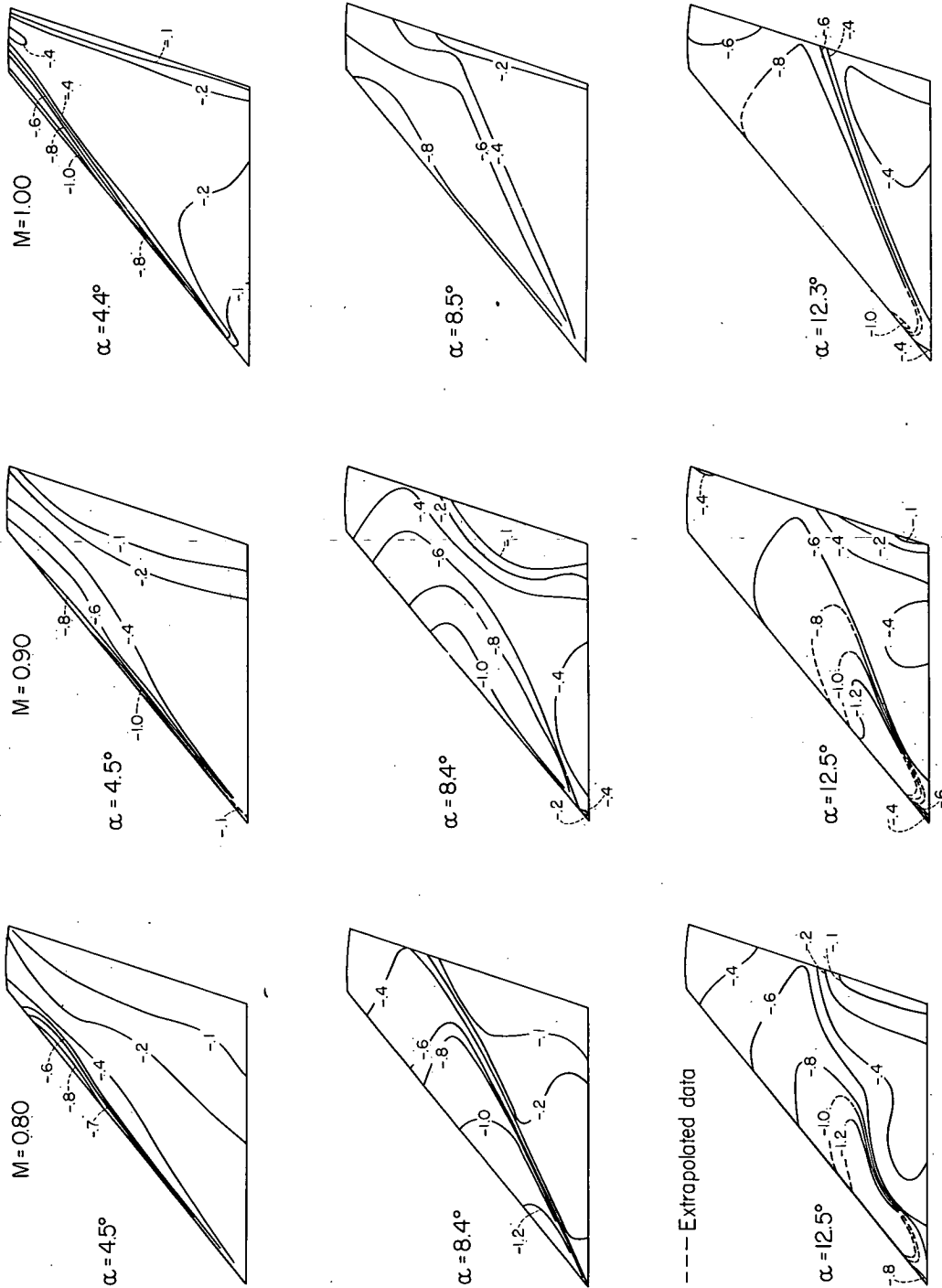
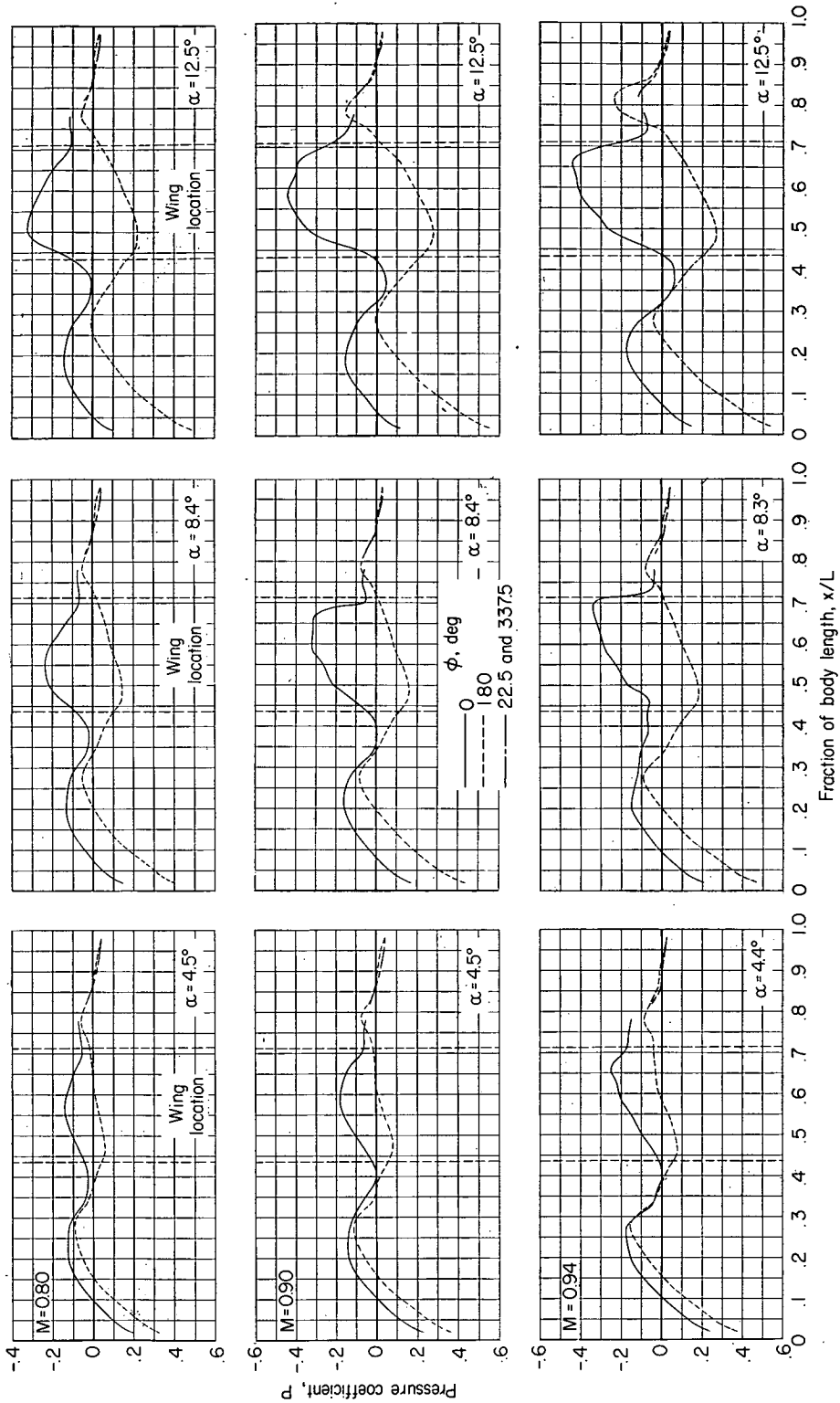
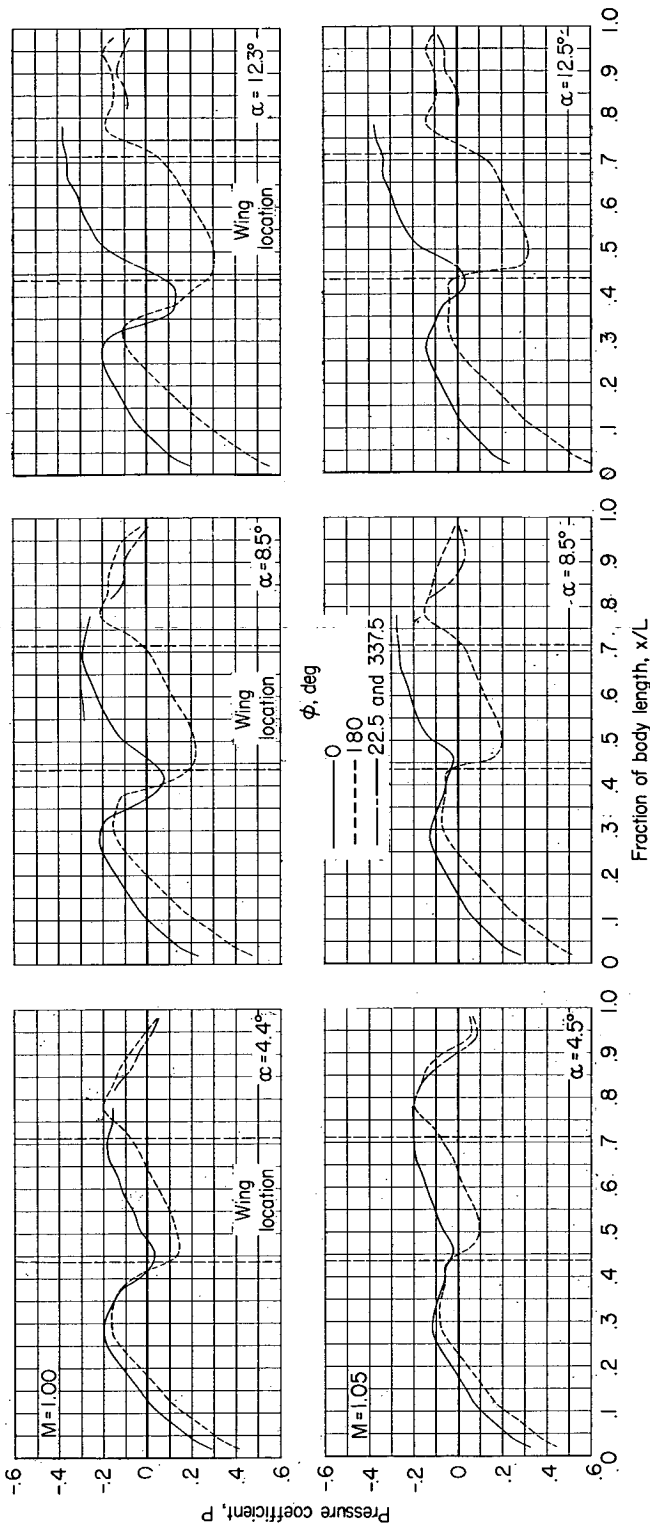


Figure 6.-- Contours of constant pressure coefficient on upper surface of wing.



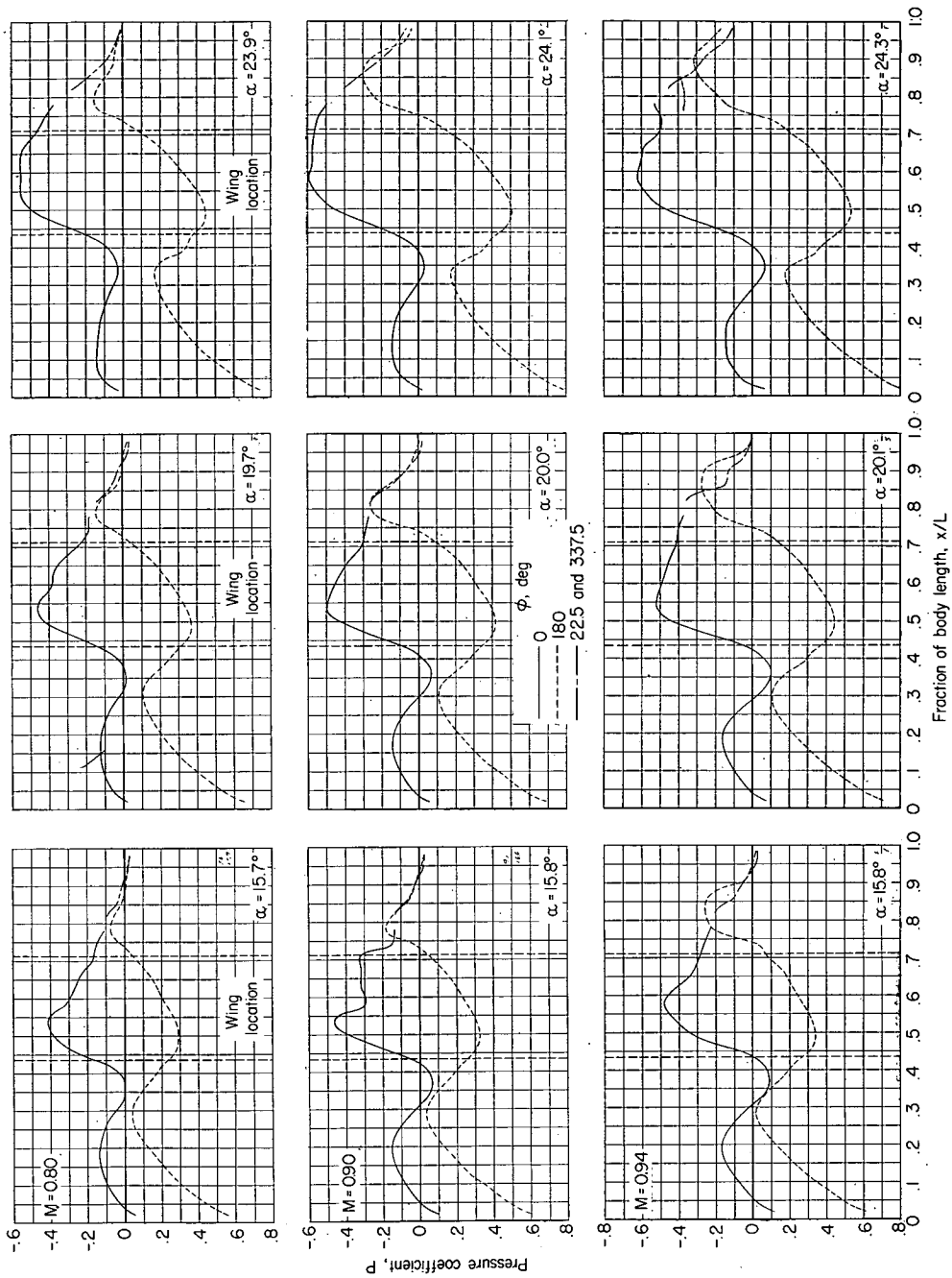
(a)  $\alpha \approx 4.4^\circ, 8.5^\circ, \text{ and } 12.6^\circ$ .  
 numbers and angles of attack.





(b)  $\alpha \approx 4.4^\circ$ ,  $8.5^\circ$ , and  $12.6^\circ$ .

Figure 7.- Continued.



(c)  $\alpha \approx 16^\circ, 20^\circ, \text{ and } 24^\circ$ .

Figure 7.- Concluded.

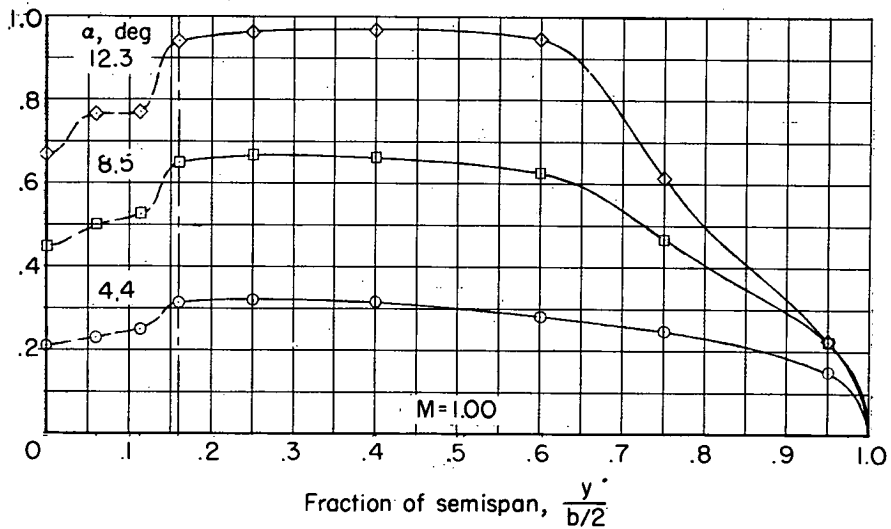
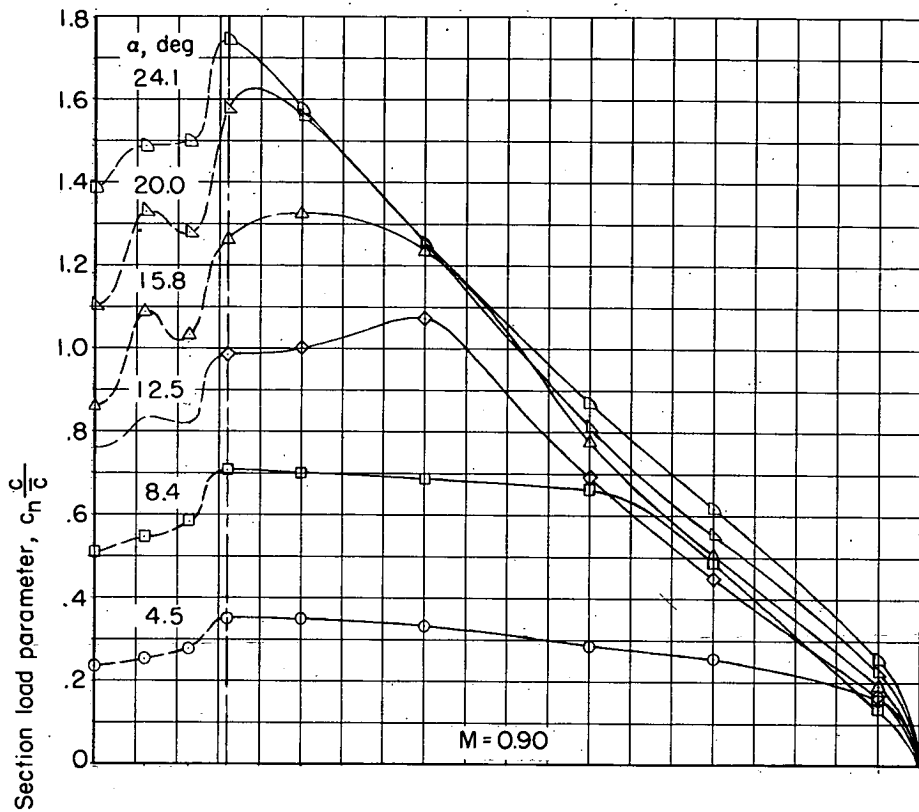
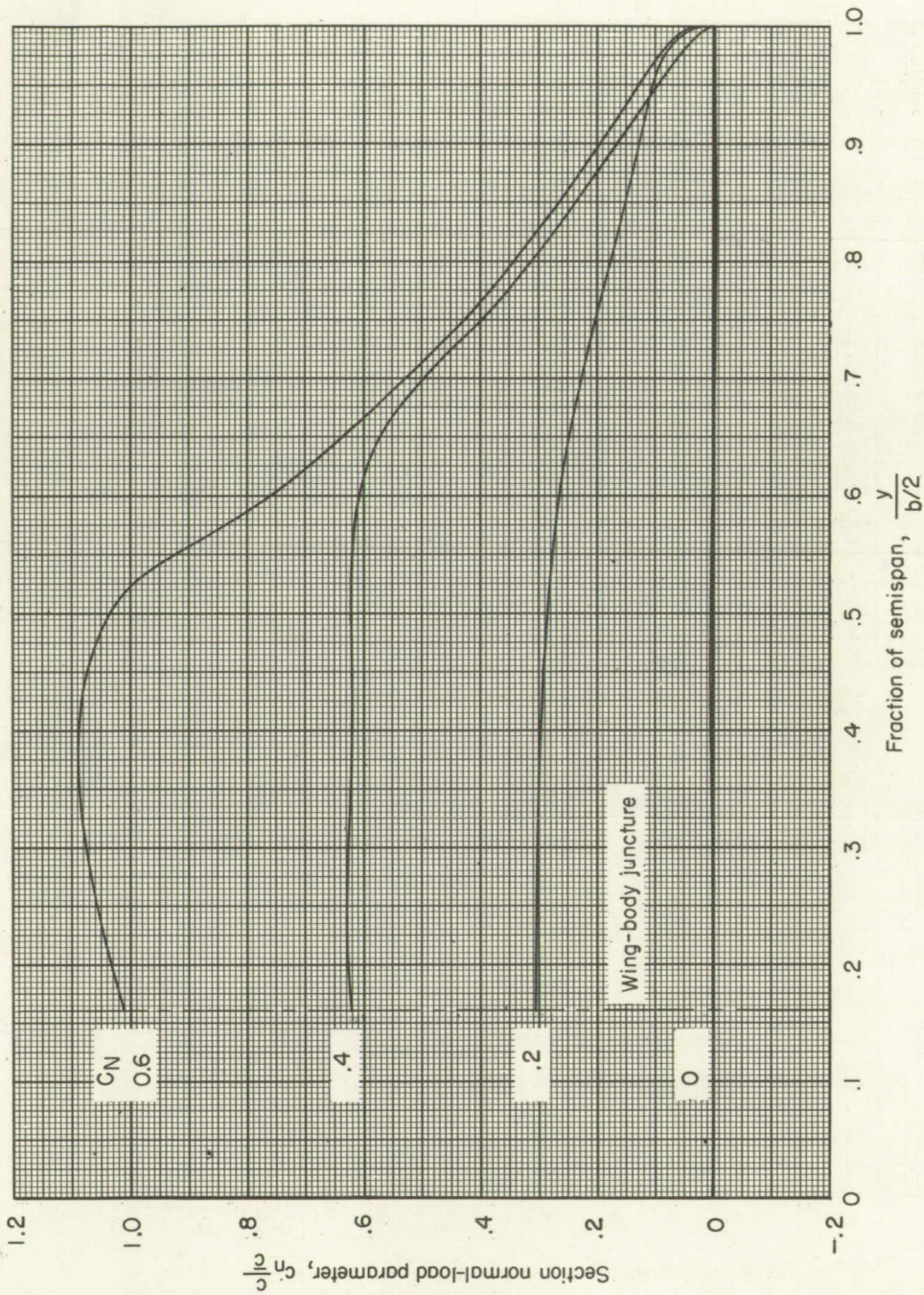


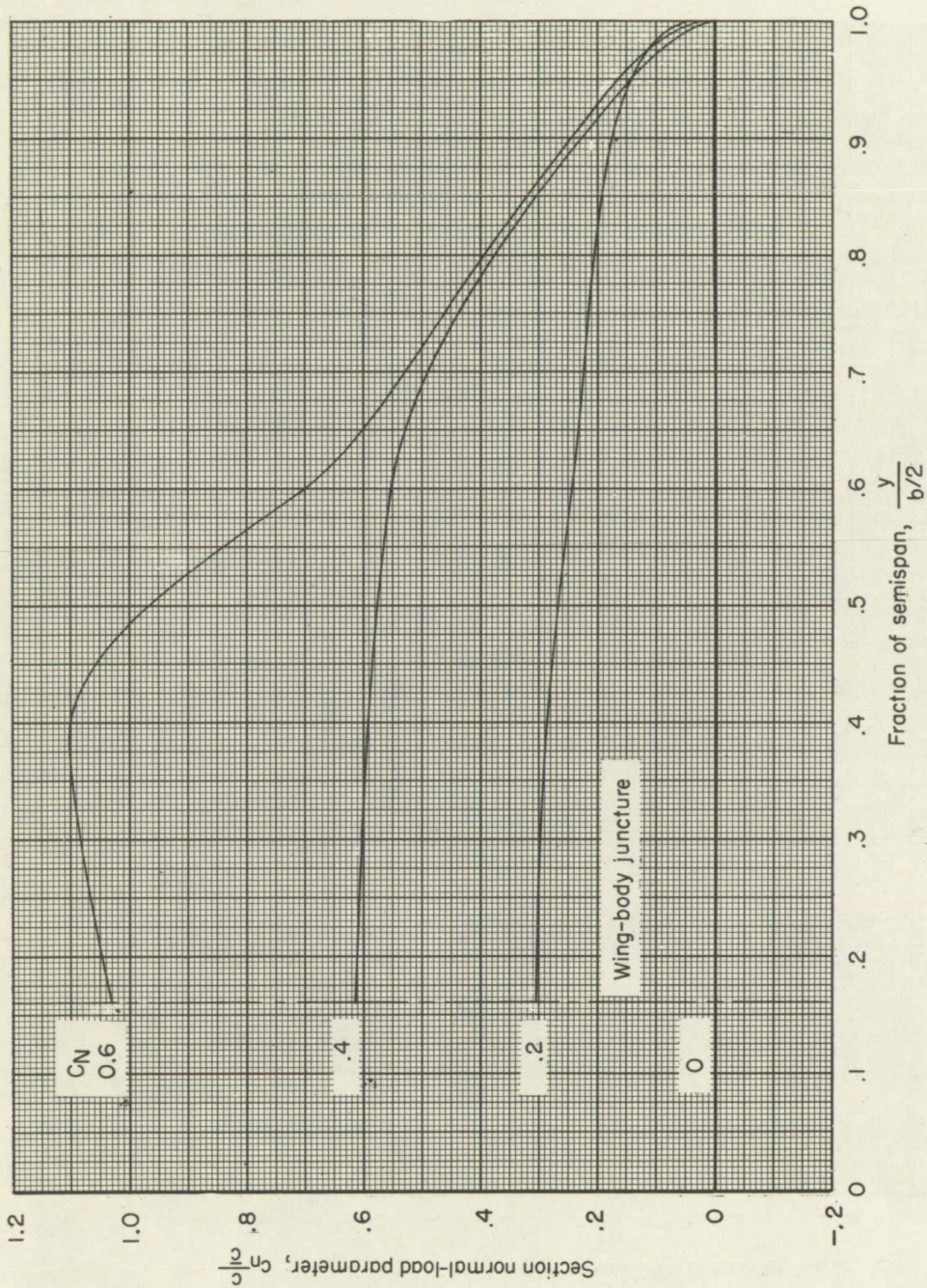
Figure 8.- Typical spanwise variation of section load parameter including loading over the body.



(a)  $M = 0.80$ .

Figure 9.- Spanwise variation of section normal-load parameter with normal-force coefficient for several Mach numbers.

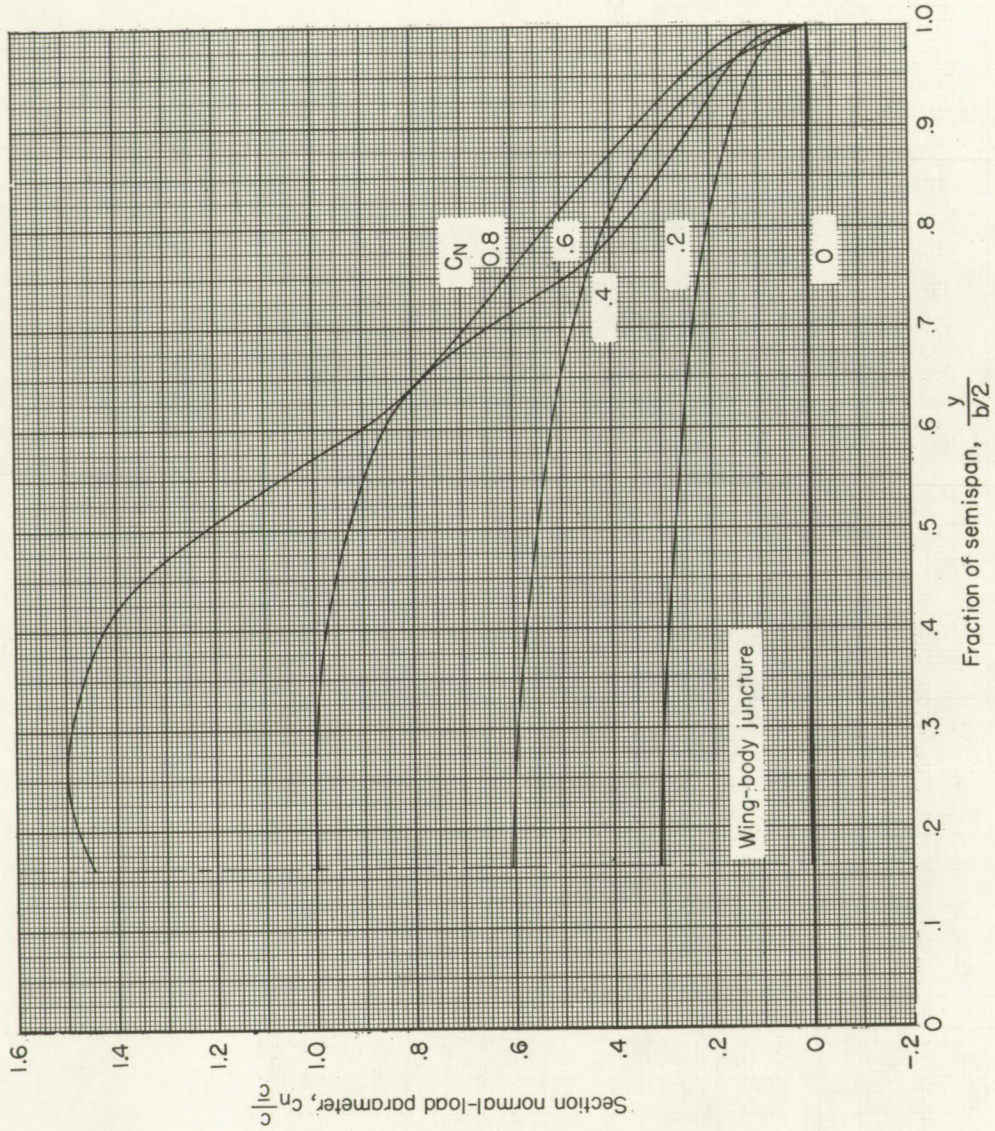




(b)  $M = 0.90$ .

Figure 9.- Continued.

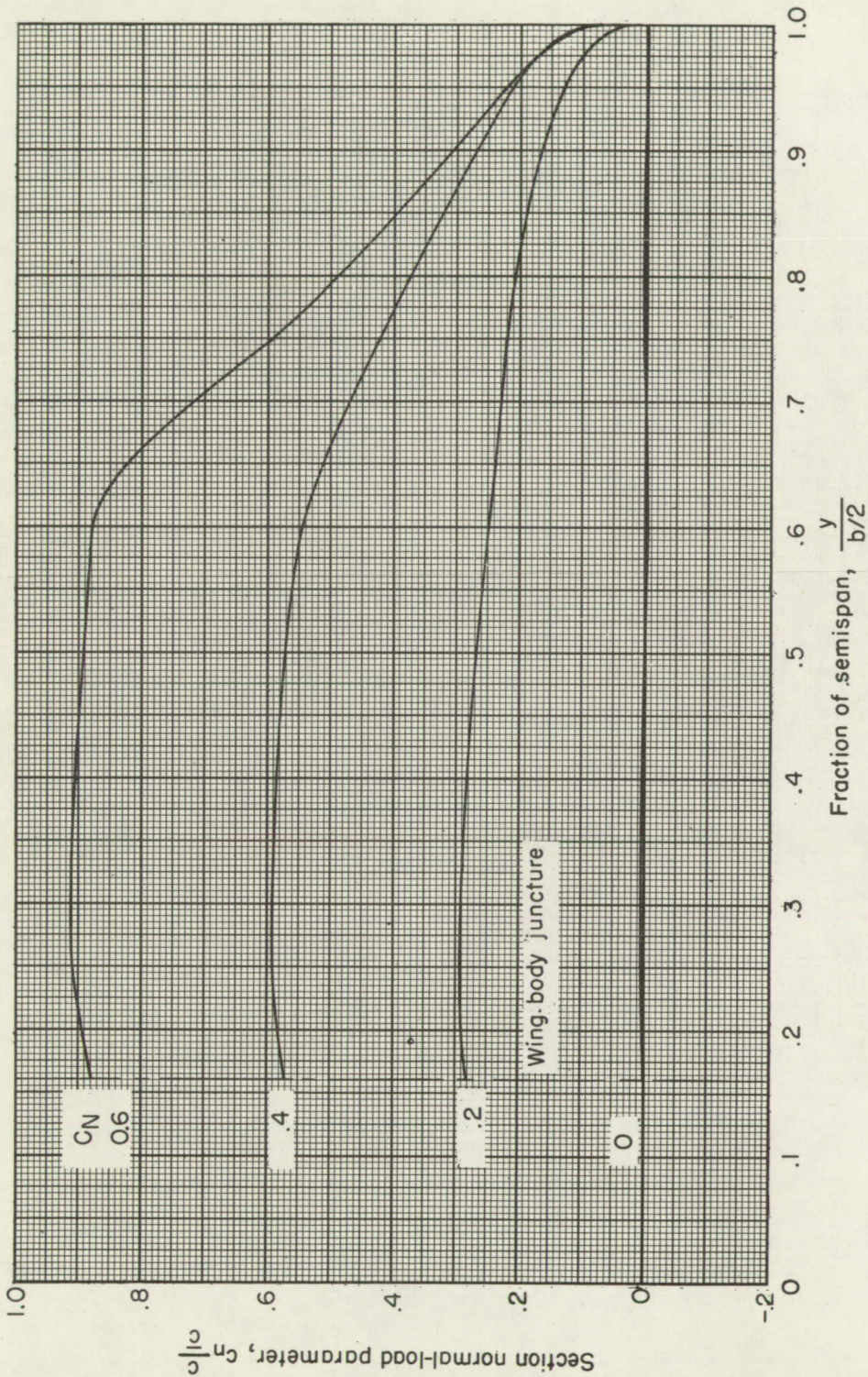




(c)  $M = 0.94$ .

Figure 9.- Continued.

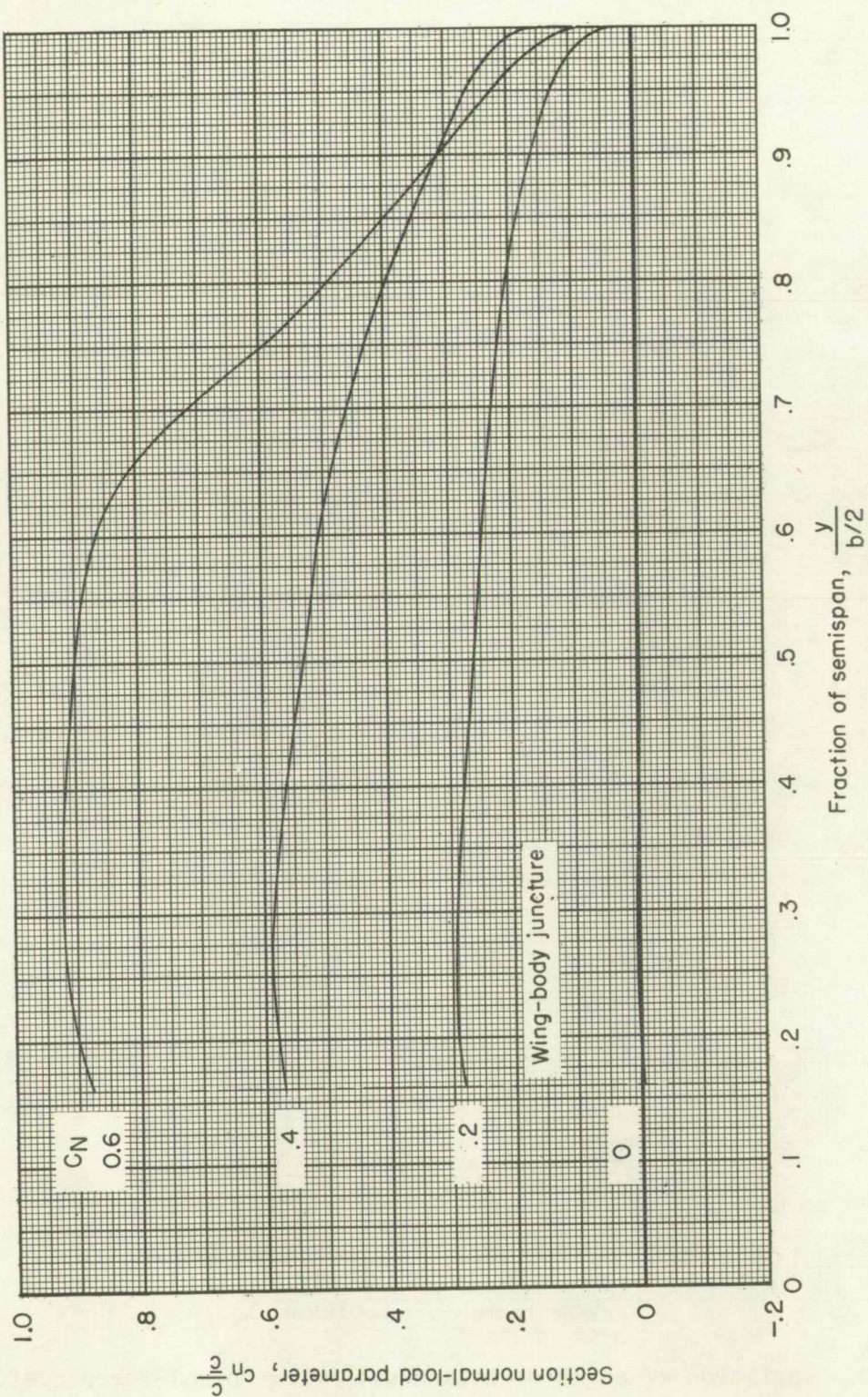




(d)  $M = 1.00$ .

Figure 9.- Continued.





(e)  $M = 1.05$ .

Figure 9.- Concluded.



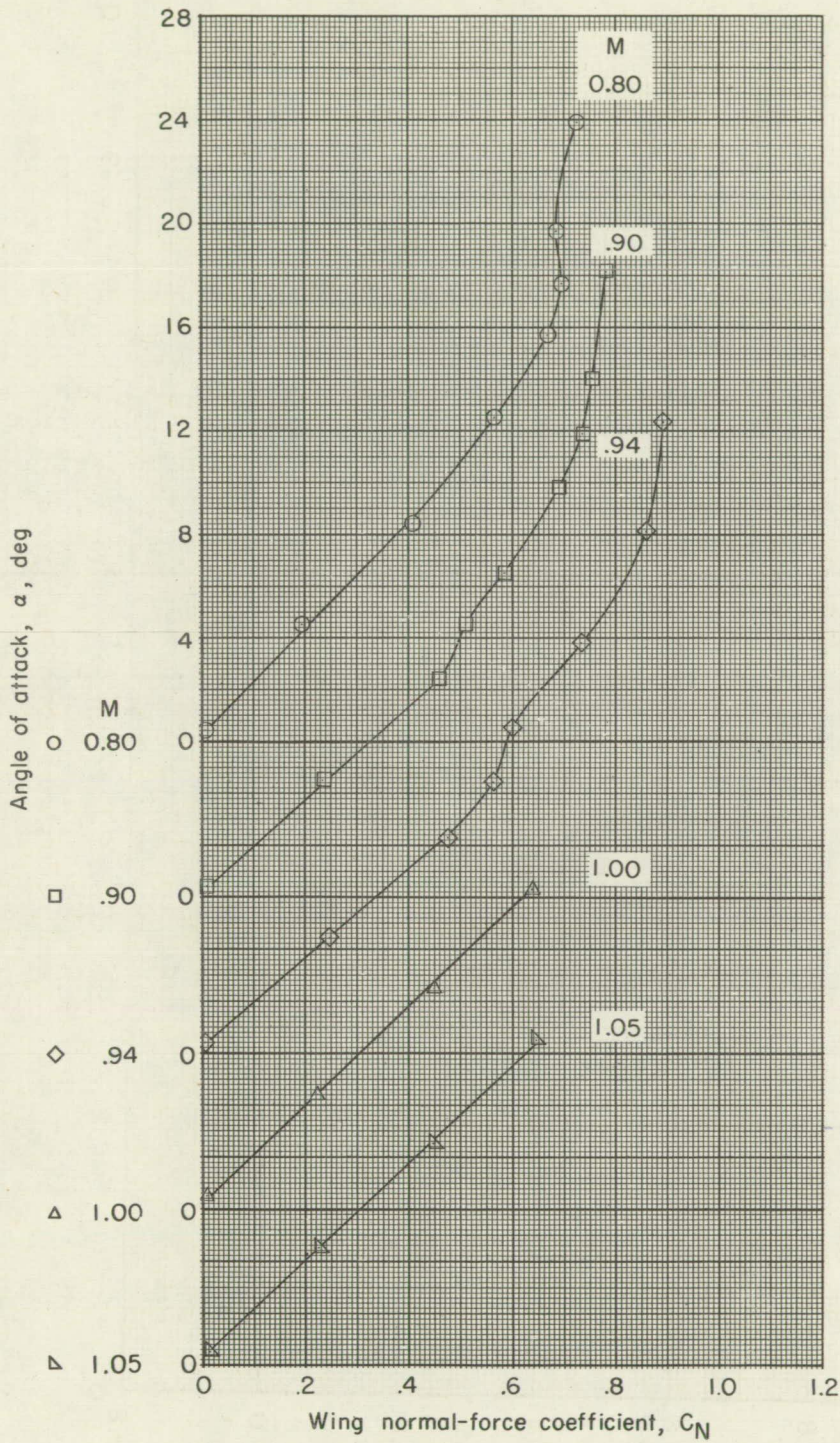
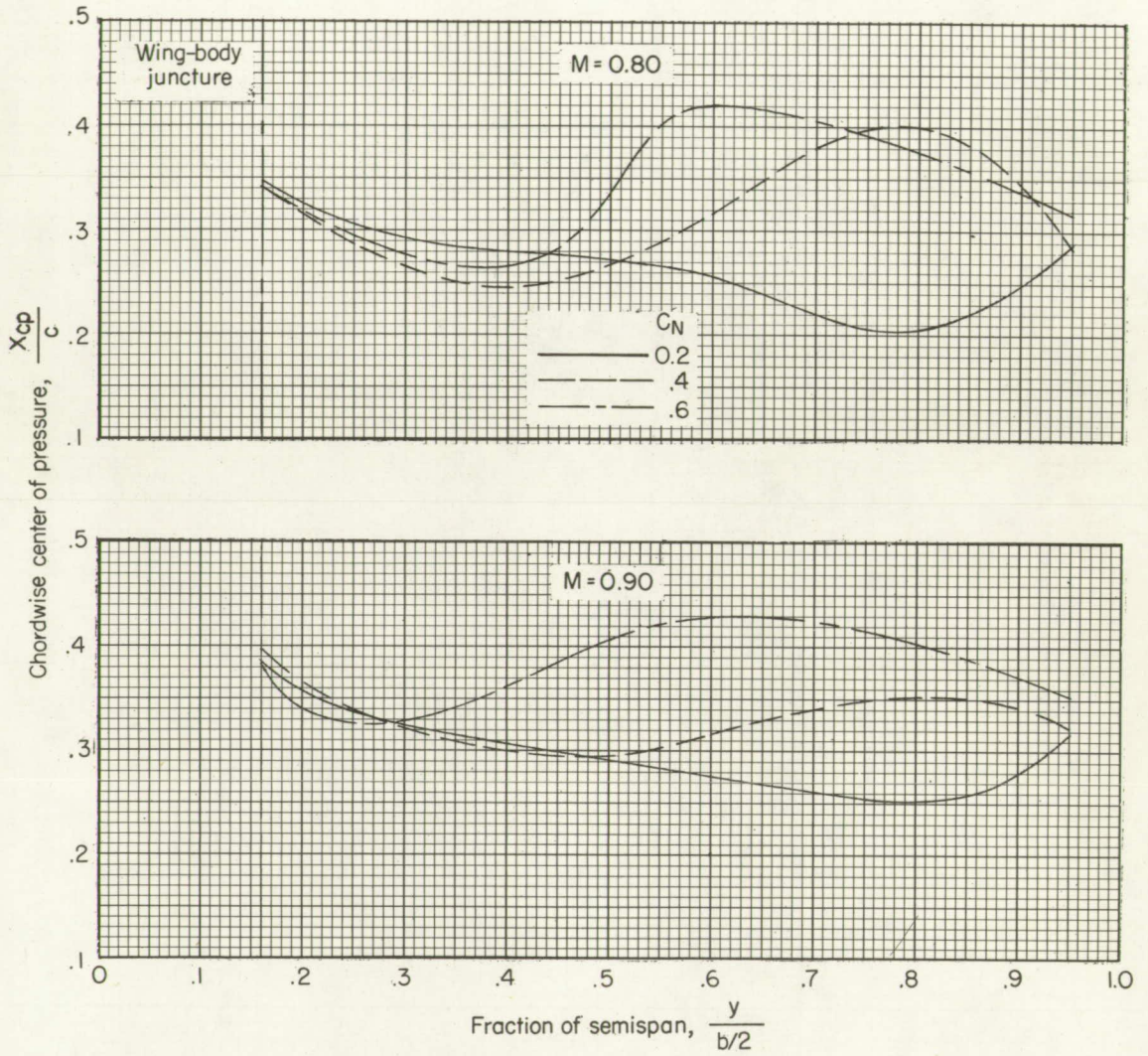


Figure 10.- Variation of angle of attack with wing normal-force coefficient for several Mach numbers.

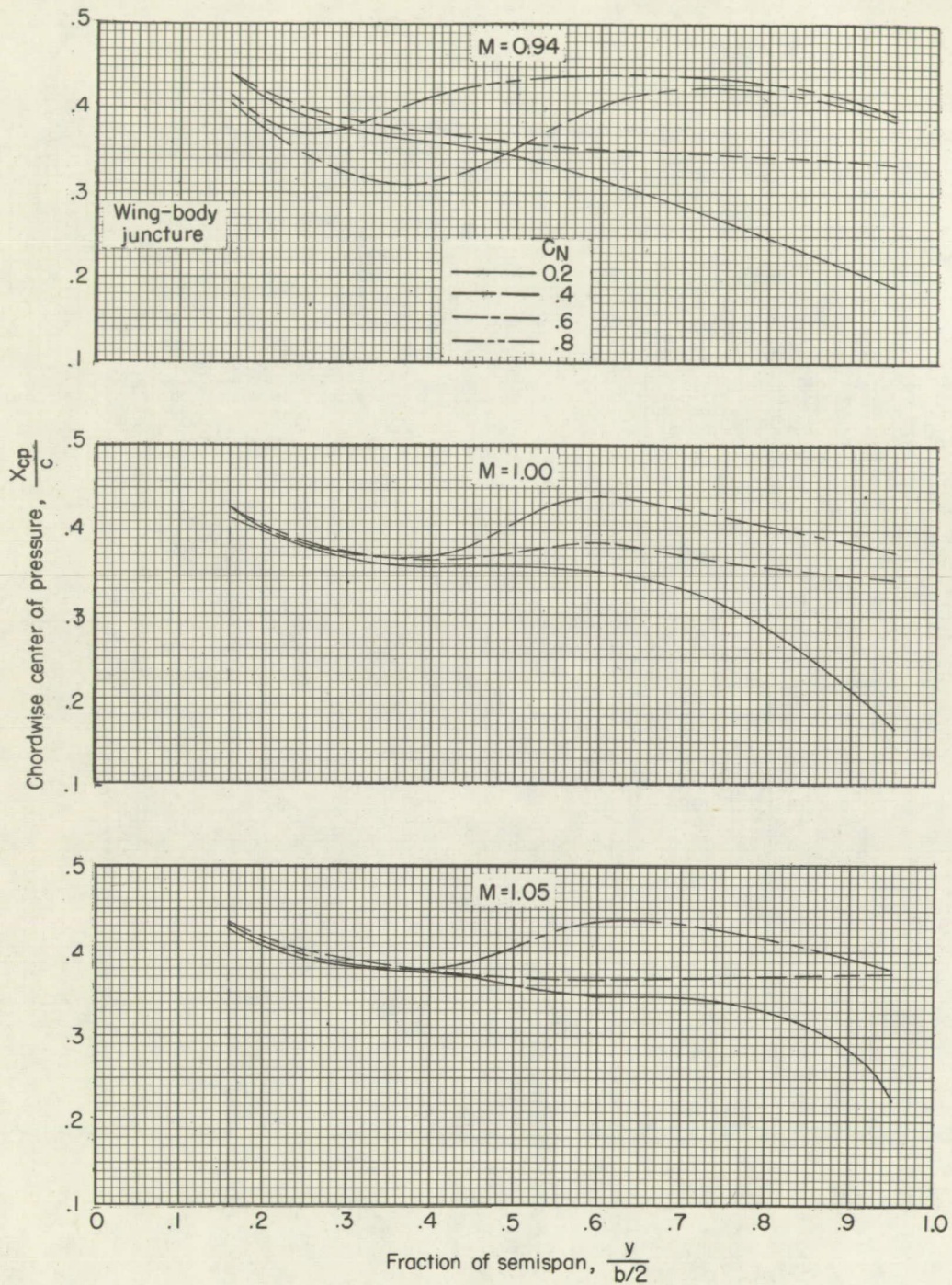




(a)  $M = 0.80$  and  $0.90$ .

Figure 11.- Section chordwise center-of-pressure characteristics.





(b)  $M = 0.94, 1.00, \text{ and } 1.05.$

Figure 11.- Concluded.



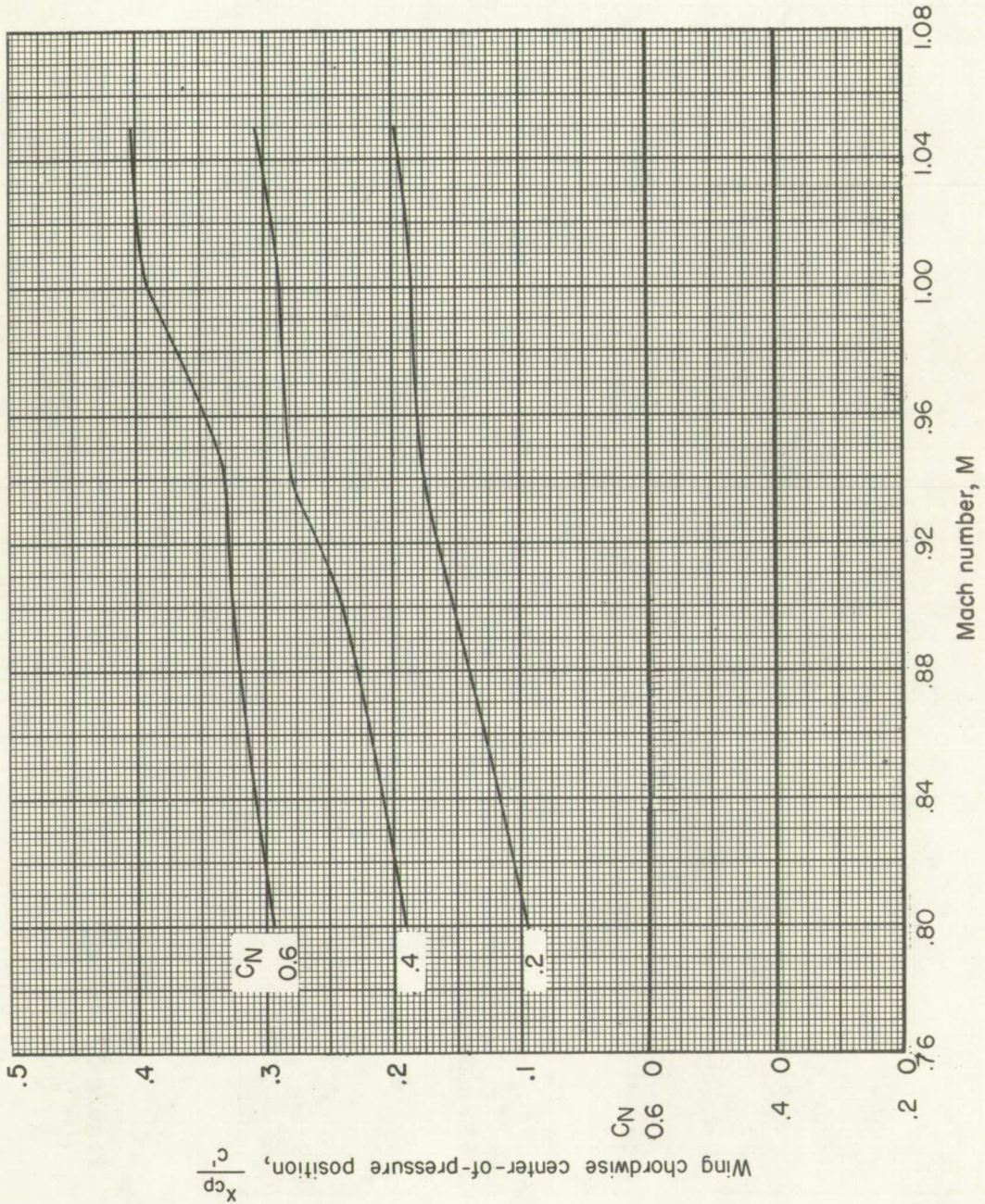


Figure 12.- Wing chordwise center-of-pressure characteristics.

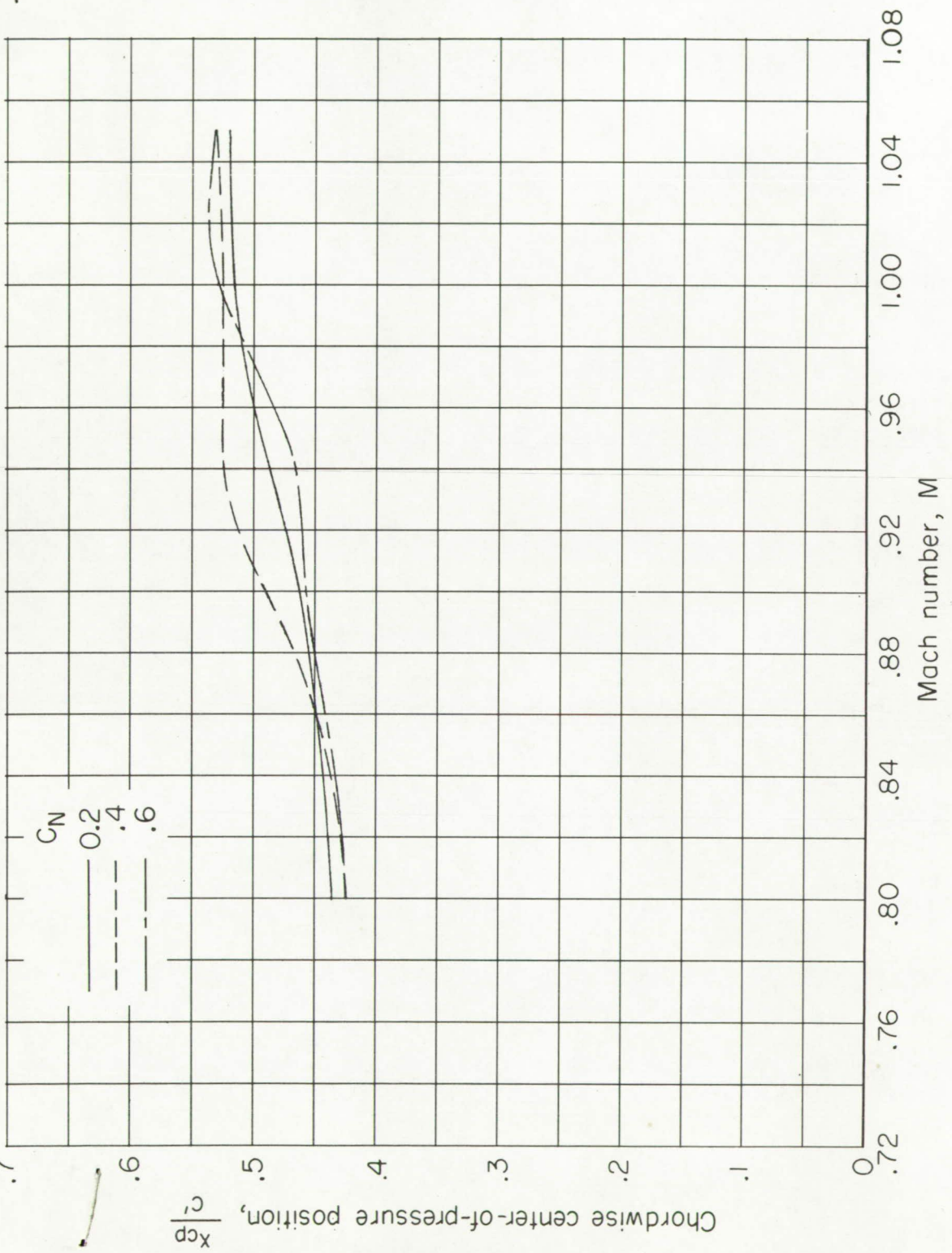


Figure 12.- Wing chordwise center-of-pressure characteristics.



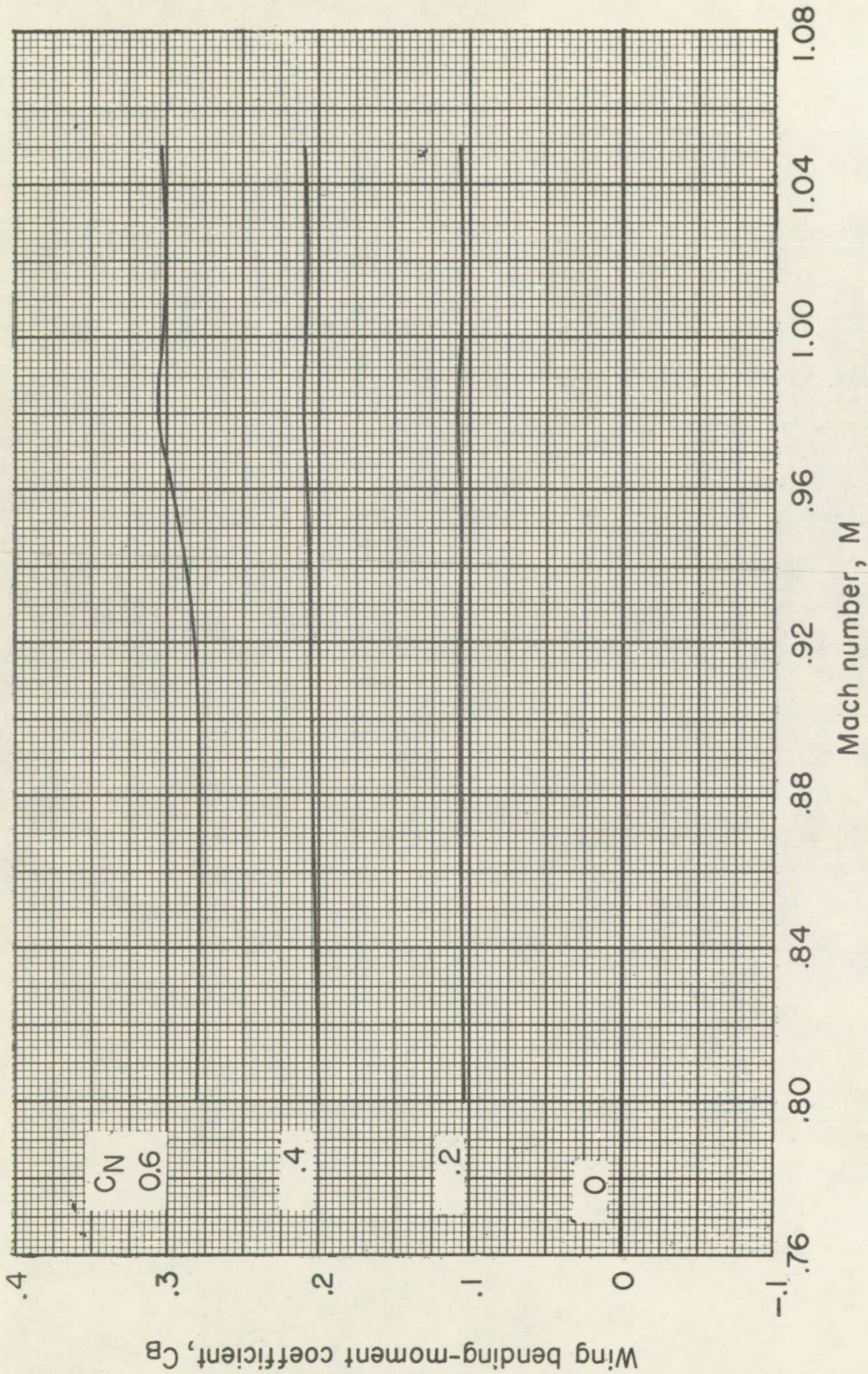


Figure 13.- Variation with Mach number of wing bending-moment coefficient at several normal-force coefficients.



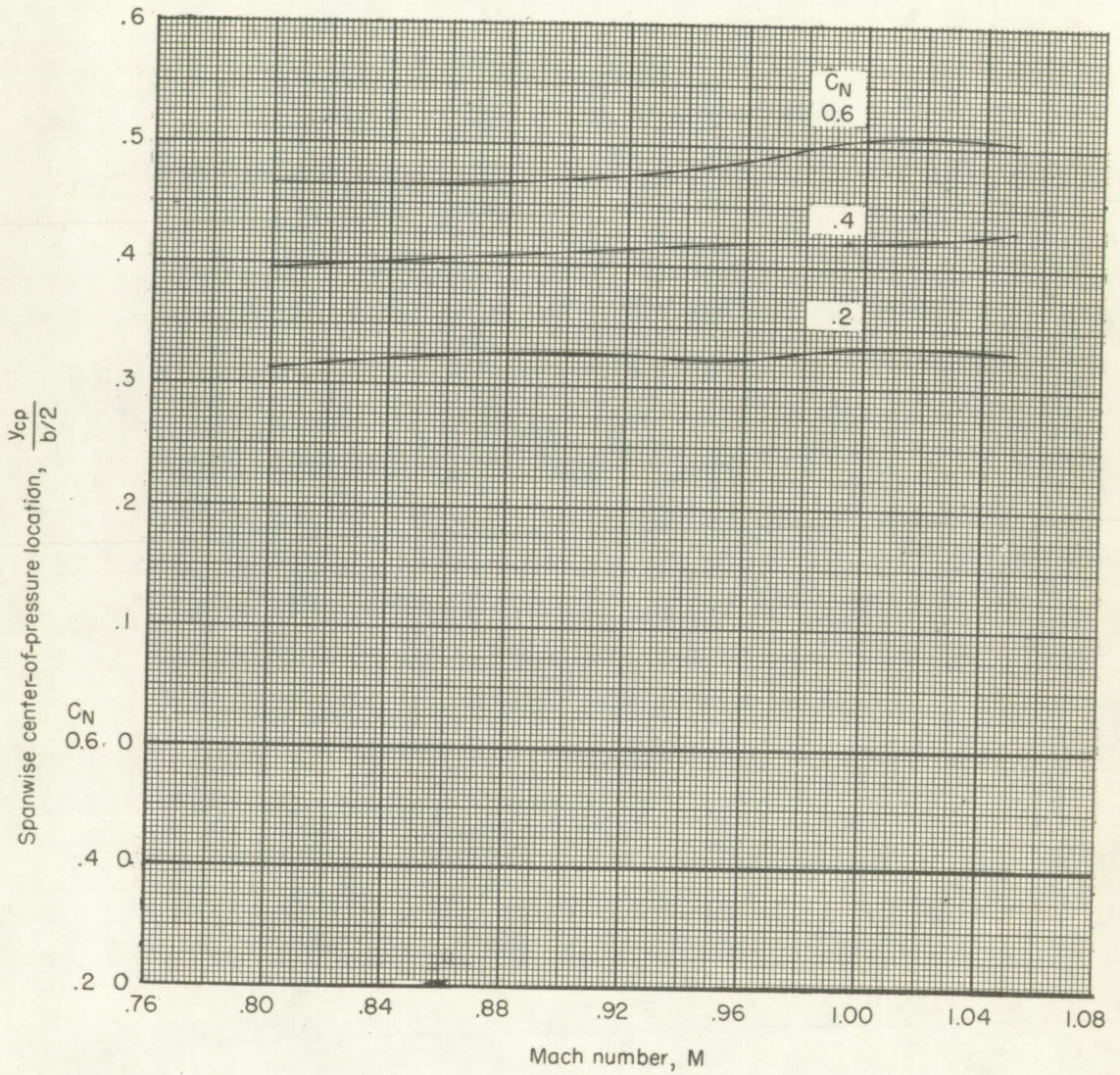


Figure 14.- Wing spanwise center-of-pressure characteristics.

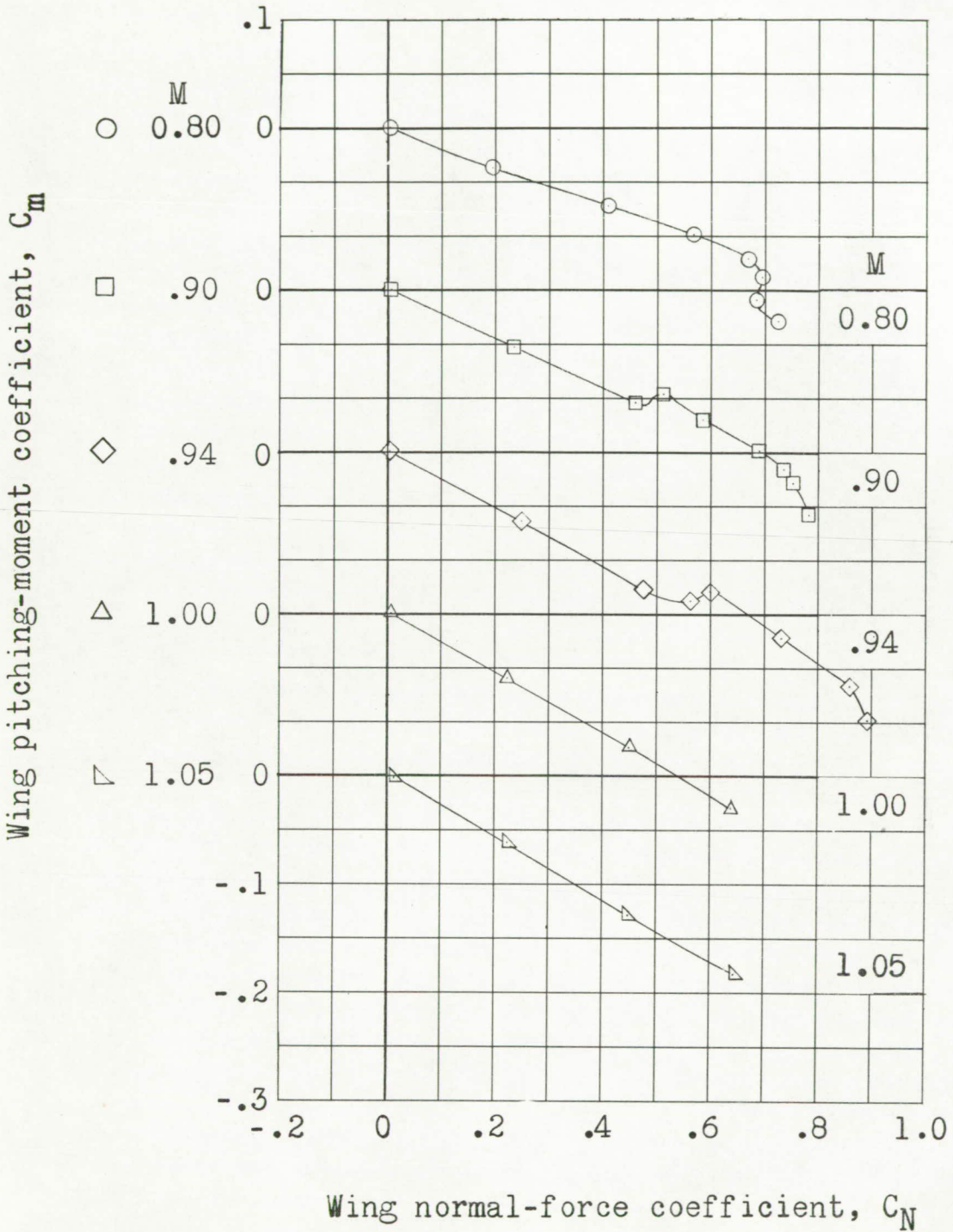


Figure 15.- Variation of wing pitching-moment coefficient with wing normal-force coefficient for several Mach numbers.



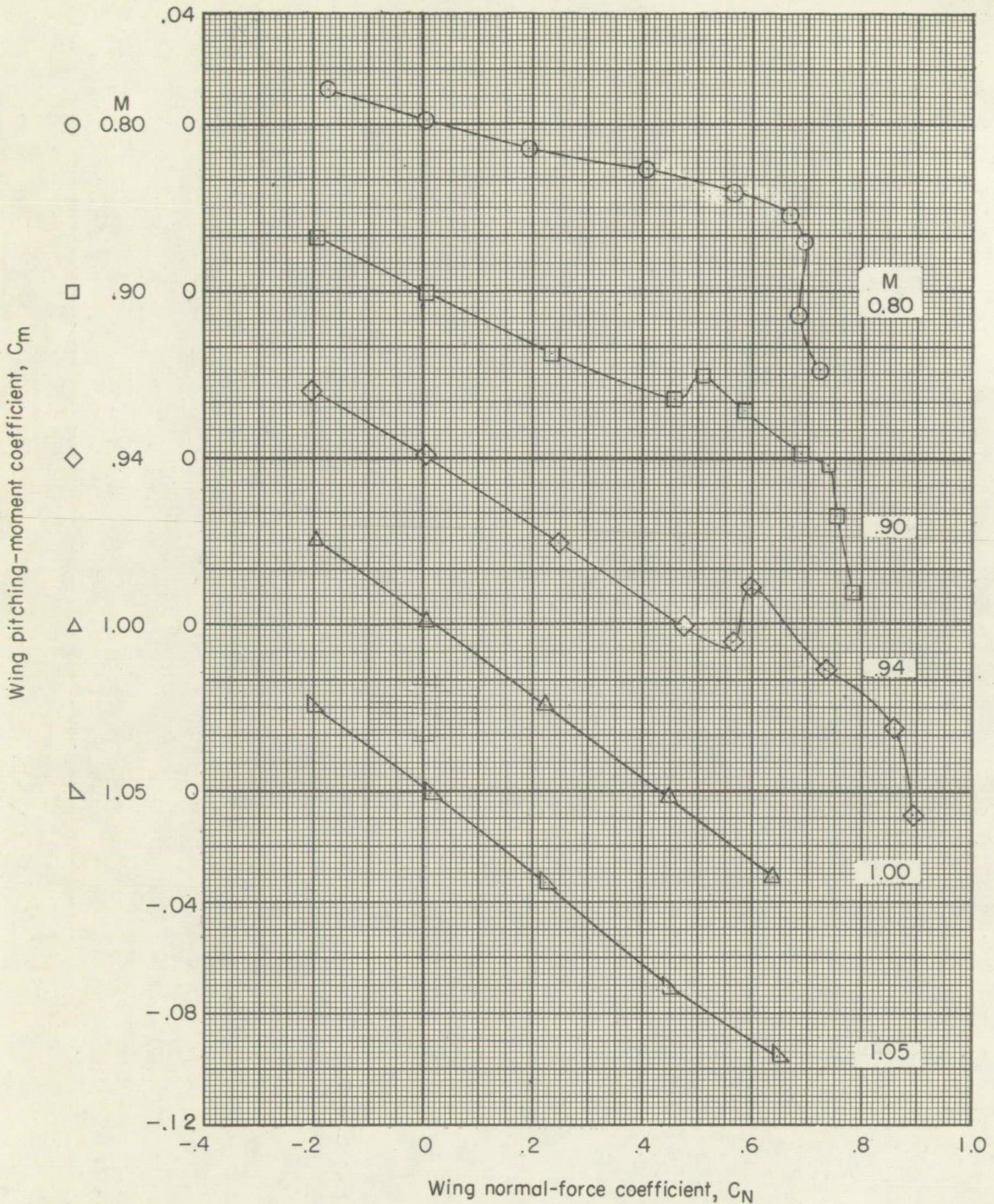


Figure 15.- Variation of wing pitching-moment coefficient with wing normal-force coefficient for several Mach numbers.



CONFIDENTIAL

CONFIDENTIAL